July 2016

# Structure and Dynamics of Charged Colloidal Disks in Colloid-Polymer Mixtures

Suhasini Kishore
*University of Massachusetts Amherst*

# STRUCTURE AND DYNAMICS OF CHARGED COLLOIDAL DISKS IN COLLOID-POLYMER MIXTURES

A Dissertation Presented

by

SUHASINI KISHORE

Submitted to the Graduate School of the
University of Massachusetts Amherst in partial fulfillment
of the requirements for the degree of

DOCTOR OF PHILOSOPHY

May 2016

Department of Chemical Engineering

**STRUCTURE AND DYNAMICS OF CHARGED COLLOIDAL DISKS IN COLLOID-POLYMER MIXTURES**

A Dissertation Presented

by

SUHASINI KISHORE

Approved as to style and content by:

_____
Surita R. Bhatia, Chair

_____
Michael A. Henson, Member

_____
David M. Ford, Member

_____
Christian D. Santangelo, Outside Member

_____
John Klier, Department Head
Department of Chemical Engineering

**DEDICATION**

*To my family and Vivek*

**ACKNOWLEDGMENTS**

It is a privilege to be a part of the Chemical Engineering department at UMass and I consider myself very fortunate to be amidst an excellent group of students. The environment in the department has always been conducive to promoting interactions with students, both on the educational and the social front and I have always felt that this is something very unique to this department alone.

I would like to thank my thesis advisor Prof. Surita Bhatia for her kind and generous support throughout my PhD work. Along the course of my research work, she has made me a better researcher, mentor and a better person all together. She has been immensely patient with me and has been an excellent source for guidance both on the research side and on the personal side. She is always there for help.

Our lab moved to Stony Brook in 2012 and it was a pretty rough time back then as I did not know if I wanted to move or stay back. Even now when I think of those times, I feel I did make the right decision to move as I would never have had a better advisor and I had also developed a lot of interest in rheology and colloid science. I had the privilege of setting up the lab at Stony Brook and I appreciate Surita for showing some confidence in me and in my ability to get things up and running. I would also like to thank her for letting me play with her kids, Julian and Evan, whenever I needed a break from all the craziness in the lab. I enjoyed my brief role as their beloved Indian Santa. It probably was the only time when I did not have the necessity to behave like an adult and I guess this was my way of taking the work stress out of my system. My days at Stony Brook would not have been enjoyable or even remotely tolerable without their abundant love and infectious cuteness. I will miss them very much! I hope they will

always remember me in the future. They probably would say “Mommy had a crazy student who would come over every day to watch us play”, but it is okay. It needs a lot of patience and perseverance to begin to like a place like Long Island and I think the kids helped make things a little easier for me during the transition period.

I would also like to thank my thesis committee members, Prof. Chris Santangelo, Prof. Mike Henson and Prof. David Ford for their guidance and support. Prof. Chris guided me through my very first simulation project. Although I could not pursue much in that direction I was able to learn a lot from him. I wish I had some more time in grad school to finish what I had originally started on. I also had the opportunity to discuss my work with Prof. Dave’s student, Raghuram Thyagarajan, who helped me understand the different facets of colloidal science through his computational research.

I have had some great times working in the lab along with my lab co-workers: Joe, Erika, Anand and Dave while at UMass and Wendy, Xiao and Bing while at Stony Brook. Joe and Anand trained me on all the instruments in the lab when I first joined the Bhatia Research Lab. This probably gave me the confidence to be able to handle the lab setup work at Stony Brook with ease. I owe Joe a lot of gratitude because he was always okay with the idea of driving down to Stony Brook to help me out during the lab setup period and with the task of aligning the laser. He is very tall and can pretty much lean on the goniometer without needing a foot stool! He took the responsibility to ensure that I plotted all my graphs the proper way and was a great desk-buddy at Elab II. I pretty much failed to understand his dry humor but I think I have improved over time. I am really happy that we were able to start working on the ALP project and it looks like some very exciting results are going to come out of it. I also had the opportunity to accompany Erika

on her trip to NIST to help her conduct neutron scattering experiments. I learnt a lot from that trip as I was able to work as a team to study some fabulous hydrogels that Erika had made with her collaborators from the Polymer Science Department.

I also thank my undergraduate researchers: Pradeep, Ying, Robert, Katie, Christina and Max for helping me with all my experiments and data analysis work. Pradeep built the templates for analyzing the light scattering data and I really appreciate his help with this. All my undergraduate students were very good at learning techniques quickly.

I would like to gratefully acknowledge the financial support that made this work possible: NSF awards CBET-0853551 and CBET-1335787 and Xerox Corporation. Use of the Advanced Photon Source at Argonne National Laboratory was supported by the U.S. Department of Energy Office of Science under contract DE-AC02-06CH11357.

I would like to thank my family for their unconditional love, encouragement and support. They worked hard all their life to give me and my brother a very good education. They sent us both to one of the best elementary schools in India and did not deny us of a good higher education despite not having all the money. I am very grateful to them.

Lastly, this dissertation would not have been written, if not for my husband who, although arrived at a later part of my life as a graduate student, has been a constant source for support and motivation. I think it takes a lot of patience to listen to reasoning and complaining when one is also traversing through the dark tunnel of the unknown. I thank him for being there for me through the last stages of my research work.

## ABSTRACT

STRUCTURE AND DYNAMICS OF CHARGED COLLOIDAL DISKS IN COLLOID-POLYMER MIXTURES

MAY 2016

SUHASINI KISHORE, B.Tech., ANNA UNIVERSITY

Ph.D., UNIVERSITY OF MASSACHUSETTS AMHERST

Directed by: Professor Surita R. Bhatia

Complex fluid mixtures of colloids and polymers are extensively used in several conventional and emerging technological applications. Particles self-assemble under different conditions to form colloidal glasses and gels and it often leads to the development of unusual viscoelastic features. In the case of aspherical particles, shape anisotropy and physical aging effects add to the existing complexities so the implementation of a strategic formulation method to improve performance and stability remains a critical challenge.

This thesis presents a comprehensive analysis of particle interactions in mixtures of charged disk-shaped colloids and weakly-adsorbing polymers like poly(ethylene oxide) (PEO). Here, we discuss the behavior of suspensions containing laponite® and PEO of molecular weights ($M_w$) varying between 4.6 and 300 kg/mol and at concentrations within the dilute through concentrated regimes. Techniques such as rheology, light (DLS) and x-ray scattering (XPCS and USAXS) were used to understand and characterize the effect of chain number and length on the macroscopic behavior, microstructure and dynamics of particles in these colloid-polymer mixtures.

Laponite® suspensions gradually transition from a homogeneous fluid to a structurally arrested phase. With the addition of polymers, rheological measurements show that in addition to the typical re-entrant behavior observed in the dilute polymer phase, there is another onset of stabilization close to the semi dilute polymer regime. While DLS and XPCS results show three different regimes in the microstructural dynamics along these transitions, USAXS measurements indicate the presence of only finite sized ellipsoidal structures that are directed by polymer-particle interactions. We believe that the arrested phase is a glassy system as no large scale structure is observed. On the other hand, adding high $M_w$ PEO results in the formation of strong colloidal gels where laponite® particles act as junctions in the colloid-polymer network. Nanometer to micron-sized clusters form with the addition of PEO chains larger than the minimum required for polymer-clay bridging. Increasing the concentration of PEO changes the density of clusters and this directly affects the bulk elasticity of the material. The results thus serve as an excellent benchmark to understand how to effectively formulate an anisotropic colloid-polymer mixture for an application.

## TABLE OF CONTENTS

Page

## LIST OF TABLES

Table Page

## LIST OF FIGURES

Figure Page

# CHAPTER 1

# BACKGROUND AND MOTIVATION

## 1.1 Introduction

### 1.1.1 Overview

Colloids are multiphase substances that are prevalent in nature and find frequent use in the industry as well. A few examples of such materials include paints, cosmetics, printing inks, cements, and so on. These materials have also been of great interest to the academic world because of their underlying rich physics. The types of colloids depend on the nature of the dispersed and continuous phases, and typically for a colloidal system the characteristic size of the dispersed phase is usually between 10 nm and a few microns. Some of the colloidal systems that are of great interest for applications are dispersions, emulsions and foams. The rheological properties of these systems can be tuned to achieve a desired consistency, which can be exploited to make the dispersions easier to process. For instance, with increasing solid concentration in a colloidal dispersion, the viscosity of the system increases to an extent that it ceases to flow unless a sufficient pressure is applied. However, as discussed later in Chapter 2, certain types of additives such as polymers may be used to decrease the viscosity and promote easier handling. Additionally, as we look more deeply into these systems, we find that the microstructure may gradually evolve with time, leading to a change in the properties that may be unfavorable for an industrial application.

The use of colloidal clays has garnered much attention in recent years, as clays can serve as model anisotropic colloids and form dispersions with a qualitatively rich phase

behavior. Laponite® is a synthetic clay that is widely used as a rheological modifier in many industrial applications. Figure 1.1 shows the structure and dimensions of a single laponite® disk. This disk-shaped colloid has an aspect ratio of 1:25. A single laponite® disk has a structure that closely resembles the structure of common phyllosilicates, where sheets of octahedrally coordinated magnesium oxide are present in between two sheets of tetrahedrally-coordinated silica. A single laponite® crystal comprises of approx. 1500 units cells[1] with an empirical formula $Na^{+}_{0.7}[(Si_8Mg_{5.5}Li_{0.3})O_{22}(OH)_4]^{-0.7}$.

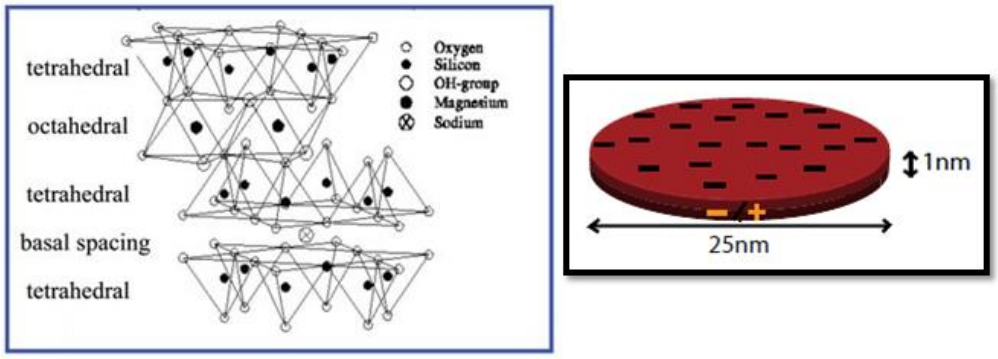


Figure 1.1 : Structure and dimensions of a laponite® platelet[1]. Laponite® has a diameter of ~25nm and a thickness of ~1nm

When laponite® is dispersed in water, the face develops a negative charge as the intercalated sodium ions are released into the medium, and a double layer forms around the face of the disk. On the other hand, the protonation of the $OH^-$ groups leads to the formation of surface charges along the rim. However, the charge distribution along the rim varies with pH, and several somewhat conflicting observations about the effective charge distribution on laponite® particles have been made over the years. A number of studies have indicated that the edge has a net positive charge, with the positive nature decreasing with increasing pH for $pH \leq 11$[2,3]. Dispersions of laponite® are generally

considered to be monodisperse, but this largely depends on the extent of hydration and exfoliation of particles present in the solution. Experimental observations made by different groups have indicated a certain magnitude of polydispersity, where about 20% of the particles exist as dimers in solution[4].

As mentioned earlier in this section, the phase behavior of a colloidal system largely relies on its microstructure and the nature of interactions between particles in the system. In addition to the excluded volume interactions, the particles also experience an electrostatic interaction as they are charged colloids. However, depending on how they are oriented in the volume the electrostatic interaction can either be repulsive (face-face, rim-rim) or attractive (rim-face). The following section will discuss the phase behavior of laponite® under different experimental conditions.

### 1.1.2 Phase diagram of laponite®

Laponite® exhibits phase behavior that depends on experimental parameters like particle concentration, salt/ion concentration, pH, temperature and also on the presence of additives/surfactants like polymers. The phase diagram of laponite® was first observed and described by Mourchid and co-workers[5,6]. In this work, they reported the phase behavior for various particle concentrations and ionic strengths through rheology and osmometry. In a recent review by Ruzicka and Zacarelli[7], a new unifying state diagram was proposed, and this state diagram takes into account the different results and observations that were made from several experimental and theoretical studies. The state diagram, as shown in Figure 1.2, considers the fact that laponite® systems exhibit an aging behavior, and that the final state behavior depends highly on the protocol for sample preparation. Thus, because some of the regions are equilibrium phases while

others are path-dependent, kinetically trapped states, we refer to the overall diagram as a state diagram.

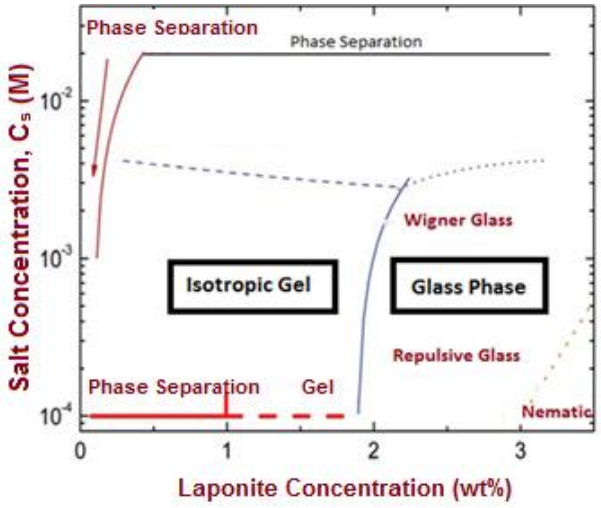


Figure 1.2: State diagram of laponite® proposed according to recent results from various experiments and simulations[6].

At salt-free conditions, laponite® exists in four different phases/states depending upon particle concentration $C_L$. For very low concentrations ($C_L$ < 1%), the dispersion exists as an isotropic liquid, and an extremely slow gas-liquid phase separation takes place[8]. However, with increasing particle concentration, an equilibrium gel state is observed because of anisotropic attractive interactions present within the system. As we keep increasing the concentration, repulsive interactions begin to dominate and a glassy state is formed. This glassy state was proposed to be a Wigner glass[9]. Glasses are described more quantitatively below in section 1.1.2. For concentrations higher than 3%, a nematic phase was observed, and this state is characterized by the presence of birefringence in the sample volume. Salt concentrations can change the nature of particle interactions and this in turn can alter the dynamics and the mechanism of structural arrest

in the system. The addition of salts causes an increase in the attractive interactions because of electrostatic screening. For salt concentrations up to 2mM, the formation of attractive glasses/gels was observed in the range of low and intermediate particle concentrations[10]. Several groups have worked on the aging dynamics, mechanism of structural arrest, and rheology of laponite® suspensions with added salt. For example, Joshi and coworkers demonstrate that at high salt concentration, the recovery behavior showed a large viscous deformation, implying a state of less homogeneity, which suggests that particles experience a weak interparticle attraction with the addition of salt[11]. On the other hand, at salt concentrations above 20mM, flocculation takes place at an accelerated rate and the aggregates begin to sediment[6,12]. Alternatively, the dynamics in clay suspensions can be altered by the addition of surfactants or polymers. The following section will briefly describe the phase behavior of colloids with polymers in the medium.

### 1.1.3 Colloid-polymer mixtures

Hard spheres are often used as fundamental models to understand colloidal behavior. In this case, the particles do not interact over distances greater than their diameter, and they remain impenetrable because of infinite repulsions when they touch each other[13]. The control parameter in such a system is the volume fraction, $\varphi$. For $\varphi < 0.49$, the suspension is a fluid and for $0.545 < \varphi < 0.74$, the equilibrium state is a crystal[14]. In this intermediate range two phases co-exist; some particles crystallize while some remain in the fluid, with constant exchange between the two. But when $\varphi \sim 0.58$, if nucleation is avoided through sufficient polydispersity, the system arrests to form a solid and is far from the equilibrium ordered phase[15]. This structurally disordered and frozen phase is

termed as a glass (also called as repulsive glass). In a hard sphere suspension, particles are free to move and undergo Brownian motion, so the time-averaged properties are equal to the ensemble average, and such a system is ergodic in nature. By contrast, in a glass, particles are confined to small regions of space within the cage created by nearest neighbors, and the system so no longer meets the conditions of ergodicity; these states are called non-ergodic systems[16].

The addition of non-adsorbing polymer chains to a hard sphere colloidal system can induce an effective attraction, leading to different types of phase behavior. Therefore, this colloid-polymer system serves as an excellent model to understand the behavior in many complex fluids that are used in the industry. The range and magnitude of the attractive interaction can be controlled such that the mixtures may form non-equilibrium gels or a network of particles that essentially percolates across the sample volume to form a soft solid[17]. It is well-known that non-adsorbing polymer chains can induce depletion effects as a result of polymer chain exclusion from the volume between two colloidal particles. If the depletion attractions are large enough, the system might phase separate[18]. Cluster formation is known to be the driving force for a system to form a soft solid. It has been shown that as the system phase separates, clusters tend to form. Alternatively, the kinetics of particle diffusion might drive the particles to permanently adhere to its nearest neighbors thus resulting in cluster growth[19]. In this case, cluster growth continues until either the cluster completely spans the system or is large and dense enough to precipitate. However, experiments conducted by Peter Lu and co-workers on sterically stabilized PMMA spheres suspended in an organic solvent mixture showed stable clusters freely

diffusing in a phase that is very close to the gel transition[20]; in other words, a phase corresponding to a "liquid" of stable, freely diffusing clusters.

### 1.1.4 Re-entrant behavior in colloid-polymer mixtures

Figure 1.3 shows the state diagram of colloids as a function of attractive strength (represented by a dimensionless temperature) and volume fraction[21]. In the case where there is no attraction in the system, or where thermal fluctuations due to motions dominate, the system behaves more or less like a glass. However, as we keep increasing the strength of attraction, the particles begin to stick to each other to form attractive bonds with a certain lifetime. Under these conditions, the distribution of particles within the system becomes inhomogeneous, and spatial voids are generated as a result of which particles find it easier to explore nearby volumes. At this stage they behave like fluids, and particles diffuse more easily.

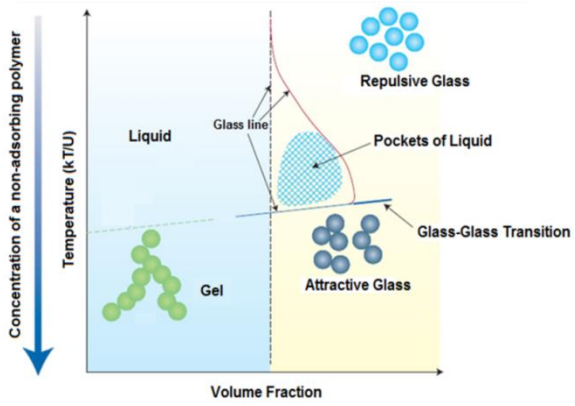


Figure 1.3 : The effect of change in the attractive strength on the phase behavior of colloids. The temperature here is the dimensionless temperature, normalized by the attractive interaction potential. This phase diagram has been adapted from Sciortino's review on disordered colloidal states[21].

However, as the attraction strength further increases, the system begins to slow down as the inter-particle attractive bonds become stronger. This state is generally known as an

attractive glass, although there is a lot of debate about whether the state is really a glass or a gel. The state diagram depicted above is a classic illustration of the re-entrant behavior where systems transition from glass to liquid and then back to another glassy state, at a fixed particle concentration. Recent studies however, have pointed out that there are some singularities within this transition line, where the dynamics are distinctly different from both the glassy states. There are very few experimental studies in the literature that actually confirm the existence of the singularities in the phase behavior. In any case, dynamics of systems near these glass-liquid and glass-glass transition lines still proves to be an interesting physical problem to consider.

Clay-polymer materials are known exhibit a similar type of phase/state diagram behavior, although at densities lower than when compared to a hard sphere colloidal system. The effective interactions become more complex when short-range attractions are coupled with long-range repulsions. In addition to this, the fact that these systems exhibit aging behavior (e.g., structures and properties that evolve very slowly over time) makes this a more challenging physical problem. Experimental results from our group have shown that re-entrant behavior does occur for clay particles with polymer chains[22]. However, unlike the glass-liquid-glass transition, they instead follow a glass-liquid-gel behavior. Studies have indicated that this behavior can further proceed (by further addition of chains) to a phase where they begin to gel instead of phase separating.

In spite of much study of re-entrant behavior in colloid-polymer systems, the behavior of clay particles with more concentrated polymer chains has not been observed so far. The primary motivation behind this work is to understand the role of significant polymer-polymer interactions and polymer-clay interactions on the phase behavior of

clay-polymer systems. Thus, we will investigate systems where polymer concentrations approach the semi-dilute regime.

### 1.2 Overview

The thesis is organized in the following manner. Chapter 2 discusses the phase behavior of laponite® and illustrates the effects of molecular weight and concentration of a weakly adsorbing polymer like poly(ethylene glycol) on its aging dynamics. Chapter 3 discusses the use of x-ray photon correlation spectroscopy to describe the particle-scale dynamics in colloid-polymer systems. Lastly, Chapter 4 discusses the microstructural changes occurring in different clay-polymer systems and its contribution to the formation of different arrested phases in this system.

### 1.3 References


1. Avery, R. G.; Ramsay, J. D. F., Colloidal Properties of Synthetic Hectorite Clay Dispersions. *J. Colloid Interface Sci.* **1986,** *109*, 448-454.

2. Tawari, S. L.; Koch, D. L.; Cohen, C., Electrical double-layer effects on the brownian diffusivity and aggregation rate of laponite clay particles. *Journal of Colloid and Interface Science* **2001,** *240* (1), 54-66.

3. C. Martin, F. Pignon, J.-M. Piau, A. Magnin, P. Lindner and B. Cabane, *Phys. Rev. E: Stat., Nonlinear, Soft Matter Phys.*, **2002**,66, 021401.

4. Balnois, E., Durand-Vidal, S., & Levitz, P., Probing the morphology of Laponite clay colloids by atomic force microscopy. *Langmuir*, **2003**, *19*(17), 6633-6637.

5. Mourchid, A.; Delville, A.; Levitz, P., Sol-gel transition of colloidal suspensions of anisotropic particles of laponite. *Faraday Discussions* **1995,** *101* (0), 275-285.

6. Mourchid, A.; Lecolier, E.; Van Damme, H.; Levitz, P., On Viscoelastic, Birefringent, and Swelling Properties of Laponite Clay Suspensions: Revisited Phase Diagram. *Langmuir* **1998,** *14*, 4718

7. Ruzicka, B.; Zaccarelli, E., A fresh look at the Laponite phase diagram. *Soft Matter* **2011,** *7* (4), 1268-1286.

8. Ruzicka, B., Zaccarelli, E., Zulian, L., Angelini, R., Sztucki, M., Moussaïd, A., Sciortino, F., Observation of empty liquids and equilibrium gels in a colloidal clay. *Nature materials*, **2011**. *10*(1), 56-60.

9. Ruzicka, B.; Zulian, L.; Ruocco, G., Routes to Gelation in a Clay Suspension. *Phys. Rev. Lett.* **2004,** *93*, 258301.

10. Jabbari-Farouji, S.; Tanaka, H.; Wegdam, G. H.; Bonn, D., Multiple nonergodic disordered states in Laponite suspensions: A phase diagram. *Physical Review E* **2008,** *78* (6), 061405.

11. Joshi, Y. M., Model for cage formation in colloidal suspension of laponite. *J. Chem. Phys.* **2007,** *127*, 081102.

12. Mongondry, P.; Tassin, J. F.; Nicolai, T., Revised state diagram of Laponite dispersions. *Journal of colloid and interface science* **2005,** *283* (2), 397-405.

13. Hansen, J. P., & McDonald, I. R., *Theory of Simple Liquids: With Applications to Soft Matter*. Academic Press.

14. Pusey, P. N., van Megen, W., Underwood, S. M., Bartlett, P., & Ottewill, R. H., Colloidal fluids, crystals and glasses. *Journal of Physics: Condensed Matter*, **1990**, *2*(S), SA373.

15. Sciortino, F.; Tartaglia, P.; Zaccarelli, E., One Dimensional Cluster Growth and Branching Gels in Colloidal Systems with Short-Range Depletion Attractive and Screened Electrostatic Repulsion. *J. Phys. Chem. B* **2005,** *109*, 21942.

16. Pusey, P.; Van Megen, W., Dynamic light scattering by non-ergodic media. *Physica A: Statistical Mechanics and its Applications* **1989,** *157* (2), 705-741.

17. Segre, P. N., Prasad, V., Schofield, A. B., & Weitz, D. A., Glasslike kinetic arrest at the colloidal-gelation transition. *Physical Review Letters*, **2001**, *86*(26), 6042.

18. Sciortino, F.; Mossa, S.; Zaccarelli, E.; Tartaglia, P., Equilibrium cluster phases and low-density arrested disordered states: the role of short-range attraction and long-range repulsion. *Physical review letters* **2004,** *93* (5), 055701.

19. Meakin, P., Formation of fractal clusters and networks by irreversible diffusion-limited aggregation. *Physical Review Letters* **1983,** *51* (13), 1119.

20. Lu, P. J.; Conrad, J. C.; Wyss, H. M.; Schofield, A. B.; Weitz, D. A., Fluids of Clusters in Attractive Colloids. *Phys. Rev. Lett.* **2006,** *96*, 028306.

21. Sciortino, F., Disordered materials: One liquid, two glasses. *Nature materials* **2002,** *1* (3), 145-146.

22. Baghdadi, H. A.; Parrella, J.; Bhatia, S. R., Long-term aging effects on the rheology of neat laponite and laponite-PEO dispersions. *Rheologica Acta* **2008,** *47* (3), 349-357.

# CHAPTER 2

# THE EFFECT OF PARTICLE-SCALE DYNAMICS ON THE MACROSCOPIC PROPERTIES OF DISK-SHAPED COLLOID-POLYMER SYSTEMS

## 2.1 Introduction

Colloid-polymer mixtures are of interest for a range of conventional and emerging industrial applications. In recent years, the use of anisotropic colloids has gained attention, as their geometry facilitates tunable phase behavior and properties, oftentimes at lower particle volume fractions than in spherical colloids. Mixtures containing natural/synthetic clays with polymers are one amongst the many suspensions that are frequently used in industries that manufacture paints, cosmetics, food, and so on[1]. However, maintaining the stability of these mixtures still remains an industrial challenge, and the conditions under which they are manipulated and processed have a strong bearing on the effective interactions in the system. Therefore, it is critical to understand the rheological features arising from the complex interactions between the nanoparticles and polymers.

Laponite® RD is a charged disk-shaped synthetic clay which is often used as a model to understand interactions within an anisotropic colloid-polymer system. This 25 nm wide, 1 nm thick disk has a negatively-charged face and an edge whose charge depends on the pH of the dispersing medium. Under more basic conditions, the edge is primarily negative, and when the pH is <9 the edge develops a small positive charge[2]. Aqueous dispersions of laponite® exhibit a time-dependent phase behavior that is highly sensitive to conditions like pH, temperature, ion/particle concentration and the presence of other

macromolecules in the system. These experimental conditions are known to change the interactions between particles in a way that leads to the formation of different arrested states like gels and glasses[3,4] yet the formation of these states and their physical behavior is not understood well.

The pH of the medium in which these particles are suspended plays a vital role in influencing particle interactions, and in turn their relevance in applications across different fields. At pH values below 9, the edges are positive and the particles form a house-of-cards structure as a result of face-rim attractions. This structure is widely exploited in the bioengineering field as they shear thin and self-assemble to form structures in aqueous media[5]. Recent experiments have shown that polymer hydrogels containing laponite® also show enhanced mechanical properties when immersed in phosphate buffer saline (PBS), which is often used in studies involving cell growth[6]. Studies have also shown that the particles are compatible with stem cells and various animal cell lines[7,8] and laponite®-based systems have been explored as vehicles for drug delivery[9]. At pH > 9 and at very low ionic strengths, the interactions between particles are largely repulsive. The electrostatic repulsions in the system primarily dominate, and the system slowly evolves to form a repulsive glassy phase with structural and dynamic heterogeneities present across length scales[10]. However, in a more recent and detailed study conducted by Ruzicka and co-workers, it was observed that the systems that exist as repulsive glasses at early waiting times undergo a glass-glass transition to behave like an attractive glass at longer time scales[11]. Upon increasing the ionic strength by adding salts, the electrostatic screening by the counter ion cloud changes the kinetics of aggregation, and this has a direct influence on the aging behavior of the system[12-15].

Besides salt/ion effects, polymer chains can alter the structure and macroscopic properties of a colloidal dispersion. A number of rich state transitions have been observed both through experiments and theoretical studies for dispersions containing either adsorbing or non-adsorbing polymers[16,17,18]. For polymer chains that adsorb onto surfaces of colloids, steric and bridging effects play an important role in deciding the effective interaction between particles, and this in turn influences the aging behavior of the system. However, the transitions in behavior will depend on fundamental polymer chain characteristics like chain length, concentration, and the nature of the polymer itself. PEO is a weakly adsorbing, neutral, hydrophilic homopolymer that is often used as a simple model polymer to observe colloidal behavior. The extent of adsorption of PEO on a surface depends not only on its length but also on the way chains arrange themselves on a surface. The chains assume a loop, train and tail configuration on a particle surface, as the adsorption of a polymer segment on one site dictates the steric configuration of the segment next to it. Numerical experiments on spherical particles with weakly interacting polymers have shown that for long polymer chains the fraction of tails is greater when compared to smaller chains which predominantly form loops with multiple contacts close to the surface[19]. NMR, dynamic light scattering (DLS) and small angle neutron scattering (SANS) studies conducted by Cosgrove and co-workers on dilute solutions of laponite® and PEO (20-986 kDa) reveal that the adsorbed polymer chains have a flat conformation with a thickness that agrees with the Scheutjens-Fleer theory[20,21]. This observation was found to be in agreement with the first SANS study conducted by Lal and co-workers[22,23]. They also observed that the thickness along the edge had a weak dependence on the

molecular weight of PEO, which suggests that the chains begin to wrap around the edge and trail along the opposite face or extend in solution.

The presence of a weakly adsorbing chain like PEO in a colloidal suspension can either slow down or speed up the aging process of the system, and this typically depends on the chain length of the polymer. The impact of chain length on the kinetics of this aging behavior has been investigated by several groups. In an experimental work conducted by Baghdadi and co-workers, the rheological behavior of laponite®-PEO dispersions with PEO at two concentrations 1% and 2% and at different molecular weights ($M_w$: 13-700 kg $mol^{-1}$) was observed over a period of time[24]. In this study, two distinct features were observed: (1) retardation of aging behavior for PEO < 83 kg $mol^{-1}$ as a result of steric effects and (2) faster aging behavior for PEO > 83 kg $mol^{-1}$ due to polymer bridging effects. Concurrently, in another study by De Lisi and co-workers, techniques like SANS and viscometry were used to understand the behavior of laponite® with a range of low molecular weight PEO ($M_w$ = 0.2-35 kg $mol^{-1}$) at a concentration of 2.2%[25]. Their SANS results indicate an attractive interaction in the system which increases with increasing laponite® concentrations. The results also suggest that the gelation kinetics speed up for the low molecular weight case but this effect is reversed for chains larger than 1 kg $mol^{-1}$. Similar observations were also made in a study by Mongondry and co-workers where the aggregation kinetics of dilute laponite® dispersions with dilute concentrations of pyrophosphate and poly(ethylene oxide) was tracked using light scattering[26]. Though the qualitative observations may seem different, they bring out the importance of how different polymer and laponite® concentrations could possibly influence the competing interactions between particles in the system.

There are studies which discuss the effects of concentration on the bulk and microstructural behavior of laponite® with both high and low molecular weight PEO. The addition of a high molecular weight PEO results in the formation of a gel-like network predominantly due to polymer-particle bridging. This behavior was first observed by Schmidt's group who conducted a systematic study on the microstructure of systems with PEO at molecular weights greater than 1000 kg $mol^{-1}$ [27]. Shake gels were later observed within a narrow range of concentrations, at molecular weights between 200 and 600 kg $mol^{-1}$, and this state was attributed to bridging which was a consequence of partial saturation of a laponite® surface[28]. A qualitative state diagram was later proposed by Okay and co-workers to define this shake gel region[29]. A dual aging behavior in a laponite® suspension with 100 and 200 kg $mol^{-1}$ was recently proposed by Ruzicka and group[30]. In this experimental work, the group investigated the aging dynamics of dispersions at a fixed laponite® concentration of 2% and varied the concentration of PEO between 0.05 and 0.5%. Fast and slow aging dynamics were observed and the existence of a critical concentration (at 0.38%) marked the transition between the two physical features.

The behavior of laponite® with shorter polymer chains is rather difficult to understand, as the polymers contribute to a variety of interactions depending upon their concentration and molecular weight. In a recent work by Tong and co-workers, a universal scaling was established to understand the dynamic response of suspensions containing laponite® and different concentrations of 35 kg $mol^{-1}$ PEO (0.1%–1%)[31]. Interestingly, the results suggest that irrespective of the concentration of polymer in the suspension, the systems still followed the universal route of aging as seen in a clay

suspension with no polymer added to it. Morariu and co-workers studied the effects of varying concentrations of a 10 kg $mol^{-1}$ PEO on the rheology and electrokinetic features of dilute laponite® solutions at 1% [32]. They also examined the temperature dependence of the aggregation kinetics for a 2% laponite® dispersion with different concentrations of 35 kg $mol^{-1}$ PEO[33]. Through oscillatory and steady flow measurements, they observed that the gelation kinetics increased not only with temperatures above 30°C but also with increasing clay concentration.

In a recent work from our group, we looked at the dynamics and rheological behavior of laponite® at a fixed concentration of 2% with a 20 kg $mol^{-1}$ PEO at concentrations varying between 0.25% and 2%. The aging behavior of these suspensions was observed for a period of 90 days. We have shown that the addition of polymers retards the aging behavior of the clay system, and as samples age, they all transition to an arrested state with a time scale that depends on the concentration of the polymer. Qualitative state diagrams were proposed to show the effects of concentration, molecular weight and aging time on the dynamics of the system.

Even with a number of previous studies on laponite®-PEO systems, we still lack a complete understanding of the dynamics in the system, and several observations that have been reported are still being debated. This may be due to the different approaches and sample preparation protocols taken by several groups to answer a specific physical problem. In addition to this, the main focus in the research community has often been on studying laponite® systems with or without high molecular weight PEO. There are very few systematic studies that focus on laponite® with short PEO chains with concentrations spanning all the way from a very dilute regime to the semi-dilute region, where polymer-

polymer interactions begin to matter in addition to the existing polymer-particle and particle-particle interactions.

In this chapter, we report the behavior of mixtures containing laponite® and PEO with a constant particle concentration of 2%. Three sets of dispersions were prepared by varying the concentrations of 35,000 g/mol (35K), 20,000 g/mol (20K) and 4,600 g/mol (4K) PEO from the dilute to the semi-dilute regime. Our study shows different transitions in behavior as the polymer concentrations are increased. Irrespective of the molecular weight, the addition of polymer was found to hinder the dynamics as compared to the neat laponite® system, similar to the re-entrant behavior previously observed. However, as the polymer concentration approaches the semi-dilute regime, the dynamics display an interesting second minima, beyond which the dynamics in the system again slow down.

**2.2 Materials and Methods**

Laponite® RD was procured from Southern Clay Products (Gonzales, TX, USA) and poly (ethylene) oxide (PEO) with number-average molecular weight, $M_n$, of 4.6, 20, 35 kg $mol^{-1}$ were purchased from Sigma Aldrich and used without any further purification. The polydispersity index of the polymers were estimated using GPC and were found to be close to 1.1. Table 2.1 lists the intrinsic viscosity ($[\eta]$), radius of gyration ($R_g$) and overlap concentrations ($c^*$) of the polymers used in this experiment. Laponite® dispersions were first prepared by adding a calculated amount of clay to de-ionized water at pH 10. A T25 UltraTurrax homogenizer was used for about 1 minute to disperse particles thoroughly. The solutions were then agitated for 20 minutes and filtered through a 0.45μm filter to remove large aggregates. PEO was then added to obtain the desired concentration. The samples were stirred until the polymer completely dissolved. For

dynamic light scattering experiments, a required amount of the suspension was transferred to a sample holder and then capped. This avoids any shear generated by removing DLS samples from a stock solution via pipetting. Samples for rheology were transferred from a stock solution to the rheometer at prescribed time points using a scoop, rather than pipetting, again to avoid excessive shear on the sample prior to measurement. The samples for both rheology and dynamic light scattering were then sealed and stored at 25°C to allow them to spontaneously age with time, and the aging time is measured from the time $t_0$ when the samples are initially sealed and stored.

Table 2.1 : Physical characteristics of the PEO chains used in this study

| $M_n$ (kDa) | $[\eta]$[a] $*10^2$ ml/g | $R_g$[b] (nm) | Mean end-to-end distance[c] (nm) | Hydrodynamic Radius[d] (nm) | $c^*$[e] (%) | Adsorbed amount $\Gamma$(mg/m$^2$)[f] | Particle-Surface Saturation $c_{sat}$ (%) |
|---|---|---|---|---|---|---|---|
| 4.6 | 3.08 | 2.84 | 7.31 | 1.82 | 8.74 | 0.14 | 0.25 |
| 20 | 35.3 ±4.5 | 6.67 | 17.15 | 4.27 | 2.93 | 0.55 | 0.99 |
| 35 | 51.4 ±6.9 | 9.22 | 23.73 | 5.90 | 1.94 | 0.59 | 1.06 |

[a]Intrinsic viscosity $[\eta] = 4.33 \times 10^{-4} * M_w^{0.67\pm0.009}$ (dl/g); Mark-Houwink-Sakurada equation for PEO with $M_w$ greater than 6000 g/mol in water at 25°C; for PEO $M_w$< 6000 g/mol the exponent in the MHS equation is 0.50 [34]

[b]Radius of gyration calculated from the *z*-averaged mean squared radius[35], $R_g = \langle S_2 \rangle_z^{1/2}$ and $\langle S_2 \rangle_z = 4.08 \times 10^{-4} * M_w^{1.16}$ [34]

[c]Mean end-to-end distance ~ $(R_g * 6^{1/2})/ 0.952$ for a good solvent

[d]Hydrodynamic radius $R_h = 0.640\ R_g$

[e] Overlap concentration, $c^* = 3M_w/4\pi N_A \langle S_2 \rangle_z^{3/2}$

[f]The adsorbed amount of PEO estimated from SANS experiment, as measured by Nelson and Cosgrove for systems containing 0.5%(w/v) laponite® and 0.35%(w/v) PEO[20]

### 2.2.1 Rheological Characterization

Laponite®-PEO systems were characterized using a TA Instruments AR-G2 controlled stress rheometer with a 40 mm 2° cone and Peltier plate temperature control system. The experiments were conducted at 25°C and the fluctuations in the temperature

were found to be ±0.009°C. A solvent trap was used to prevent any sample evaporation and to maintain a good temperature control in the sample environment. Prior to the start of an experiment all samples were allowed to equilibrate for 15-20 minutes, to allow any loading induced microstructural perturbations to relax. Oscillatory stress sweeps were conducted at 1 Hz to determine the linear viscoelastic (LVE) region. Using a suitable amplitude within the bounds of the LVE region, frequency sweep tests were conducted to determine material response. The variations in the viscoelastic response between replicates were within 5% and this small variance is expected as the starting suspensions are homogeneous and they age uniformly throughout its sample volume.

### 2.2.2 Dynamic Light Scattering

Dynamic light scattering experiments were performed with a 488 nm wavelength, 200mW Coherent Ar-ion laser and a BI-9000AT Brookhaven Instruments correlator. The intensity fluctuations were collected at a scattering angle of 90° and the systems were sampled for 30 seconds with a delay time window between 0.025μs and $10^7$μs. Samples were measured several times, with a slight rotation after each run since each rotation samples a different position or volume in the sample space. The autocorrelation function, $g_2(\tau)$ is calculated by averaging the values of $g_2(\tau)$ over the 10-25 number of runs at each delay time[36]. The non-negative least square (NNLS) analysis was used to obtain size distributions for each sample.

## 2.3 Results and Discussion

Both the macroscopic properties and the microstructure of laponite® and the colloid-polymer mixture have been found to evolve with time, suggesting that the non-equilibrium system may contain particles that undergo spatial rearrangements in this

state. Results from previous experiments on this system, however, have shown that the dynamics slow down at longer aging times[37,38] indicating that the system may have entered a pseudo-equilibrium state where rearrangements are minimal or infrequent. Hence this study will focus primarily on the early aging behavior (e.g., 0-30 days after preparation) where particle scale dynamics can still be understood within the time scales of observation. We report variations in the viscoelastic moduli $G'$ and $G''$ in the discussion that will follow; additional rheological data on tan delta (tan $\delta$) and complex viscosity ($\eta^*$) are in the Appendix (Figures A1-A5; Appendix A). The average relaxation times obtained from rheology are estimated from the frequency at which $G'(\omega)$ is equal to $G''(\omega)$, and the calculated values are listed in Table A1 provided in the Appendix.

Figures 2.1-2.3 show the variation in the viscoelastic moduli, $G'$ and $G''$, with changes in polymer concentration, $c_p$, for samples with 35K, 20K and 4K PEO, respectively. After an aging time of 21 days, mixtures with low polymer concentrations behave rheologically as soft solids, with an storage modulus $G'$ that exhibits a weak dependence on the values of frequencies explored in this study, while the loss modulus $G''$ exhibits a shallow minimum that can be well described within the framework of the mode coupling theory (MCT) for soft glassy systems[39]. As shown in Figure 2.1, for the 35K PEO, $G'$ gradually decreases as $c_p$ increases, and at a polymer concentration of 0.5% the viscoelastic moduli begin to show large frequency dependence. The sample at this concentration behaves like a viscoelastic fluid with a distinct crossover at ca. 0.06Hz. Upon further increasing $c_p$, the dependence of $G'$ on $c_p$ is non-monotonic. The magnitude of $G'$ initially increases for polymer concentrations up to 0.75%, but beyond this concentration we observe a steady decrease in $G'$ up to a concentration of 1.5%. At this

concentration, the system exhibits an elasticity that is much weaker than what is observed at 0.5%. The crossover of $G'$ and $G''$ now shifts to a higher frequency ($10^0$ – $10^1$ Hz). At concentrations higher than 1.5%, the system regains elasticity and reverts back to a soft solid behavior and the viscoelastic moduli show reduced frequency dependence in this region. At the highest polymer concentration considered in this study, the storage modulus is comparable to the sample at the lowest polymer concentration (0.25%), and the minimum in $G''$ shifts to a higher frequency.

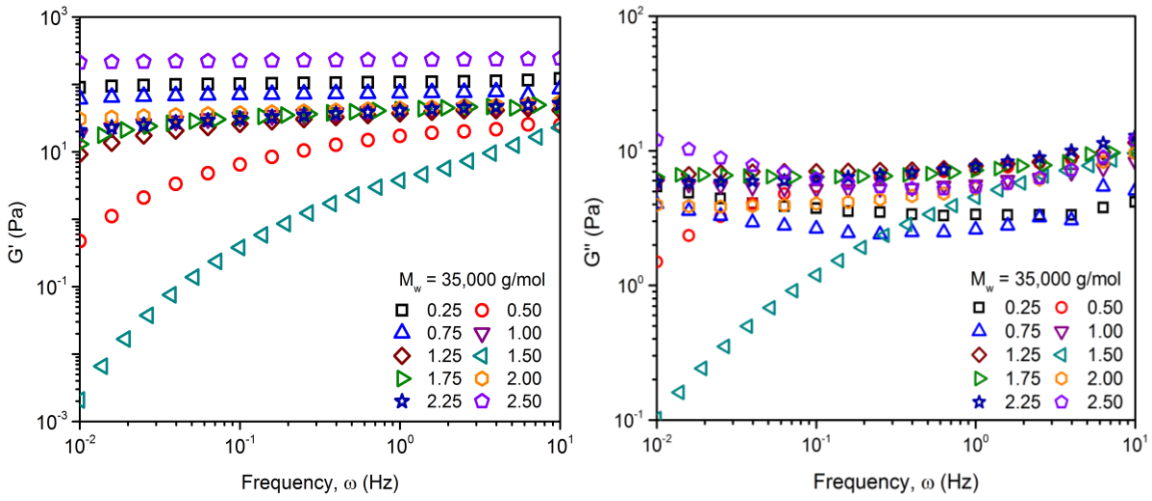


Figure 2.1 : Frequency dependence of the viscoelastic moduli at different polymer concentrations of 35K PEO, (a) $G'$, and (b) $G''$. Legends represent $c_p$ in % (w/w). All samples were tested after an aging time of 21 days.

To understand how the qualitative trends vary for different polymer chain lengths, we examined suspensions having the same particle-polymer compositions but with a shorter chain instead. In the case of the 20K PEO (Figure 2.2), both $G'$ and $G''$ begin to exhibit a gradually increasing frequency dependence for concentrations up to 1%. The crossover that was observed at the lowest frequency for the 0.5% 20K PEO mixture now

shifts to a higher frequency as concentrations go up to 1.0%, indicating that the suspension is more liquid like at this concentration. As the polymer concentration is increased further, the magnitude of $G'$ gradually rises and the system exhibits a weak solid/gel like behavior until $c_p$ reaches 1.75%. At higher concentrations the elasticity drops at 2.25%, before we observe a viscoelastic behavior again at 2.5%. The second transition around 2.25% is similar to what was observed in the 35K PEO system.

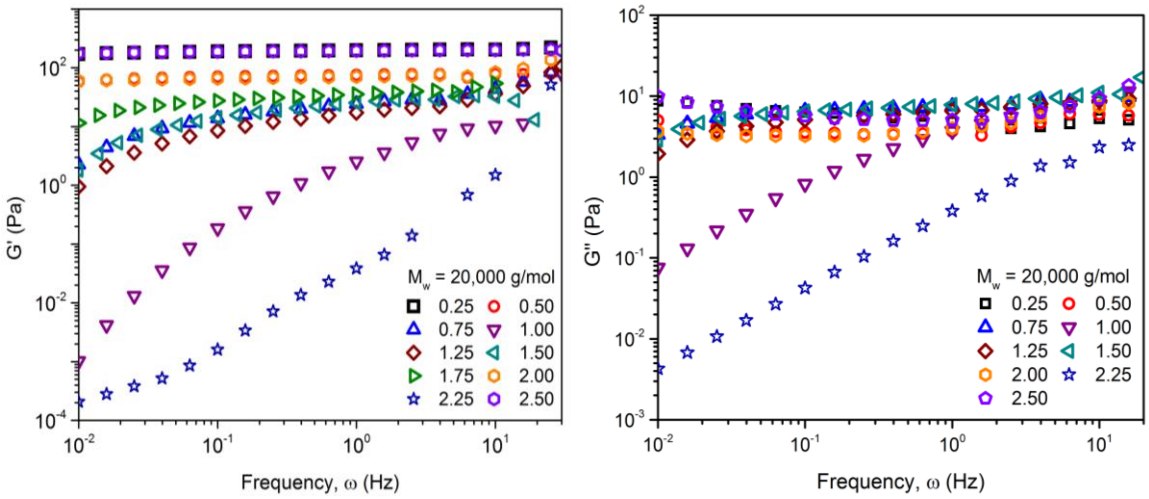


Figure 2.2 : Frequency dependence of the viscoelastic moduli at different polymer concentrations of 20K PEO, (a) $G'$ and (b) $G''$. Legends represent $c_p$ in % (w/w). All samples were tested after an aging time of 21 days.

The transitions in the rheological behavior with $c_p$ that occur for dispersions with the 20K and the 35K PEO seem to qualitatively follow similar trends. However, we do see some variation in the trends for very short 4K PEO chains (Figure 2.3). In this case, $G'$ decreases with the addition of a small number of chains to the system, but increases for polymer concentrations between 0.25% and 0.75%. However, the variation in $G'$ is more non-uniform along intermediate polymer concentrations, and beyond 1.75% we observe a steady decrease in $G'$ until $c_p$ reaches 2.25%. Interestingly, even with the 4K PEO we see

that $G'$ at the highest polymer concentration is comparable to those systems with a small number of chains.

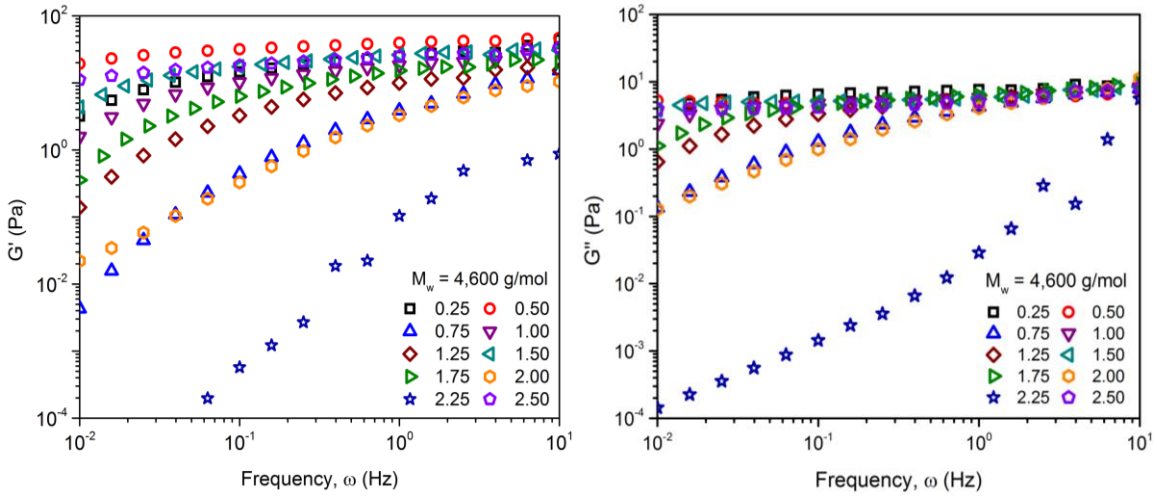


Figure 2.3 : Frequency dependence of the viscoelastic moduli at different polymer concentrations of 4K PEO, (a) $G'$ and (b) $G''$. Legends represent $c_p$ in % (w/w). All samples were tested after an aging time of 21 days.

The behavior of laponite® in the presence of a weakly adsorbing polymer like PEO typically depends on three physical conditions: (i) the polymer chain length, (ii) the extent of particle surface coverage as a result of polymer chain adsorption and (iii) the free polymer chain density in the medium. As alluded to above, we are mainly interested in (iii), and exploring variations in the behavior for systems with PEO concentrations transitioning into the semi-dilute region. In order to understand the effects that these parameters have on the macroscopic features, we look at the variations in $G'$ with $c_p$ scaled with the overlap concentration ($c^*$) of each PEO molecular weight in order to gain some insight into the behavior of the polymer chains in the bulk medium. Figure 2.4(a-c) shows the plots of $G'$ for each PEO chain length at four different frequencies, 0.01, 0.1, 1 and 10 Hz, as a function of the scaled polymer concentration ($c_p/c^*$). The variations in $G'$

with polymer concentration are more apparent at the lowest frequency of 0.01Hz than when compared to the trends at higher frequencies. In each case, we see that the storage modulus reaches a critical minimum at two different concentrations. We will henceforth refer to the 1st and 2nd minima as $c_{p,min1}$ and $c_{p,min2}$, and their corresponding storage moduli as $G'_{min1}$ and $G'_{min2}$, respectively.

After an aging time of 21 days, the $G'$ of laponite® in the absence of PEO is approximately 150 Pa (Figure A1), as neat laponite® dispersions evolve slowly with time to form a dense repulsive colloidal glass. As depicted in Figure 2.4, with the addition of a small number of polymer chains to the system, we see that $G'$ decreases as chains begin to adsorb onto any particle surface that is accessible. When the chains continue to saturate the surfaces available, the elasticity decreases gradually as the repulsive glass begins to melt and reaches the first critical minimum, $c_{p,min1}$. Within this phase space, the effect of polymer adsorption on the rheological properties is quite significant. The adsorption of polymer chains is largely dependent on the on the spatial arrangement of particles in the mixture; at a particle concentration of 2wt% and a pH of 10, the distribution at early aging times is largely bimodal with populations of both individual platelets and small clusters of particles, about 100-200 nm in size, in solution (Figure A6). Thus, the faces of particles that are within clusters might be inaccessible to PEO chains so complete adsorption as seen in the case of dilute laponite®-PEO solutions is unlikely. In this region, the magnitude of $G'$ for the 35K PEO system decreases by two orders of magnitude to reach its first minimum at $c_p/c^* \sim 0.25$ (Figure 2.4a). For the smaller 20K chain, the first minimum occurs at a higher concentration of $c_p/c^* \sim 0.4$, and $G'_{min1}$ is about $10^{-3}$ Pa (Figure 2.4b). The storage modulus of the 4K PEO in this region

does not show a distinct decrease like the 20K and the 35K PEO. It is rather interesting to note that the elasticity at $c_{p,min1}$ for the 4K system at this aging time is greater than both the 20K and 35K PEO; that is, $G'_{min1}$(4K) > $G'_{min1}$(35K) > $G'_{min1}$(20K). This is in accord with the observations made from an aging study on laponite® with different molecular weights of PEO by Baghdadi and co-workers, although the mixtures that were analyzed in that study had a higher PEO content of 1% and 2% [40].

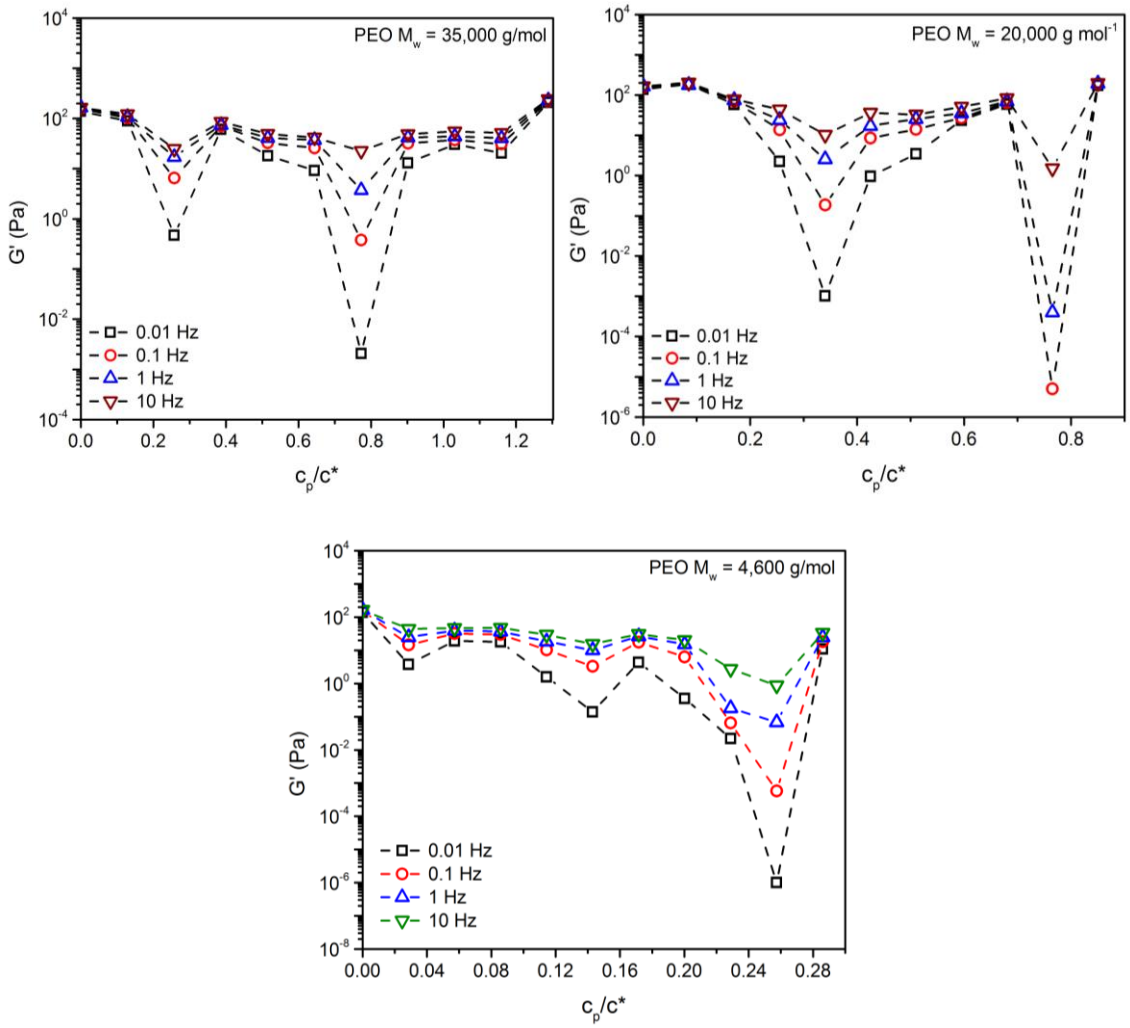


Figure 2.4 : The storage modulus $G'$ at four frequencies plotted as a function of the scaled polymer concentration, ($c_p/c^*$). (a) 35K PEO; $c^*$ = 1.94% (top) (b) 20K PEO; $c^*$ = 2.93% (center) (c) 4K PEO; $c^*$=8.74% (bottom).

As mentioned earlier, the saturation of surfaces depends on the arrangement of particles in the solution. In the SANS experiment conducted by Cosgrove et. al, dilute laponite® solutions ($c$ = 0.5%) were used to estimate the amount of PEO adsorbed on laponite® and it was inferred that the number of chains required to saturate an area on the surface decreases asymptotically with molecular weight of PEO. Using dilute systems eliminates not only any clustering that might take place as particle concentration is increased but also ensures that polymer chains have the access to all adsorption sites on a colloidal surface. With the same assumption that all particle surfaces are exposed to these polymer chains even in a 2% laponite® solution, we estimate the saturation concentration for each PEO chain and report them in Table 2.1[20]. The differences between the estimated values and the first minima, $c_{p,min1}$, observed through rheology can be attributed to the fact that in these concentrated suspensions not all surface sites are exposed to the polymers and free polymer chains present in the solution are bound to play a role in addition to the steric effects coming from chains that are adsorbed on surfaces. Increasing the concentration of polymers beyond the first minimum will only increase the number density of free polymers in the medium.

At concentrations above $c_{p,min1}$, samples display an increase in the elastic strength. In this region, as the number of free chains increase in the medium, attractive inter-particle and particle-cluster interactions are also expected to increase because the free chains contribute to a weak local depletion attraction. Because chain lengths are different in each case, the re-arrangement of particles as chains begin to adsorb or cover surfaces would be different, so this may potentially force samples to take different dynamic pathways that eventually lead to similar final states. This qualitative feature of a glassy system melting

and reforming into a solid has been observed in a previous work on laponite® with PEO of an intermediate molecular weight of 20 kg/mol[41], in laponite® with DNA strands[42] and also with sterically stabilized PMMA spheres in a polystyrene medium[43]. In all the experimental studies mentioned above, this transition was found to occur in a polydisperse particle system suspended in a dilute polymer medium where the scaled concentrations ($c_p/c^*$) were below 1. Additionally, since the polymer is dilute in this region ($c_p/c^* << 0.5$) polymer-polymer interactions are minimal in the bulk, and any free chains that may be present in the medium behave as swollen coils in a good solvent.

At polymer concentrations beyond this re-entrant phase, one may expect the elasticity to increase further due to increasing interparticle attractions, eventually leading to a macroscopic phase separation. This feature is commonly observed in hard sphere colloids with non-adsorbing polymers where the strength of depletion attractions scales with the concentration of the polymer. However, in the current study, we see that at higher $c_p$ the elasticity decreases to reach the 2nd minimum, $G'_{min2}$ at $c_{p,min2}$ but no macrophase separation is observed. For intermediate chain lengths (Figure 2.4a and 2.4b), this critical concentration lies somewhere between $c_p/c^* \sim 0.8$-$0.9$. For the series of systems containing the 4K polymer (Figure 2.4c), this transition interestingly occurs at $c_p/c^* \sim 0.3$, which is within the dilute polymer solution regime. Additionally, we also observe that the samples at $G'_{min2}$ are approx. 3 to 4 times weaker than those samples at $G'_{min1}$. To understand why we see such a remarkable difference, we look at how the polymer chains behave at the higher polymer concentrations.

In the case of the 4K polymer chain, the hydrodynamic radius is ca. 1.72 nm, and its equivalent spherical volume is very small when compared to the effective volume of

either an isolated laponite® platelet or a cluster of particles. Hence, polymer-polymer interactions do not contribute to the change in elasticity in the range of concentrations considered for the 4K PEO series. On the other hand, since the chains are small they may be more easily able to intercalate through stacks or weak clusters of laponite®. If intercalation does take place, then more chains have the opportunity to adsorb onto surfaces, thereby increasing inter-particle and inter-cluster repulsions. Given this, the distinct decrease in the storage modulus with increasing 4K chain number in the concentration region $0.08 < c_p/c^* < 0.32$ is reasonable. By contrast, for both the 35K and the 20K series, the 2nd critical concentration is close to $c^*$, the concentration where polymers begin to overlap and feel each other.

For the 20K and 35K systems, why do these transitions in the rheology occur close to, but not precisely, at $c_{sat}$ and $c^*$? To better understand the system dynamics in different regimes of polymer concentration, we consider the effect that the experimental conditions can have on the chain conformation. (1) ***The polymer chains are suspended in a medium whose volume is also shared by solid particles; therefore, the effective overlap concentration ($c_{eff}^*$) will not be equivalent to the actual overlap concentration ($c^*$) of PEO***. If the total volume of the medium is $V$ then the number density of chains would be $\upsilon$ $m^{-3}$ when the polymer is present as a single component in a mixture. In this case it would take $n^*$ chains to get to the corresponding overlap concentration, $c^*$. When the same medium has impenetrable solids that occupy volume $V_c$, the polymer chains are forced to occupy only the free volume, $V - V_c$. As a rough approximation, if we were to accommodate the same number of chains $n^*$, the overlap concentration will now be lower than the actual $c^*$, and this difference, $c^* - c_{eff}^*$ will vary with the fraction of solids in the

medium. Since PEO adsorbs onto surfaces, the effective $c^*$ will still be below the actual $c^*$, but the deviation will not be as large as in the case when all the chains are present only within the free volume that is available. (2) ***The polymer chains are suspended in a medium at a pH of 10 which may result in some aggregation or swelling of chains***[44]. Behavior of PEO in water depends on how the interactions are balanced amongst itself and the hydrogen bonds in water. Several experimental studies have been conducted to understand behavior of PEO in aqueous media,[45,46] although there is still considerable debate on the interpretation of these observations. Additionally, the chain conformation depends on the chain length of the polymer; for instance, for 100K PEO in water at pH 10, large aggregates were visually observed at concentrations above 1%. Hence, it is important to consider the notion that the chains may be present as collapsed coils or aggregates in solution along with the particles, which may also cause the actual overlap concentration to be different than what we estimate from literature. (3) ***Laponite®-PEO mixtures are known to age with time, and particle-polymer rearrangements take place more frequently during the early aging regime.*** With respect to the macroscopic behavior that we see at scaled concentrations between 0.4 and 1.4, we believe that the transition around $c_{p,min2}$ can be attributed to the physical phenomena we describe above. At the early aging times considered, we know that the samples contain both individual particles and clusters that are covered with polymer chains, and the manner in which these interact with each other changes as spatial rearrangements take place. As clusters grow and break with time, the number of chains that adsorb onto the surfaces that are created keeps varying; therefore, the sample volume right next to the adsorbed polymer layers remains depleted of polymer chains. This depleted region potentially would lead to

a weak attraction between particles, which is consistent with the increase in the elasticity for concentrations just above $c_{p,min1}$. However, as we keep increasing the chain number, the concentration of free polymers increases in the medium, and at a certain concentration it is in equilibrium with the concentration of the polymer that is adsorbed on the particle surfaces. At this point, the free polymers that are located close to adsorbed layer interface begin to interact with each other, thus forcing the system to stabilize in order to bring it to the nearest stable non-equilibrium state. This particular behavior where systems re-stabilize at high polymer concentrations has been previously observed experimentally in systems containing dextran and erythrocytes[47], gold nanoparticles with PEO[48], and theories have been proposed by several groups[49,50,51]. Although depletion induced attraction and re-stabilization in the systems mentioned above are found to occur at $c^*$ and $c^{**}$ respectively, the fact that the interactions between particles are anisotropic and that the laponite®-PEO mixtures are aging systems, makes this behavior a little more complex to understand.

The magnitude of the storage modulus increases with time for all the particle-polymer mixtures considered in this study. As an example of this aging phenomenon, we plot the storage modulus at 1Hz for an aging time of 21 and 30 days (Figure 2.5). At an aging time of 30 days, we observe that along the concentrations falling within the region around the 1st transition, the samples now behave as solids/gels with the samples at $c_{p,min1}$ exhibiting a weaker elastic behavior when compared to other mixtures in the same series. On the other hand, for samples along the 2nd transition the samples at $c_{p,min2}$, especially in the case of the 20K and the 4K PEO, still behave as viscoelastic fluids but with a slightly higher elastic response. The behavior suggests that for very small chain lengths, the

mixtures that re-stabilize at higher concentrations age very slowly. We believe that this mixture contains clusters that remain stable in solution over a relatively longer time. Such mixtures containing long living clusters have been observed in a previous work on laponite®-PEO by Baghdadi and co-workers. In this particular study, suspensions containing 2% laponite® and 2% of an intermediate molecular weight PEO still behaved as viscoelastic fluids even at a longer aging time of 80 days[40,52].

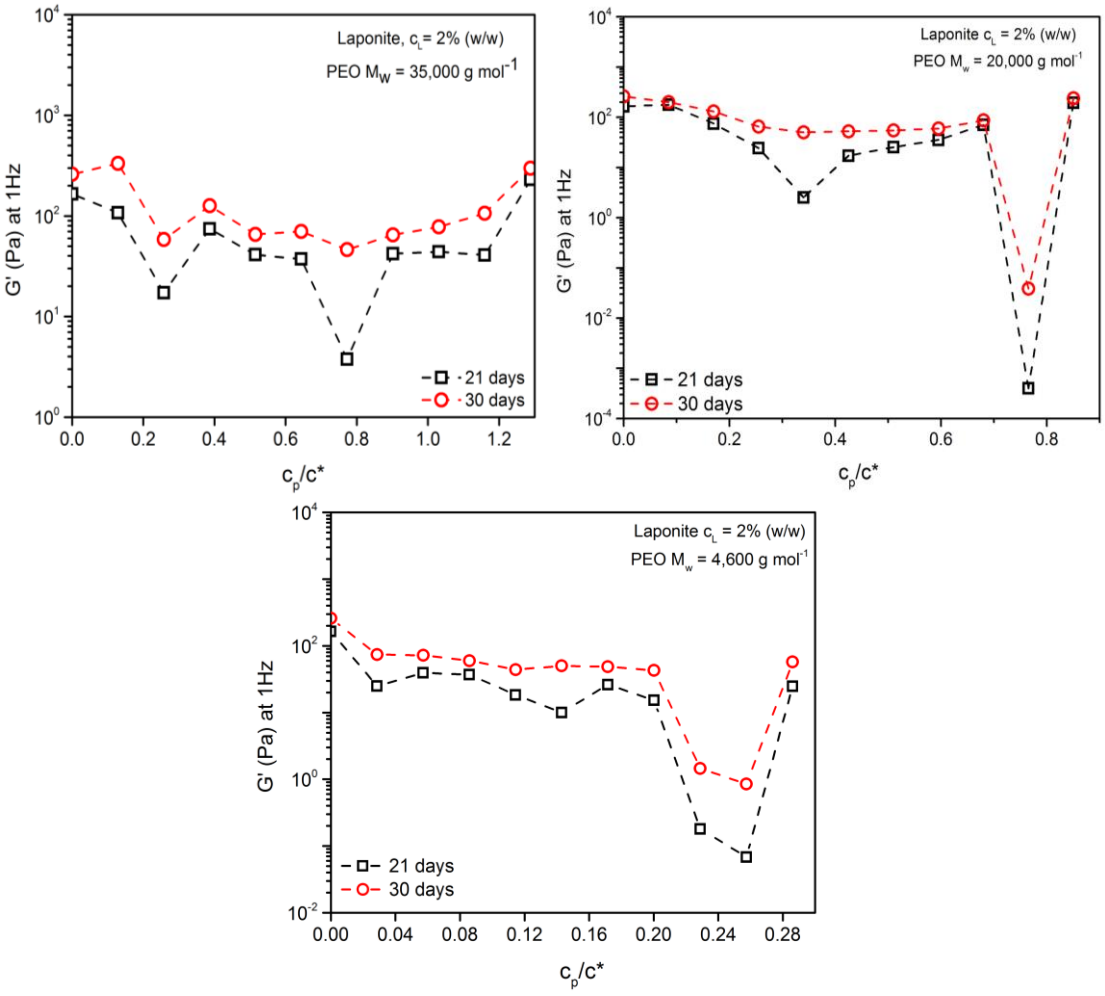


Figure 2.5 : Storage modulus *G'* at 1 Hz versus the scaled polymer concentration ($c_p/c^*$) at an aging time of 21 days (black squares) and 30 days (red circles). (a) 35K PEO; $c^*$ = 1.94% (top) (b) 20K PEO; $c^*$ = 2.93% (center) (c) 4K PEO; $c^*$ = 8.74% (bottom).

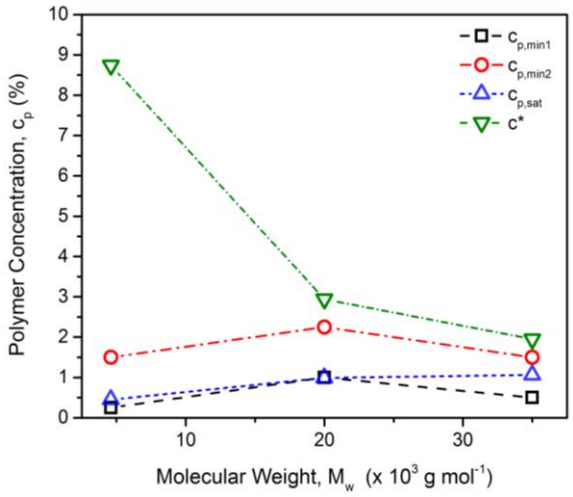


Figure 2.6 : The overall polymer chain length and number dependence on the particle scale dynamics showing the overlap concentration ($c^*$) (green inverted triangle), surface saturation concentration ($c_{sat}$) (blue triangle), first ($c_{p,min1}$) and second minimum ($c_{p,min2}$).

The theoretical calculations and the experimental observations of critical concentrations are summarized in Figure 2.6. It can be seen that for intermediate chain lengths the second transition lies close to the onset of the overlap concentration of PEO, indicating that there is a critical chain length which triggers the re-stabilization of mixtures at high polymer concentrations. However, in the lower chain length limit, the second minimum occurs well within the dilute concentration regime, suggesting that there may be other physical processes that lead to dispersing clusters in solution. On the other hand, in the long chain limit, chain polydispersity might result in preferential adsorption of chains, thus leading to a decrease in viscosity at higher polymer concentrations (Figure A6).

Dynamic light scattering experiments were conducted to correlate particle dynamics and features observed on the macroscopic scale. The structure and dynamics of samples were probed during an aging time between 20 and 30 days, at a scattering angle of 90°.

The equivalent scattering wave vector, $q$, at 90° is estimated to be ca. 0.0319 $nm^{-1}$ and this corresponds to a real space length scale of approx. 200 nm. The normalized intensity autocorrelation function $g_2(\tau)$ obtained for each sample is fit to a function that empirically describes the two-step relaxation process that is commonly observed in glassy colloid-polymer systems[37,53-55]. This function which is a squared sum of an exponential and a stretched exponential is given below:

$$g_2(\tau) = A[\left(pe^{\left(-\frac{t}{\tau_1}\right)}\right) + (1-p)e^{\left(-\left(\frac{t}{\tau_2}\right)^{\beta}\right)}]^2 + C$$

From the above function, we obtain values for the fitting parameters, $A$, $p$, $\tau_1$, $\tau_2$, $\beta$ and $C$. A majority of studies in the literature interchangeably refer to $\tau_1$ and $\tau_2$ as the beta and alpha relaxation processes so to be generic and clear we will henceforth refer to these as fast and slow relaxation parameter. In theory, the first relaxation process is governed by the time scale $\tau_1$ which represents the short time diffusion of a particle within a cage that is formed by its nearest neighbors. The second or the slow relaxation process which is governed by a timescale $\tau_2$ describes the characteristic time taken for a particle to potentially break away from its cage. With aging, this process tends to slow down as particle motions are more constrained. Hence $\tau_2$ increases with aging time. In this case, the systems go from being ergodic, where fluctuations decay within experimental time scales at an early aging time to being non-ergodic, where the fluctuations in the density are large because particle dynamics slow down and appear to be frozen.

At very early aging times (e.g. 2 days), the intensity auto-correlation function for all samples decays to zero, and samples remain ergodic. However, this decay shifts to a longer delay time with aging, indicating that particle or cluster motions are slowing down. The autocorrelation function at different polymer concentrations is used as a

measure to qualitatively analyze the dynamics of the system. Figure A9 shows the time dependence of the fast and slow relaxation parameters for systems containing the 35K PEO. Since the systems age gradually we look at the dynamics at five different aging times: 2 days (5600 mins), 7 days (~10000 mins), 14 days (~20000 mins), 21 days (~30000 mins) and 30 days (45000 mins).

The fast ($\tau_1$) and slow relaxation ($\tau_2$) parameters increase with aging as typically observed in other laponite®-PEO systems[17]. At a very early aging time of 5600 minutes (2 days), the contribution to the effective interactions due to aging is rather small so the parameters essentially describe the initial dynamics present in the system. $\tau_1$ and $\tau_2$, at this aging time, show non-monotonic changes with increasing concentration of PEO. In the dilute polymer phase, the increase in both parameters with the addition of a small amount of PEO indicates the formation of small laponite®-PEO complexes in the dispersion. However we observe a remarkable decrease in the parameters upon further addition of polymers (from 0.25% to 0.5%) and this can be attributed to the melting of the repulsive glass due to increasing attractions in the system. The dynamics at this concentration is faster than the dynamics that is seen in a neat laponite® dispersion and it exhibits a slower aging kinetics than the neat dispersion. This supports the observation of the first minimum at 0.5% from our rheological experiments. Beyond this concentration, $\tau_1$ increases with increase in PEO concentrations from 0.75% to 2.50%. On the other hand, $\tau_2$ which describes the structural rearrangements in the system exhibits some interesting behavior in this range of polymer concentration. Even though we see a systematic increase in the first relaxation time, the structural re-arrangements are surprisingly faster

than laponite® itself. The growth of the slow relaxation parameter is slower than what is seen in neat laponite® systems.

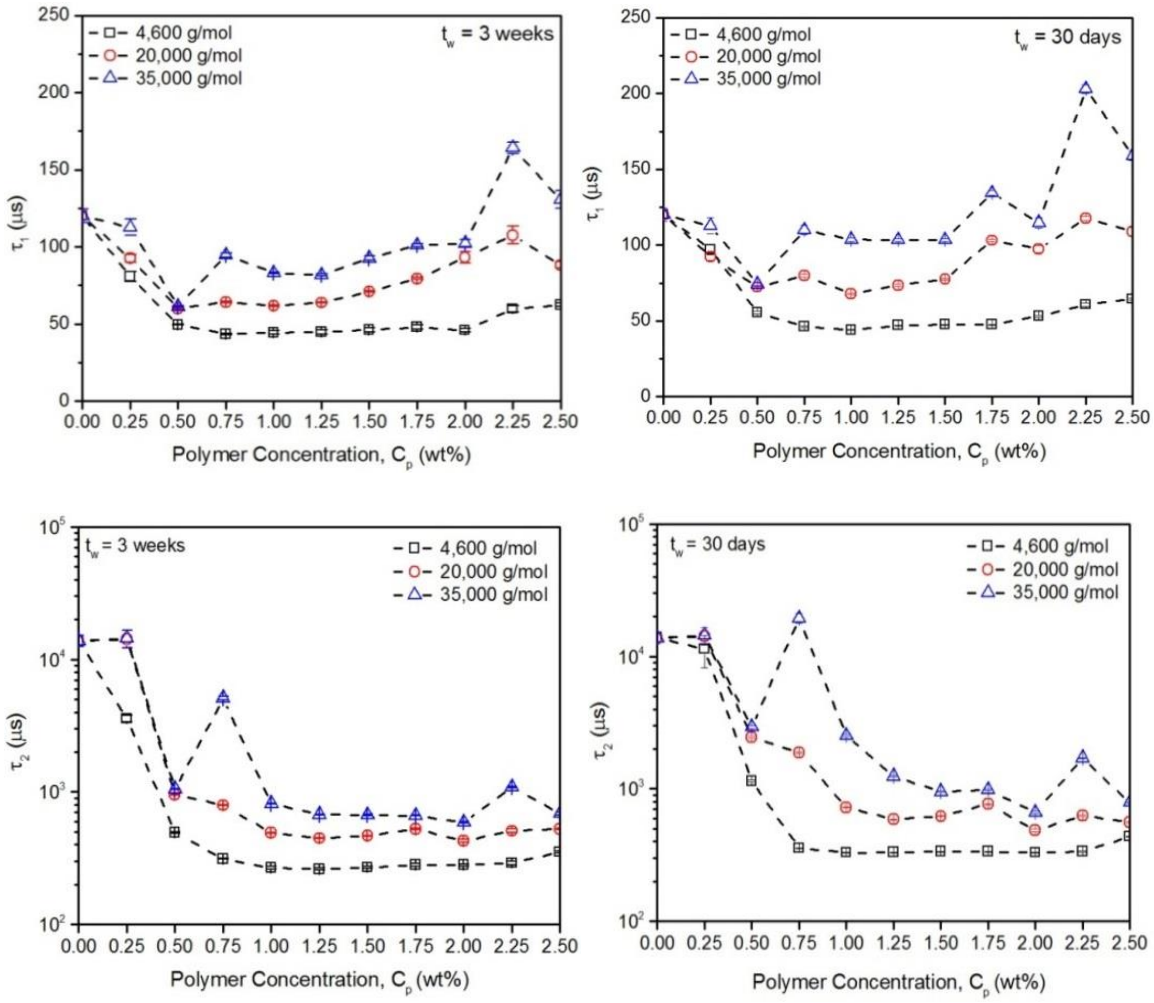


Figure 2.7 : Variation of the fast ($\tau_1$) and slow ($\tau_2$) relaxation processes with the polymer concentration at 21 days (left) and 30 days (right) for (i) 4.6kDa (black squares); (ii) 20kDa (red circles) and (iii) 35kDa (blue upper triangle). The error bars is each graph represent the deviation in the values obtained by fitting $g_2(\tau)$ to the empirical function that describes the dynamics in these mixtures.

The state of a laponite®-PEO dispersion at longer aging time relies greatly on the aging kinetics of the system. After 21 days, laponite® exhibits non-ergodic behavior with the long time decay saturating at ~ 0.02. However, with the addition of chains, the

relaxation processes speed up and the correlation decays within the observation window. As an example, the normalized autocorrelation functions for a 2% laponite® dispersion with various concentrations of the 35K PEO is shown in the appendix (Figure A8). We show in Figure 2.7 the variation of the fast and slow relaxation times with polymer concentration, at a longer aging time of 21 days and 30 days. The dynamics that we observe through DLS qualitatively mirrors the structure observed on the macroscopic scale.

Figure 2.8 gives an overview of the structural changes that we believe are consistent with the various changes in the dynamics that we have observed. After 21 days, laponite® forms a colloidal glass (Figure 2.8a), with a slow relaxation process that has a characteric time scale of about $10^4$ μs. As we add polymer chains to the sample the relaxations speed up as a function of PEO chain length. Both $\tau_1$ and $\tau_2$ decrease as steric repulsions increase due to the presence of adsorbed polymer chains on the surface (Figure 2.8b). As we approach the surface saturation concentration, in the case of intermediate chain lengths, the particles are able to diffuse out of their cages within a millisecond, and this is consistent with diffuse clusters in these suspensions (Figure 2.8b). At intermediate polymer concentrations however, we expect that the clusters will begin to segregate because of increasing repulsions. For a particle that is diffusing within a tight cluster arrangement, it takes a longer time for the particle to perturb its neighboring particle volume. Hence $\tau_1$ increases along this range of concentration. In the same way, as clusters begin to re-stabilize (Figure 2.8c and 2.8d), the second relaxation times decreases, reaches a minimum and then increases for higher polymer concentrations.

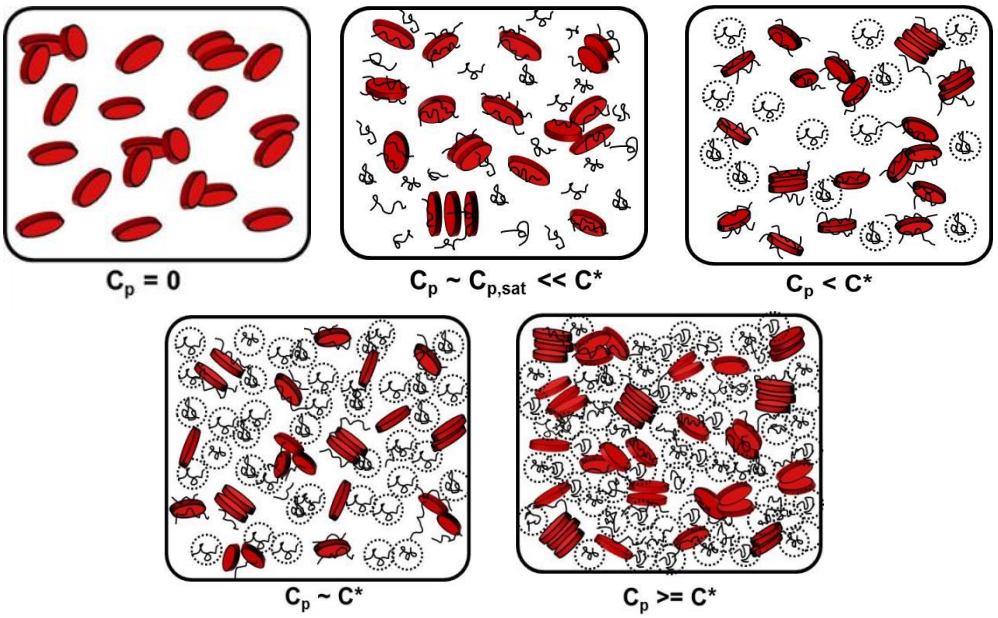


Figure 2.8 : Schematic representation of the structural arrangement of laponite® in a polymer solution. Neat laponite® solutions form a colloidal glass (a). Addition of polymer chains increases attractions; repulsive glass melts (b). Beyond saturation, free chains increase depletion attractions to result in aggregation (c). As chain numbers increase, interactions between adsorbed layers and free chains result in re-stabilization of clusters (d). Beyond c*, cluster-cluster attractions increase and the attractions are now long ranged (e).

While the structure proposed in Figure 2.8 is consistent with our data on dynamics and previous observations of PEO adsorption onto laponite®, ideally structural studies such as SANS could be used to confirm the presence and detailed structure of particle clusters. However, although the dynamics in these different regimes are dramatically different, the structural changes we expect are somewhat subtle. Preliminary SANS studies result in spectra that are dominated by the form factor of individual disks, although ultra-small angle scattering spectra (USANS) as well as cryo-TEM have both confirmed the presence of clusters[56]. Ultra-small angle x-ray scattering (USAXS) experiments are planned to further elucidate the larger-scale structure in these samples.

## 2.4 Conclusions

We have shown that complex interactions between polymers and particles can result in unusual rheological features in an anisotropic colloidal dispersion. The early aging behavior of three sets of dispersions with laponite® at a fixed concentration of 2wt% and various amounts of PEO with $M_n$ of 4.6, 20 and 35 kg mol$^{-1}$ was observed through rheometry and dynamic light scattering experiments. With increasing concentrations of PEO, three distinct transitions in behavior were observed, but the qualitative trend overall was found to be independent of the chain length of PEO.

Initial addition of PEO to a dispersion at $c_p < c_{sat}$ results in a decrease in the storage modulus and the aging kinetics is slow in this concentration phase space. Close to the particle surface saturation concentration ($c_{sat}$ or $c_{p,min1}$), the samples are present as viscous fluids. Upon increasing the concentration further ($c_p > c_{sat}$) they progress to a second arrested state. This glass-liquid-glass transition is reminiscent of the re-entrant glass transition in colloids with non-adsorbing polymers and is a consequence of depletion effects arising from free chains in solution. Interestingly, a second critical concentration minimum ($c_{p,min2}$) is observed as the PEO concentration transitions into the semi-dilute regime. Through a qualitative analysis of the DLS data, we find that this minimum is characterized by a retardation in the relaxation processes for the case of the intermediate chain length PEO.

## 2.5 References

1. Israelachvili, J. N., *Intermolecular and surface forces: revised third edition*. Academic press: 2011.

2. Tawari, S. L.; Koch, D. L.; Cohen, C., Electrical double-layer effects on the brownian diffusivity and aggregation rate of laponite clay particles. *Journal of Colloid and Interface Science* **2001,** *240* (1), 54-66.

3. Zaccarelli, E.; Poon, W. C., Colloidal glasses and gels: The interplay of bonding and caging. *Proceedings of the National Academy of Sciences* **2009,** *106* (36), 15203-15208

4. Tanaka, H.; Meunier, J.; Bonn, D., Nonergodic states of charged colloidal suspensions: Repulsive and attractive glasses and gels. *Physical Review E* **2004,** *69* (3).

5. Ruzicka, B.; Zaccarelli, E., A fresh look at the Laponite phase diagram. *Soft Matter* **2011,** *7* (4), 1268-1286.

6. Liu, X.; Bhatia, S. R., Laponite® and Laponite®-PEO hydrogels with enhanced elasticity in phosphate-buffered saline. *Polymers for Advanced Technologies* **2015**.

7. Gaharwar, A. K.; Avery, R. K.; Assmann, A.; Paul, A.; McKinley, G. H.; Khademhosseini, A.; Olsen, B. D., Shear-Thinning Nanocomposite Hydrogels for the Treatment of Hemorrhage. *ACS nano* **2014,** *8* (10), 9833-9842.

8. Gaharwar, A. K.; Schexnailder, P.; Kaul, V.; Akkus, O.; Zakharov, D.; Seifert, S.; Schmidt, G., Highly Extensible Bio-Nanocomposite Films with Direction-Dependent Properties. *Advanced Functional Materials* **2010,** *20* (3), 429-436.

9. Viseras, C.; Cerezo, P.; Sanchez, R.; Salcedo, I.; Aguzzi, C., Current challenges in clay minerals for drug delivery. *Applied Clay Science* **2010,** *48* (3), 291-295.

10. Jabbari-Farouji, S.; Zargar, R.; Wegdam, G.; Bonn, D., Dynamical heterogeneity in aging colloidal glasses of Laponite. *Soft Matter* **2012,** *8* (20), 5507-5512.

11. Angelini, R.; Zaccarelli, E.; de Melo Marques, F. A.; Sztucki, M.; Fluerasu, A.; Ruocco, G.; Ruzicka, B., Glass–glass transition during aging of a colloidal clay. *Nature Communications* **2014,** *5*.

12. Joshi, Y. M.; Reddy, G. R. K., Aging in a colloidal glass in creep flow: Time-stress superposition. *Phys. Rev. E* **2008,** *77*, 021501.

13. Nicolai, T.; Cocard, S., Structure of gels and aggregates of disk-like colloids. *The European Physical Journal E* **2001,** *5* (2), 221-227

14. Kroon, M.; Vos, W. L.; Wegdam, G. H., Structure and formation of a gel of colloidal disks. *Physical Review E* **1998,** *57* (2), 1962-1970

15. Saha, D.; Bandyopadhyay, R.; Joshi, Y. M., A Dynamic Light Scattering Study and DLVO Analysis of Physicochemical Interactions in Colloidal Suspensions of Charged Disks. *Langmuir* **2015**.

16. Laurati, M.; Petekidis, G.; Koumakis, N.; Cardinaux, F.; Schofield, A. B.; Brader, J. M.; Fuchs, M.; Egelhaaf, S. U., Rheology, Structure and Dynamics of Colloid-Polymer Mixtures: from Liquids to Gels. *J. Chem. Phys.* **2009,** *130*, 134907

17. Ilett, S. M.; Orrock, A.; Poon, W.; Pusey, P., Phase behavior of a model colloid-polymer mixture. *Physical Review E* **1995,** *51* (2), 1344.

18. Zulian, L.; Ruzicka, B.; Ruocco, G., Influence of an adsorbing polymer on the aging dynamics of Laponite clay suspensions. *Philosophical Magazine* **2008,** *88* (33-35), 4213-4221.

19. Surve, M.; Pryamitsyn, V.; Ganesan, V., Nanoparticles in solutions of adsorbing polymers: Pair interactions, percolation, and phase behavior. *Langmuir* **2006,** *22* (3), 969-981.

20. Nelson, A.; Cosgrove, T., A small-angle neutron scattering study of adsorbed poly (ethylene oxide) on laponite. *Langmuir* **2004,** *20* (6), 2298.

21. Nelson, A.; Cosgrove, T., Dynamic light scattering studies of poly(ethylene oxide) adsorbed on laponite: Layer conformation and its effect on particle stability. *Langmuir* **2004,** *20* (24), 10382-10388.

22. Lal, J.; Auvray, L., Interaction of polymer with clays. *J. Appl. Crystallogr.* **2000,** *33* (1), 673; Lal, J.; Auvray, L., Interaction of polymer with discotic clay particles. *Mol. Cryst. Liq. Cryst.* **2001,** *356*, 503.

23. Baghdadi, H. A.; Sardinha, H.; Bhatia, S. R., Rheology and gelation kinetics in laponite dispersions containing poly (ethylene oxide). *J. Polym. Sci., Part B: Polym. Phys.* **2005,** *43* (2), 233.

24. De Lisi, R.; Gradzielski, M.; Lazzara, G.; Milioto, S.; Muratore, N.; Prevost, S., Aqueous Laponite Clay Dispersions in the Presence of Poly (ethylene oxide) or Poly (propylene oxide) Oligomers and their Triblock Copolymers. *J. Phys. Chem. B* **2008,** *112*, 9328.

25. Mongondry, P.; Nicolai, T.; Tassin, J. F., Influence of Pyrophosphate or Polyethylene Oxide on the Aggregation and Gelation of Aqueous Laponite Dispersions. *J. Colloid Interface Sci.* **2004,** *275*, 191.

26. Loizou, E.; Porcar, L.; Schexnailder, P.; Schmidt, G.; Butler, P., Shear-Induced Nanometer and Micrometer Structural Responses in Nanocomposite Hydrogels. *Macromolecules* **2009,** *43* (2), 1041-1049.

27. Zebrowski, J.; Prasad, V.; Zhang, W.; Walker, L. M.; Weitz, D. A., Shake-gels: shear-induced gelation of laponite–PEO mixtures. *Colloids Surf., A* **2003,** *213* (2−3), 189.

28. Can, V.; Okay, O., Shake gels based on Laponite-PEO mixtures: effect of polymer molecular weight. *Des. Monomers Polym.* **2005,** *8* (5), 453.

29. Zulian, L.; de Melo Marques, F. A.; Emilitri, E.; Ruocco, G.; Ruzicka, B., Dual aging behaviour in a clay–polymer dispersion. *Soft matter* **2014,** *10* (25), 4513-4521.

30. Sun, W.; Wang, T.; Wang, C.; Liu, X.; Tong, Z., Scaling of the dynamic response of hectorite clay suspensions containing poly (ethylene glycol) along the universal route of aging. *Soft Matter* **2013,** *9* (27), 6263-6269.

31. Morariu, S.; Bercea, M., Influence of Poly (ethylene oxide) on the Aggregation and Gelation of Laponite Dispersions in Water. *Rev. Roum. Chim.* **2007,** *52*, 147.

32. Morariu, S.; Bercea, M., Effect of Temperature and Aging Time on the Rheological Behavior of Aqueous Poly(ethylene glycol)/Laponite RD Dispersions. *The Journal of Physical Chemistry B* **2011,** *116* (1), 48-54.

33. Kawaguchi, S.; Imai, G.; Suzuki, J.; Miyahara, A.; Kitano, T.; Ito, K., Aqueous solution properties of oligo-and poly (ethylene oxide) by static light scattering and intrinsic viscosity. *Polymer* **1997,** *38* (12), 2885-2891.

34. De Gennes, P.-G., *Scaling concepts in polymer physics*. Cornell university press: 1979.

35. Pusey, P.; Van Megen, W., Dynamic light scattering by non-ergodic media. *Physica A: Statistical Mechanics and its Applications* **1989,** *157* (2), 705-741.

36. Bellour, M.; Knaebel, A.; Harden, J.; Lequeux, F.; Munch, J.-P., Aging processes and scale dependence in soft glassy colloidal suspensions. *Physical review E* **2003,** *67* (3), 031405.

37. Joshi, Y. M.; Reddy, G. R. K.; Kulkarni, A. L.; Kumar, N.; Chhabra, R. P., Rheological behaviour of aqueous suspensions of laponite: new insights into the ageing phenomena. *Proceedings of the Royal Society A: Mathematical, Physical and Engineering Science* **2008,** *464* (2090), 469-489.

38. Cipelletti, L.; Ramos, L., Slow dynamics in glassy soft matter. *Journal of Physics: Condensed Matter* **2005,** *17* (6), R253.

39. Baghdadi, H. A.; Jensen, E. C.; Easwar, N.; Bhatia, S. R., Evidence of Re-Entrant Behavior in Laponite-PEO Systems. *Rheol. Acta* **2008,** *47,* 121.

40. Atmuri, A. K.; Peklaris, G. A.; Kishore, S.; Bhatia, S. R., A Re-Entrant Glass Transition in Colloidal Disks with Adsorbing Polymer. *Soft Matter* **2012,** *8,* 8965.

41. Arfin, N.; Bohidar, H., Ergodic-to-nonergodic phase inversion and reentrant ergodicity transition in DNA–nanoclay dispersions. *Soft matter* **2014,** *10* (1), 149-156.

42. Eckert, T.; Bartsch, E., Re-Entrant Glass Transition in a Colloid-Polymer Mixture with Depletion Attraction. *Phys. Rev. Lett.* **2002,** *89,* 125701.

43. Alessi, M. L., Coil-to-Helix Transition of Poly (ethylene oxide) in Solution. **2004**.

44. Adam, M.; Delsanti, M., Dynamical behavior of semidilute polymer solutions in a θ (theta) solvent: quasi-elastic light scattering experiments. *Macromolecules* **1985,** *18* (9), 1760-1770

45. Magda, J.; Fredrickson, G.; Larson, R.; Helfand, E., Dimensions of a polymer chain in a mixed solvent. *Macromolecules* **1988,** *21* (3), 726-732.

46. Van Oss, C.; Arnold, K.; Coakley, W., Depletion flocculation and depletion stabilization of erythrocytes. *Cell biophysics* **1990,** *17* (1), 1-10.

47. Zhang, X.; Servos, M. R.; Liu, J., Ultrahigh nanoparticle stability against salt, pH, and solvent with retained surface accessibility via depletion stabilization. *Journal of the American Chemical Society* **2012,** *134* (24), 9910-9913.

48. Feigin, R. I.; Napper, D. H., Depletion stabilization and depletion flocculation. *Journal of Colloid and Interface Science* **1980,** *75* (2), 525-541

49. Ogden, A.; Lewis, J., Effect of nonadsorbed polymer on the stability of weakly flocculated suspensions. *Langmuir* **1996,** *12* (14), 3413-3424

50. Sciortino, F.; Mossa, S.; Zaccarelli, E.; Tartaglia, P., Equilibrium cluster phases and low-density arrested disordered states: the role of short-range attraction and long-range repulsion. *Physical review letters* **2004,** *93* (5), 055701.

51. Baghdadi, H. A.; Parrella, J.; Bhatia, S. R., Long-term aging effects on the rheology of neat laponite and laponite-PEO dispersions. *Rheologica Acta* **2008,** *47* (3), 349-357.

52. Knaebel, A.; Bellour, M.; Munch, J. P.; Viasnoff, V.; Lequeux, F.; Harden, J. L., Aging behavior of Laponite clay particle suspensions. *Europhysics Letters* **2000,** *52* (1), 73-79

53. Megen, W. V.; Underwood, S. M., Glass Transition in Colloidal Hard Spheres: Measurement and Mode-Coupling-Theory Analysis of the Coherent Intermediate Scattering Function. *Phys. Rev. E* **1994,** *49*, 4206

54. Abou, B.; Bonn, D.; Meunier, J., Aging dynamics in a colloidal glass. *Physical Review E* **2001,** *64* (2), 021510.

55. Baghdadi, H. A. Polymer-clay dispersions as soft glassy materials: Rheology, dynamics and structure. ProQuest, **2008**.

# CHAPTER 3

# MULTIPLE DYNAMIC REGIMES IN COLLOID-POLYMER DISPERSIONS: NEW INSIGHT USING X-RAY PHOTON CORRELATION SPECTROSCOPY (XPCS)

## 3.1 Introduction

Colloidal glasses and gels can form either as a result of crowding or as a consequence of the nature of interactions between particles as seen in the case of low density colloidal suspensions. Both these states are essentially non-equilibrium systems where particle dynamics and structure evolve gradually with time and the dynamics begin to slow down. For instance, in the case of a hard sphere colloidal suspension they can form either by increasing the volume fraction towards glass transition or by increasing the attractive interactions at a lower colloidal density/volume fraction[1].

An important feature in a colloidal glass/gel is the concept of non-ergodicity. As a colloidal suspension enters a disordered arrested state, particle motions become increasingly correlated and localized. The dynamics in the non-equilibrium states are characterized in a generic sense by a distribution of relaxation processes that is observed at different length scales. The spectrum of relaxation mechanisms can be broadly classified into two categories. The fast relaxation mechanism corresponds to the motion of a single particle or entity within its nearest neighbor cage. The slow relaxation modes correspond to time scale at which structural rearrangements take place. In other words, it is the time taken for the structure to take up its nearest equilibrium configuration. Theories such as the mode coupling theory (MCT) were initially proposed to understand

the slow dynamics in suspensions interacting via a hard sphere potential[2]. Since then, improvements on the mode coupling theory have been made and the theory is now applicable to a bigger class of systems; for e.g. systems with attractive interactions in the concentrated[3] and dilute limit[4]. Additionally, experimental techniques like light scattering, diffusive wave spectroscopy (DWS) and optical microscopy are often used as tools to quantify and understand the slow dynamics in these systems. Through experimental and theoretical work, it was observed that the fast relaxation mechanism is diffusive and independent of aging while the slow relaxation mechanism is hyper-diffusive and varies with aging.

Often times, the use of a light scattering apparatus to investigate the slow relaxations in arrested phases becomes very cumbersome as the duration of an experiment becomes long. X-ray photon correlation spectroscopy is a technique that was recently developed in order to overcome such drawbacks in other experimental techniques. Since this technique makes use of x-rays, this technique can probe dynamics at smaller length scales and at longer time scales making it suitable to examine the dynamics in all kinds of systems.

### 3.1.1 X-ray photon correlation spectroscopy – Technique

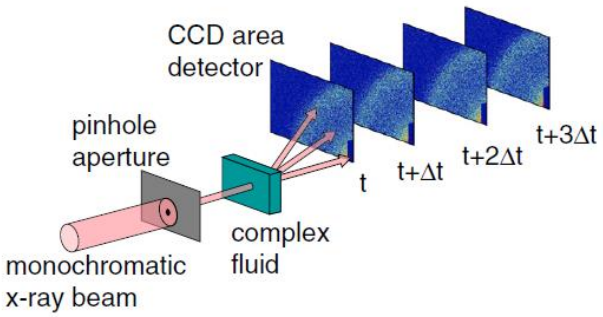


Figure 3.1 : Adapted from a recent review paper by Bob Leheny. Schematic representation of an XPCS measurement. A partially coherent beam is allowed to pass through the material of interest and the speckled scattering intensity is recorded over a range of scattering wave vectors and at different times to record a statistically significant and smooth autocorrelation function.

X-ray photon correlation spectroscopy is a useful tool to investigate the slow dynamics at the nanometer length scale in many materials. Figure 3.1 is a schematic representation of an XPCS measurement. A partially coherent X-ray beam of energy between 6 and 30keV is allowed to pass through an aperture to select an approximate coherence length before it traverses through the material to be tested. This small coherence length has an advantage of avoiding multiple scattering as seen in the case of a DLS experiment. On the other hand, a compromise is made on the intensity because of the fact that only a small fraction of the beam is used, hence brightness and high intensity x-ray beams are required.

When the partially coherent beam passes through a sample, a speckled scattering pattern is obtained and the temporal evolution of this scattering pattern provides information about the dynamics in the system. Now in addition to this, the use of an area detector helps in recording multiple speckle patterns in a single experimental run.

Therefore, the scattering is determined over a range of wave vectors in a single measurement and at a set of time intervals. The intensity autocorrelation function is now measured both as a function of time and at different wave vectors. This is given below:

$$g_2(\vec{Q},t) = \frac{\langle I_{ij}(\vec{Q},t')I_{ij}(\vec{Q},t'+t)\rangle}{\langle I_{ij}(\vec{Q},t)\rangle\langle I_{ij}(\vec{Q},t'+t)\rangle}$$

where, $I_{ij}(\vec{Q},t')$ is the intensity measured at time *t'* and the brackets <..> indicate the average over time and over each pixel *i* and *j* at equivalent scattering vectors. The largest accessible delay time in this technique is limited by the measurement stability and also by issues concerning the over exposure of materials to an x-ray beam.

### 3.1.2 Relaxation and dynamics in colloidal glasses

Colloidal dispersions exhibit complex phase behavior, with the formation of equilibrium phases such as fluids and crystals, as well as disordered non-equilibrium dynamically arrested states, such as glasses and gels[5-8]. For repulsive colloids, the formation of a disordered solid accompanied by dynamic arrest occurs through a glass transition[9], whereas for attractive particles, dynamic arrest can occur through gelation or via formation of an attractive glass[10]. For weakly attractive systems, a re-entrant glass transition can occur, whereby a repulsive glass initially melts into a liquid state as attractions are increased, and then re-forms an arrested attractive glass state; this phenomenon has been predicted theoretically and observed experimentally[11-13].

Hard spheres are often used as models to understand glassy behavior in colloidal systems. Sterically stabilized PMMA spheres have been found to behave like hard spheres and they form a repulsive glass at volume fractions close to the glass transition.

Experimental[14] and theoretical work[15] have shown that the addition of a short ranged attractive interaction can melt the repulsive glass as particle attractions increase the free volume, thus giving way to more particle movements in the system. However, as the strength of attraction is increased an attractive glass is formed. The repulsive glass-liquid transition and the liquid-attractive glass transition meet at a region where both caging effects and attractive interactions are comparable. The dynamics observed around this region has a logarithmic decay feature. Several experimental techniques have been used to distinguish these two phases. Light scattering experiments suggest that the non-ergodicity factor or the Debye-Waller factor, $F(q, t\rightarrow\infty)$, for an attractive glass is much larger than that for the repulsive glass, as motions are more restrained in the former than in the latter phase[16]. In addition to this, rheological experiments conducted to understand the re-entrant behavior of solutions containing diblock copolymer micelles have shown that the elastic modulus $G'$ of an attractive glassy phase was larger than that of the repulsive phase, by a factor of 2. This feature was observed to be in agreement with the mode coupling theory[17].

Laponite systems also show the existence of a very rich phase behavior but this system is rather interesting as the disordered states form at volume fractions much lower than that of the hard sphere system. Studies with varying particle and salt concentrations have contributed to our understanding of a variety of dynamic states from ergodic liquids to non-ergodic glasses, gels and amorphous aggregates. With increasing particle concentration, the phase behavior changes from an isotropic liquid to a nematic state where particles begin to exhibit some orientational ordering[18]. Since the particles are charged, the electrostatic interactions between particles can be tuned by the addition of

salts to form gels and amorphous aggregates at intermediate particle concentrations[19-21]. Alternatively, the effective interactions between particles can also be tuned by changing the pH of the medium. At a pH greater than 9, dominant repulsive interactions lead to the formation of repulsive Wigner glasses and as the pH is lowered attractive face-rim interactions between particles trigger the formation of a house-of-cards structure[22]. Changes in pH also affect the dissolution properties of laponite® and in turn the chemical stability of the system with time[23]. Experiments show that the dissolution occurs significantly when the pH is less than 9 and that the particles remain stable with no surface charge change when the pH is close to 10.

Laponite® exhibits a time-dependent phase behavior with an aging kinetics that has been extensively studied and it is shown that the aging process is strongly correlated with the structural arrangement of particles within the system[24,25]. The structural dependencies on aging and its related phase transitions have been studied using experimental methods like light scattering, rheology and also through simulations. Rheological experiments show that the particles exhibit a glassy behavior and the relation between microscopic dynamics and rheology is well described within the framework of the mode coupling theory (MCT)[26,27]. The aging in glassy colloidal systems has been studied to some extent and comparisons have been made to the aging of quenched polymer melts and molecular liquids[28-30]. Structural arrest and aging in the latter is typically driven by temperature, while in the former this is often governed by the relaxation of residual stresses present in the system after the cessation of flow. Osuji and co-workers utilized rheological methods to understand stress mediated structural arrests and dynamics in colloidal glasses[31-33]. The evolution of the complex modulus, $G^*(t)$, after the application of various magnitudes of

stresses and at different flow cessation rates was observed for suspensions containing ~3%-5% laponite® XLG. It was shown that they are essentially frustrated out of-equilibrium systems and the pathway to structural arrest and aging depend on the relaxation of the residual stresses in the system.

The dynamics occurring in glassy colloidal systems during structural arrest and physical aging are characterized by a two-step relaxation process and much work in the literature has involved the use of light scattering to explain these features [24,26,34]. Aging usually is characterized by an increase in density fluctuations and correlations in particle motions. Bonn and co-workers utilized light scattering and conductivity experiments to classify dispersions of laponite® into three different arrested states; (i) gels ($c_l$ < 1.5wt%), (ii) repulsive glasses ($c_l$ > 1.5wt%) and (iii) attractive glasses ($c_l$ < 1.5wt%, high salt conc.), based on the evolution of the slow relaxation parameter with time[35]. Using polarized light scattering experiments the diffusion of particles within laponite® glasses ($c_l$ ~ 3wt%) was observed by Bonn and co-workers and it was shown that the decoupling of rotational and translational diffusion of particles during aging and the increase in the distribution width of the slow relaxation process were attributed to dynamic heterogeneities in the system[36]. The aging of laponite® can be understood from the qualitative manner in which both the fast and the slow relaxation processes change with time and the relaxation mechanisms can be measured using diffusive wave spectroscopy (DWS) and dynamic light scattering (DLS)[37]. Experiments with higher laponite® concentrations reveal two different regimes in the aging process: (i) early aging where cage formation is primitive and (ii) full aging regime where the particle motions become increasingly restrictive since the cage formation is now complete. Light scattering

experiments were conducted to observe the $q$-dependence of the relaxation processes with aging time. In an experimental work by Abou and co-workers, the relaxation time $\tau$ varied as $q^{-2}$ which suggested that the process was diffusive in nature[34]. However, another study on a similar system by Bellour and co-workers showed that this dependence was valid only within the early aging regime where the characteristic time varied exponentially with aging. They also observed that beyond an aging crossover, the $q$ dependence was ~1.3 and this regime was termed as the full aging regime where the slow relaxation process varied linearly with aging time[38].

In a recent XPCS experiment that was conducted on laponite by Bandyopadhyay and co-workers, a $q^{-1}$ scaling was observed in the high $q$ region, which suggests that the slow relaxation mechanisms might be due to ballistic particle motions. A similar observation was made in other systems like fractal colloidal gels[39,40] and emulsion droplets[41]. In addition to this, they also found that the dynamic structure factor took a compressed exponential form, $F(q,t) \sim exp[-(t/\tau)^{\beta}]$ with $\beta$ larger than 1. Experiments that were later conducted to understand this behavior suggest that this was a result of internal stress relaxations taking place at the particle scale level. In other words, due to local synergistic rearrangements occurring at particle length scales there is a local strain field that translates across length scales and this essentially drives the decay in the slow relaxation process[41]. In the case of the laponite system, it was suggested that the increasing interparticle repulsions due to ion dissociation generated the internal stresses in the system[42]. Similar arguments have been made with respect to other systems like multi-lamellar vescicles (MLV) and the observations were verified through complementary rheological experiments[43].

The interactions between colloids can be tweaked in a way to derive new materials with better properties. For instance, the behavior of sterically stabilized colloids can be controlled by changing the interactions between the grafted chains. In the case of colloids with non-adsorbing polymers, the range of attractions can be tuned by changing the polymer chain length and the strength of the attraction can be increased by increasing its concentration. The dynamic behavior of the new phases that form by changing such parameters is quite abstruse and still remains a topic of great interest to the world of physicists.

In the presence of macromolecules, the structure and dynamic pathways leading to an arrested state is rather complicated and still remains unresolved. Polymers contribute to a variety of interactions depending on its fundamental physical property and the nature of its interactions with nanoparticles in solution. It is known that the addition of polymers to a colloidal dispersion induces an attractive interaction and can lead to re-entrant behavior and glass-glass transitions[44-46]. Though most experimental and theoretical observations have been derived from systems containing hard-sphere colloids and non-adsorbing polymers, it was recently shown that a similar phenomenon is also seen in laponite® dispersions with weakly adsorbing polymers, such as poly(ethylene oxide) (PEO)[45,47].

The adsorption of PEO on laponite® has been extensively studied by Cosgrove, Lal and others using dynamic light scattering and small angle neutron scattering techniques[48-51]. Results have shown that the thickness and the amount of polymer present in the adsorbed layer on the face of the particle did not vary greatly with the molecular weight of the polymer, and that the thickness of the adsorbed layer on the face is ~ 1.6 nm. On

the other hand, the thickness along the edge of the particle was found to show some dependence on the polymer molecular weight (~$M_w^{0.13}$). The scaling exponent was found to be smaller than that observed in the case of PEO chains on spherical latex surfaces (~$M_w^{0.4}$)[52]. The results thus suggest that the adsorbed polymer layer on a laponite® surface is flat and compact and a large fraction of these chains are present as trains, and the fraction of loops and tails is more or less constant. The increasing edge thickness, however, indicates that as the polymer chain length increases, the chains are now long enough to wrap around the edge of the particle. The characterization of the adsorption of PEO on a laponite® surface, thus, is of importance as it provides as a basis to understand how it influences the formation of different arrested phases either via steric stabilization or via bridging flocculation.

Studies also show that the repulsive colloidal glass melts with the addition of polymer chains of intermediate chain lengths but forms another arrested state when excess free polymers are present in solution. Additionally, the rate at which arrested states form is dependent upon the polymer chain length. When chains are too short to bridge between particles, samples age slowly due to steric effects of chains in solution, whereas if chains are long enough to bridge between particles, the rate of aging to a glass or gel state increases[53,54]. For a laponite® concentration of 2 wt%, the transition between these two types of behaviors occurs at approximately $M_w$ < 83kg mol$^{-1}$. When chains are long enough to bridge between particles, (approximately 200-600 kg mol$^{-1}$ for laponite® dispersions at particle concentrations between 1 and 2.5 wt%) reversible shake gels were observed, which was attributed to incomplete surface coverage and the dynamic equilibrium between the desorption and adsorption of chains onto colloidal surfaces[55-57].

Though the macroscopic measurements in the work mentioned above confirm the existence of new and different glass and gel phases[58,59], they do not completely reveal the particle scale dynamics leading to the formation of these arrested states. Thus, laponite®-polymer dispersions provide an ideal system to study such phenomenon, as the magnitude and range of interparticle interactions can be tuned through polymer molecular weight and concentration[58-61].

In this chapter, we investigate the dynamics observed in colloidal dispersions of laponite® nanoparticles, where interparticle interactions can be tuned with the addition of a weakly adsorbing polymer like poly(ethylene oxide), PEO. We use coherent x-ray photon correlation spectroscopy (XPCS) to investigate the glassy dynamics over a wide range of length and time scales. The laponite® composition were fixed at concentration of 2% and 3% (w/w), thereby exploring the dynamics within the phase space where it forms a repulsive glass. The amount of PEO was varied to span its dilute and semi-dilute concentrations in order to understand the effect of different polymer induced interactions. The dynamics of the different phases in laponite®-polymer dispersions, measured over multiple length scales, provides a qualitative insight to the formation of non-equilibrium states with an emphasis on its dependence on the range of polymer concentrations, molecular weights and particle concentration.

**3.2 Materials and Methods**

Laponite® RD was obtained from Southern Clay Products (Gonzales, TX, USA). Poly(ethylene oxide) ($M_n$ = 20 kg mol$^{-1}$, 35 kg mol$^{-1}$) and poly(ethylene oxide) ($M_n$ = 55 kg mol$^{-1}$) were purchased from Sigma Aldrich and Polymer Source respectively. All the materials used in this study were used without any further purification.

### 3.2.1 Sample preparation

Samples were prepared by first dispersing laponite® in deionized filtered water (resistivity of ~18.2 MΩ.cm at 25°C) whose pH was adjusted to 10 using sodium hydroxide (NaOH) to ensure stability of laponite®. The dispersions were homogenized using an Ultra Turrax homogenizer to break up any large aggregates present in the solution and then stirred for 20 minutes. The samples were filtered using a 0.45μm filter and mixed with required amounts of poly(ethylene oxide) (PEO) and stirred until the polymer completely dissolved. The vials were capped, sealed and stored to avoid any exposure to the external environment. Samples with 2% laponite® by weight % (w/w) and polymers of molecular weight, $M_n$ ~ 20, 35, 55 kg/mol are referred as $S_{M20\_L2}$, $S_{M35\_L2}$ and $S_{M55\_L2}$ respectively. Similarly, samples with 3% laponite® will be referred to as $S_{MXX\_L3}$. For all samples, the concentration of the polymer, $c_p$ % (w/w) was varied between 0.25% and 2.5%.

The amount of polymer needed to saturate a laponite® particle surface exhibits a weak power-law relationship with molecular weight ($\Gamma \sim M_w^{0.05}$). The concentration of PEO bound to the surfaces of a laponite® particle, estimated using NMR relaxation experiments, was found to be ~0.18%. This corresponds to a coverage of 0.4 mg/m$^2$, approximately. Additionally, laponite® has a specific surface area of 900m$^2$/g. Therefore, for every gram of laponite® the amount of PEO at saturation can be calculated as (900 m$^2$/g) x (adsorbed amount at saturation) x (1g/1000 mg). For a 2 wt% laponite® dispersion, the concentration of PEO needed to saturate or bind to all available particle surfaces ($c_{sat}$) was estimated to be ~0.75%. This is strictly based on the assumption that

all adsorption surfaces are available to the polymer and that there is a perfectly monodisperse particle size distribution.

The overlap concentration of polymer is estimated as, $c^* \sim \frac{3M_w}{4\pi N_A R_g^3}$ , where $N_A$ is Avogadro's number[62]. The calculated values of the overlap concentrations are shown in Figure 3.1. The hydrodynamic radius of the PEO chains was estimated as $R_h = 0.66R_g$, where $R_g$ is the radius of gyration, given by $R_g \sim 0.022M_w^{0.583}$ [62]. For all samples considered in this study, the polymer-colloid size ratio ($R_g/R$) is less than 1.

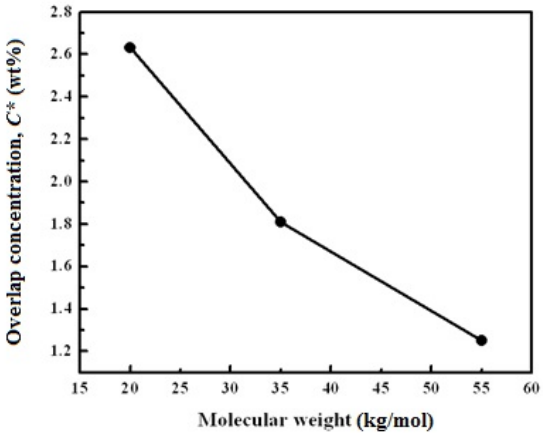


Figure 3.2 : Estimate for the overlap concentration, *c** vs. the molecular weight of the polymer used in this study

### 3.2.2 X-ray photon correlation spectroscopy

X-ray photon correlation spectroscopy (XPCS) measurements were performed at sector 8-ID-I of the Advanced Photon Source (APS). A small quantity of the dispersion sample, prepared as described above was loaded in a 1mm glass capillary tube, flame sealed, and left undisturbed at 25°C to spontaneously age for 30 days. Two different detectors were used depending on the sample dynamics to record the scattering intensity.

For samples exhibiting slow dynamics, the scattered intensity was recorded by a direct–illuminated charge coupled device (CCD) area detector (Princeton Instruments EEG model 37) at a distance of 3.4 m, covering wave vector, $q$ range from 0.002 $Å^{-1}$ to 0.03 $Å^{-1}$ with incident coherent x-rays of wavelength 0.94 $Å^{-1}$. Scattering from samples with fast dynamics was recorded using a DALSA detector which covers a $q$ range of 0.002 $Å^{-1}$ to 0.015 $Å^{-1}$.

### 3.3 Results and Discussion

The diffusion of laponite® particles become more restrictive with aging and the ergodicity breaking time depends inversely on the concentration of laponite® and is typically between 2-3 weeks for a particle concentration of 2% [63,64]. When PEO is initially added to a dispersion containing laponite®, particle-polymer complexes form in addition to presence of individual particles and free polymer chains[65-67]. The systems thus age in a complex manner to exhibit gel-like/glassy dynamics. The dynamics present in these systems depends on both, the spatial distribution of particles within the volume and the polymer-particle/cluster interactions present in the dispersion. Here we use XPCS to examine the dynamics over an extended range of time and length scales. We make a quantitative analysis of the dynamics by fitting the intensity autocorrelation function, $g_2(q,t)$, calculated from time-dependent intensity fluctuations at each $q$, to the modified Kohlrausch-William-Watts equation which is given as:

$$g_2(\mathrm{q},\mathrm{t}) = 1 + b\left\{A\, exp\left(-(t/\tau)^{\beta}\right)\right\}^2 \qquad (1)$$

where, $A$ is the short time plateau amplitude, $b$ is the Siegert factor (~0.3) and it is largely dependent on the instrument optics and is independent of the wave vector $q$, $\tau$ is the

characteristic relaxation time, and $\beta$ is the distribution width of the slow relaxation process. The parameters $A$, $\tau$ and $\beta$ are functions of the scattering wave vector $q$.

The dynamic structure factor, $F(q,t)$ for neat nanoparticles and polymer-nanoparticle dispersions shown in Figures (3.1 and 3.3), and are given by:

$$F(q,t) = A\ exp\left(-(t/\tau)^{\beta}\right) \qquad (2)$$

The fits to the data discussed herein are shown in solid black lines.

The following discussion is divided into three sections and each section focusses on the effect of polymer concentration, polymer chain length and nanoparticle concentration on the particle or cluster dynamics respectively.

### 3.3.1 Polymer concentration effects on dynamics

The dynamic structure factor, *F(q,t)* and measured relaxation dynamics for system $S_{M35\_L2,}$ obtained at various added concentrations of PEO (35 kg/mol and 2% laponite®) is shown in Figure 3.3. At an aging time of 30 days, the dynamics in a neat laponite® system is slow and we observe a non-exponential decay of *F(q,t)* at a longer delay time of $10^3$s (Figure 3.3a). The relaxation processes in systems with added PEO vary non-uniformly with increasing PEO concentration and the slow relaxation time, $\tau$, is estimated from fitting the data to Equation 2. As can be clearly seen in Figure 3.3a, with initial addition of a small amount of PEO, the early decay in the dynamic structure factor is indicative of faster relaxation mechanisms in the system. We see that the diffusion of complexes and particles in these systems is faster than what is observed in a neat laponite® system. Upon further increasing the polymer concentration from 0.25% to 0.75% (Figure 3.3d), we observe retardation in dynamics, before it once again begins to

exhibit faster dynamics at intermediate concentrations of PEO ($c_p$: 0.75% – 1.5%). As the PEO concentration transitions to a semi-dilute regime, we observe a critical concentration at which the samples begin to show slower dynamics. Beyond this critical concentration, the dynamics once again speeds up. We believe that the behavior through each of these transitions describes different particle dynamics influenced by the effective interactions present in the system.

Figure 3.3c and 3.3e illustrate the $q$-dependence of the slow relaxation time $\tau$ and exponent, $\beta$ for the series of samples containing the 35kg/mol PEO. The polymer–nanoparticle dispersions exhibit slow hyper-diffusive motion for which the relaxation time scales inversely with $q$ ($\tau \sim q^{-1}$) and $\beta$ is greater than 1. The compressed exponential form ($\beta$ >1) of the dynamic structure factor has been observed in disordered elastic media with local heterogeneous stresses and experiments show that this is a result of internal stress relaxations taking place at the particle length scales[68,69,15]. In a recent XPCS experiment that was conducted on neat laponite® dispersions by Bandyopadhyay and co-workers, a $q^{-1}$ scaling was observed in the intermediate $q$ region which suggests that the slow relaxation mechanisms might be due to ballistic particle motions as a response to local stresses developing in the system[70]. A similar feature was observed in other systems containing fractal colloidal gels and concentrated emulsion droplets[15].

In the case of the laponite® system, it was suggested that the increasing interparticle repulsions due to counter-ion dissociation generates internal stresses in the system. Across different values of $q$ we do not observe any particular scaling behavior in $\beta$ and we observe only subtle differences across of the range of length scales observed in this experiment. For the series of samples containing 3% laponite®, both with and without

PEO, the exponential factor $\beta$ *is* ~ 1.5. However, for polymer-nanoparticle dispersions at 2% laponite®, $F(q,t)$ decays with $1 \leq \beta < 1.5$. It is known that decreasing laponite® concentration slows the aging dynamics considerably[71] and the ongoing aging process may affect the stress field in a complex manner that leads to an estimate of $\beta < 1.5$. We find that on allowing samples to age for long times, ~ 90 days, correlation functions decay with the predicted value of $\beta$ ~1.5, consistent with the value of $\beta$ (~1.4 ± 0.1) observed by Leheny and co-workers for aging gel-forming systems comprising of grafted silica particles of radius 22 nm.

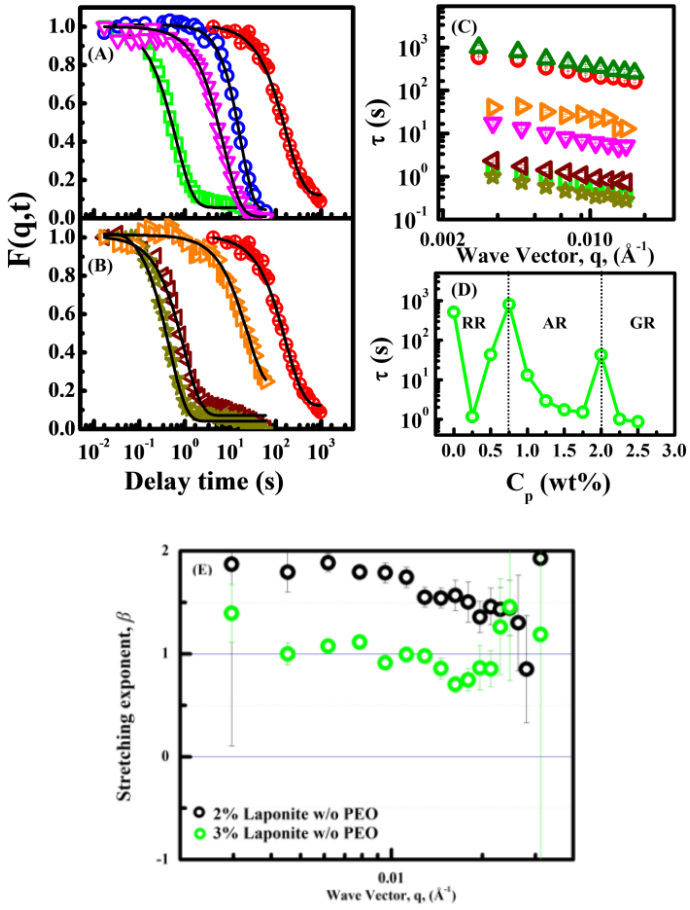

Figure 3.3 : Dynamic structure factor, $F(q,t)$ at $q$~0.009Å$^{-1}$ for (A) 2% laponite® (neat, ⊗) and with 35kg/mol PEO at 0.25% (□), 0.5%(○), 1% (▽) and (B) 2% laponite® (neat, ⊗), 1.5%(◁), 2.0%(▷) and 2.5%(☆). The solid black lines represent the fits to the data. (C) Q-dependence for the slow relaxation time $\tau$ obtained for $S_{M35\_L2}$ at PEO 0% (⊗), 0.25% (□), 0.75% (△), 1% (▽), 1.5% (◁), 2.0% (▷) and 2.5% (☆). (D) Relaxation time, $\tau$ vs $c_p$, at $q$ ~ 0.0045Å$^{-1}$. (E) Q – dependence of the stretching exponent $\beta$ for 2% and 3% laponite suspensions without PEO.

As shown in Figure 3.3d, based on the interparticle interactions resulting from the addition of polymer in each concentration regime, we refer to $c_p < c_{sat}$ (~0.75%) as the repulsive regime (RR), the regime with $c_{sat} < c_p < c^*$ (~ 1.81%) as the attractive regime (AR), and the regime at $c_p > c^*$ as the gel regime (GR). At low $c_p$ (RR), interparticle interactions are primarily repulsive. For intermediate $c_p$ (AR), short-range attractive interactions arising from depletion interactions appear to dominate. In the third regime (GR), the polymer chains behave as in a semi-dilute solution and the medium is expected to be crowded[72]. A schematic of these three regimes and an additional discussion of these three regimes is provided in the discussion of polymer molecular weight effects, below.

### 3.3.2 Polymer molecular weight effects on dynamics

To comprehensively understand the behavior in the series of samples containing the 35K PEO, we also looked at systems containing shorter (20 kg mol$^{-1}$) and longer (55 kg mol$^{-1}$) PEO chains, at the same concentration of laponite®. As shown in Figure 3.4, the microscopic dynamics with increasing $c_p$ for all the three series of samples $S_{M20\_L2}$, $S_{M35\_L2}$ and $S_{M55\_L2}$ are qualitatively similar, and we observe the three dynamic regimes (RR, AR, and GR) for all three molecular weights.

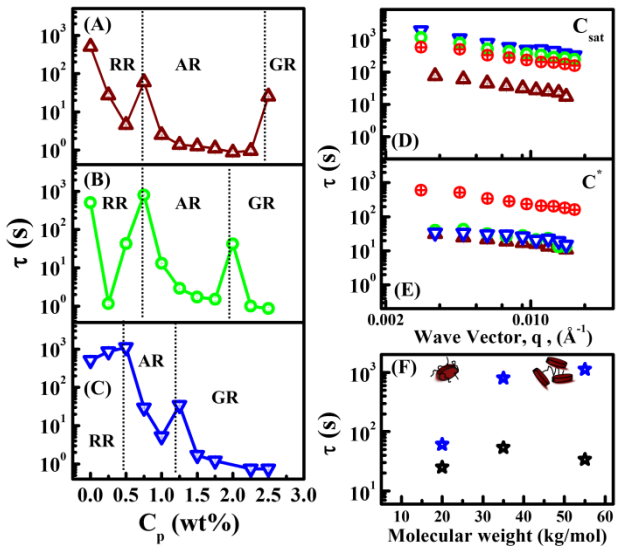


Figure 3.4 : Relaxation time, $\tau$ vs polymer concentration, $c_p$ for (A) Δ ($S_{M20\_L2}$), (B) ○ ($S_{M35\_L2}$), (C) ▽ ($S_{M55\_L2}$). The data at $c_p \sim 0\%$ corresponds to neat laponite® (2%). The maxima in relaxation time, $\tau$ observed at $c_{sat}$ and $c^*$ (dashed line) marks transition from RR-AR and AR-GR regime respectively. All data for $\tau$ are compared at $q \sim 0.0045$ Å$^{-1}$. (D, E) Q-dependence of relaxation time, $\tau$ for neat 2% laponite® (⊗), and systems with different molecular weight of PEO at their respective, $c_{sat}$ and $c^*$. (F) Relaxation time $\tau$ vs molecular weight of PEO, at $c_{sat}$ (blue ☆) and $c^*$ (black ☆). Overlap concentration, $c^*$: 2.63% (20 kg/mol); 1.81% (35 kg/mol); 1.23% (55 kg/mol)

We discuss each of these states in detail along with a schematic representation (Figure 3.5) of these dynamics and our rationale for designating these three regimes as repulsive, attractive, and gel-like below. We have not measured the detailed interparticle interactions in this study; nevertheless, these classifications are consistent with both the dynamics and structure we observe, as well as earlier work on laponite®-PEO dispersions.

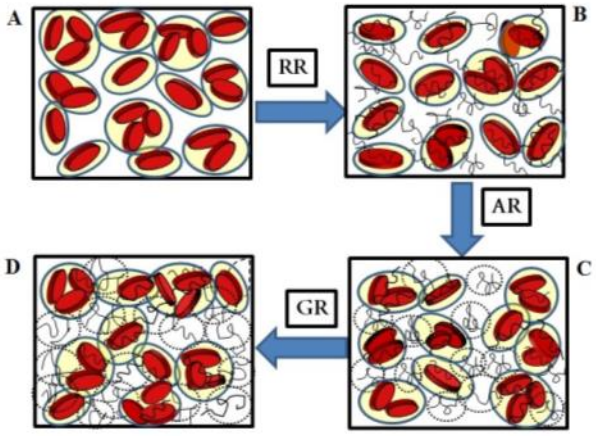


Figure 3.5 : A schematic representation of the dynamics seen in this system. With the addition of PEO to a neat laponite® system we observe a transition in the dynamics across the repulsive regime (RR) (A→B), attractive regime (AR) (B→C) and the gel regime (GR) (C→D).

For polymer-nanoparticle dispersion samples, adding polymer into the repulsive nanoparticle system (Figure 3.5a) introduces a weak attractive interparticle interaction, which affects the diffusion of the nanoparticles in a complex manner. The three regimes, RR, AR and GR are observed with dynamic transitions between different regimes at $c_{sat}$ and $c^*$. The experimentally measured AR-GR transition (Figure 3.5c→d), shown by the dashed line in Figure 3.4, agrees well with theoretical estimate of $c^*$ for all the three systems (calculated $c^*$ for different molecular weights shown in Figure A2). As far as RR-AR transitions are concerned (Figure 3.5a→c), the theoretical value of $c_{sat}$ depends very weakly on the size of the polymer chains for the range of molecular weight we explored and we expect the transition to occur at concentrations close to $c_{sat}$, if all the particle surfaces are available for polymer adsorption. However we find, the RR-AR transition for $S_{M55\_L2}$ occurs at $c_p$ = 0.5%, which is smaller than the theoretical $c_{sat}$. Recent experiments using dynamic light scattering and ultrasound attenuation

spectroscopy techniques[73] have shown that the distribution of laponite® particles in suspensions in the early time periods is bimodal, and not monodisperse as one would expect. This was attributed to the fact that there may be partially exfoliated weak aggregates/clusters of particles or stacks of two or more laponite® particles present in the system. We believe because of such cluster formation there are a number of particle surfaces inaccessible to polymer chains, which can result in saturation occurring at a lower $c_p$. Thus our studies reveal a simple method of tuning the dynamic range in the aging dispersion sample by varying either polymer concentration or molecular weight in a controlled manner.

The log-log plot of $\tau$ vs $q$ for neat laponite® (2%) and dispersions $S_{M20\_L2}$, $S_{M35\_L2}$, $S_{M55\_L2}$ at $c_{sat}$ and $c^*$ are shown in Figure 3.4d and Figure 3.4e, respectively. Irrespective of the PEO concentration and chain length of the polymer, the inverse scaling of $\tau$ with $q$ remains unchanged and is indicative of slow hyper-diffusive motion. At $c_{sat}$, the relaxation time scales increases with polymer chain length (Figure 3.4f). At and above $c^*$ (Figure 3.4d), we do not observe remarkable changes in the slow relaxation processes with changes in the polymer chain length (Figure 3.4f). The above analysis suggests that, when the polymer concentration is below the overlap concentration, the relaxation dynamics slow down with increase in polymer chain length, corresponding to an increase in resistance for motion. However, above the overlap concentration, polymer chains are in the semi-dilute regime, and motion is independent of chain length as expected. The concentration and chain length of added polymer plays an important role in the origin of multiple arrested states and aging dynamics. In the RR, polymer chains adsorb onto the particle surface, but there are not many free chains to serve as depletants, thus

interparticle interactions are primarily repulsive. However, adsorbed polymer may partially screen repulsive interactions, and therefore faster relaxation dynamics are observed in samples with polymer as compared to neat laponite® (Figure 3.4a, 3.4b and 3.4c). The degree of screening depends on both $c_p$ and chain length.

With increasing polymer molecular weight, the number of adsorbed chains per particle decreases and the system contains a finite number of larger clusters, resulting in the slow relaxation time. With further increase in $c_p$ beyond $c_{sat}$ (Figure 3.5b→c), the system enters a regime of attractive interparticle interaction through depletion caused by free polymer chains, allowing for depletion-induced melting of the repulsive glass. Above $c_{sat}$ there is a formation of small clusters which are held together via short-range attractive interactions. The formation of attractive clusters effectively results in a smaller density of nanoparticles in the solution, which is comprised of free polymer chains and nanoclusters. Thus in the AR regime (Figure 3.5c), the small nanoclusters can diffuse faster in an effectively dilute medium. The attractive depletion interaction between nanoparticles governs the dynamic response at $c_{sat} < c_p < c^*$. However, at higher polymer concentration, polymer-polymer interactions become significant and motion of the nanoclusters is limited as the solution becomes more crowded, approaching $c^*$. Consequently, a second maxima in the relaxation dynamics occurs at the overlap concentration, $c^*$.

At $c^*$ the polymer chains are expected to exist as closely packed blobs which would confine the motion of the nanoparticle clusters. The presence of a crowded environment located close to these cluster surfaces results in a hindered and restricted diffusion, and hence slow dynamics are again observed at this concentration. For $c_p \geq c^*$, in the GR

regime (Figure 3.5d), the behavior of polymer chains is dominated by their excluded volume interactions, and they behave less as depletants and more as a uniform polymer matrix. The nanoclusters and polymer coils undergo structural reorganization mediated by competing polymer-polymer and polymer-nanoparticle interactions. In the semi dilute regime, the polymer chains form a dense network[72] with characteristic length $\xi = R_g (c_p/c^*)^{-0.75}$ [74] and the characteristic length $\xi$ is always smaller than the size of the nanoclusters. Effectively in the GR regime we are measuring the diffusion of nanoclusters in a matrix where these clusters experience the macro-viscosity environment of the polymer solution, as has been predicted[75] and observed earlier in PEO solutions[74]. Since the characteristic length of polymer solution in the GR regime does not depend on polymer molecular weight, we observe a chain length-independent relaxation time (Figure 3.4f).

While we have focused primarily on how particle-particle interactions change with polymer concentration and molecular weight and how this impacts the dynamics, we also expect changes in the viscosity of the background fluid as polymer concentration and molecular weight increases. For example, one may argue that the slowdown in dynamics near the AR-GR transition may be due to the background fluid entering the semi-dilute regime. However, the large change in $\tau$ we observe at this transition is much more than one would expect from a polymer solution at the dilute/semi-dilute transition. Given the low molecular weights and concentrations used, we expect these types of effects to be minor in comparison to the dramatic changes in dynamics observed from formation of different arrested states.

### 3.3.3 Laponite® particle concentration effects on dynamics

In concentrated laponite® suspensions, the enhanced particle crowding and increased electrostatic repulsions restrict particle re-arrangements within the system and the timescales at which it reaches a structurally arrested phase is shorter. The aging of these systems thereafter in the full aging regime is slower and this can be observed from the longer relaxations in the system[76]. This is seen from the slower decay of *F(q,t)* for the 3% laponite® system in comparison with the 2% laponite® system (Figure 3.6a). Now in the presence of polymers, the qualitative behavior is quite similar to what is observed in systems with 2% laponite®. However, as shown in Figure 3.6b, we observe a shift in the transition from each dynamic regime. Additionally, the secondary peak could not be observed as the shift in the transition from the AR to the GR is believed to fall outside the experimental window. This is expected because the number density of free polymer chains in the medium decreases as more surfaces are now accessible for adsorption. The magnitude of the relaxation time scales at intermediate polymer concentrations show little differences and a qualitatively similar trend is observed within this region. This can be attributed to the sizes of clusters that form along with polymer concentration phase space and the magnitude of repulsions that influence the diffusion of these many-body clusters within the solvent. The study of the characteristic nature of these clusters using high-end x-ray techniques like ultra-small angle x-ray scattering (USAXS) is on-going and a comprehensive discussion will be presented in an upcoming publication.

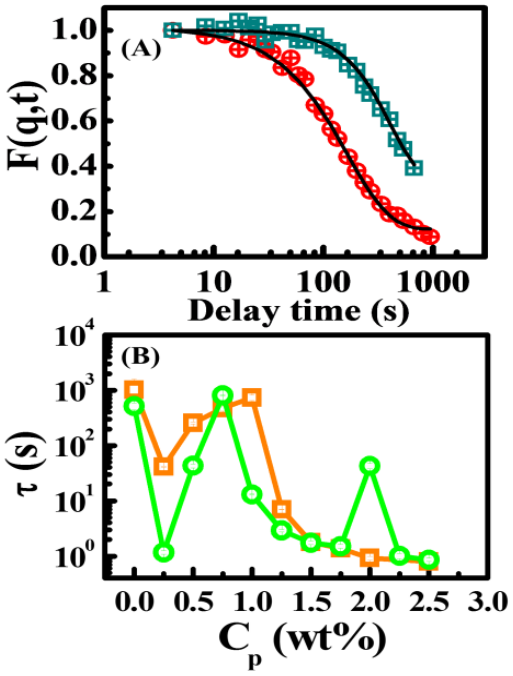


Figure 3.6 : The effect of particle concentration on colloid-polymer dynamics. (A) Dynamic structure factor, *F(q,t)* for 2% laponite® (⊗) and 3% laponite® (□). (B) Relaxation time $\tau$ vs $c_p$ for $S_{M35\_L2}$ (○) and $S_{M35\_L3}$(□)

### 3.4 Conclusions

Dynamics of multiple arrested states of nanoparticle dispersions with adsorbing polymer chains were explored using x-ray photon correlation spectroscopy. Our results indicate that the microscopic and macroscopic properties of the polymer-nanoparticle dispersion are correlated and can be tuned by altering the competing long-range repulsions and short-range attractions. The change in interparticle interactions leads to structural reorganization at the nanoscale through polymer–particle and polymer–polymer interaction, which in turn has major effects on the bulk properties and results in complex dynamic state diagram with multiple arrested states. With change in interparticle interaction, the polymer-nanoparticle dispersion exhibits dynamic behavior in three regimes: the repulsive regime (RR, for $c_p < c_{sat}$) where interparticle interactions are

primarily dominated by the long range electrostatic repulsion, the attractive regime (AR, $c_{sat} < c_p < c^*$ **)** , where liquids and attractive glasses are formed due to the formation of attractive nanoclusters via depletion interaction of the polymer, and the gel regime (GR, $c_p > c^*$**)** above the polymer overlap concentration where the macroscopic viscosity of the semi-dilute polymer solution dominates at nanoscale and exhibits fast relaxations, independent of the polymer chain length.

### 3.5 References


1. Bergenholtz, J.; Fuchs, M., Nonergodicity transitions in colloidal suspensions with attractive interactions. *Physical Review E* **1999,** *59* (5), 5706-5715

2. Goetze, W. in Liquids, Freezing and Glass Transition (eds Hansen, J. P., Levesque, D. & Zinn-Justin, J.) 287 (North Holland, Amsterdam, 1991).

3. Dawson, K. A., The glass paradigm for colloidal glasses, gels, and other arrested states driven by attractive interactions. *Current opinion in colloid & interface science* **2002,** *7* (3), 218-227.

4. Kroy, K.; Cates, M.; Poon, W., Cluster mode-coupling approach to weak gelation in attractive colloids. *Physical review letters* **2004,** *92* (14), 148302.

5. Trappe, V.; Sandkuhler, P., Colloidal gels - low-density disordered solid-like states. *Current Opinion in Colloid & Interface Science* **2004,** *8* (6), 494-500.

6. Poon, W. C. K.; Renth, F.; Evans, R. M. L.; Fairhurst, D. J.; Cates, M. E.; Pusey, P. N., Colloid-polymer mixtures at triple coexistence: Kinetic maps from free-energy landscapes. *Physical Review Letters* **1999,** *83* (6), 1239-1242

7. Zaccarelli, E., Colloidal gels: equilibrium and non-equilibrium routes. *J Phys-Condens Mat* **2007,** *19* (32), 323101.

8. Guo, H. Y.; Ramakrishnan, S.; Harden, J. L.; Leheny, R. L., Gel formation and aging in weakly attractive nanocolloid suspensions at intermediate concentrations. *J Chem Phys* **2011,** *135* (15), 154903.

9. Pusey, P. N.; Vanmegen, W., Observation of a Glass-Transition in Suspensions of Spherical Colloidal Particles. *Physical Review Letters* **1987,** *59* (18), 2083-2086.

10. Lu, P. J.; Zaccarelli, E.; Ciulla, F.; Schofield, A. B.; Sciortino, F.; Weitz, D. A., Gelation of particles with short-range attraction. *Nature* **2008,** *453* (7194), 499-U4.

11. Sciortino, F., Disordered materials - One liquid, two glasses. *Nature Materials* **2002,** *1* (3), 145-146

12. Pham, K. N.; Puertas, A. M.; Bergenholtz, J.; Egelhaaf, S. U.; Moussaid, A.; Pusey, P. N.; Schofield, A. B.; Cates, M. E.; Fuchs, M.; Poon, W. C. K., Multiple glassy states in a simple model system. *Science* **2002,** *296* (5565), 104-106

13. Bergenholtz, J.; Fuchs, M., Nonergodicity transitions in colloidal suspensions with attractive interactions. *Physical Review E* **1999,** *59* (5), 5706-5715.

14. Eckert, T.; Bartsch, E., Re-Entrant Glass Transition in a Colloid-Polymer Mixture with Depletion Attraction. *Phys. Rev. Lett.* **2002,** *89*, 125701.

15. Cipelletti, L.; Ramos, L.; Manley, S.; Pitard, E.; Weitz, D. A.; Pashkovski, E. E.; Johansson, M., Universal non-diffusive slow dynamics in aging soft matter, *Faraday Discussions* **2003,** *123*, 423-423

16. Mourchid, A.; Lecolier, E.; Van Damme, H.; Levitz, P., On Viscoelastic, Birefringent, and Swelling Properties of Laponite Clay Suspensions: Revisited Phase Diagram. *Langmuir* **1998,** *14*, 4718.

17. Pham, K.; Egelhaaf, S.; Moussaıd, A.; Pusey, P., Ensemble-averaging in dynamic light scattering by an echo technique. *Review of scientific instruments* **2004,** *75* (7), 2419-2431.

18. Grandjean, J.; Mourchid, A., Re-entrant glass transition and logarithmic decay in a jammed micellar system. Rheology and dynamics investigation. *EPL (Europhysics Letters)* **2004,** *65* (5), 712.

19. Ruzicka, B.; Zulian, L.; Ruocco, G., Ageing dynamics in Laponite dispersions at various salt concentrations. *Philosophical Magazine* **2007,** *87* (3-5), 449-458

20. Saha, D.; Bandyopadhyay, R.; Joshi, Y. M., A Dynamic Light Scattering Study and DLVO Analysis of Physicochemical Interactions in Colloidal Suspensions of Charged Disks. *Langmuir* **2015**

21. Joshi, Y. M.; Reddy, G. R. K., Aging in a colloidal glass in creep flow: Time-stress superposition. *Phys. Rev. E* **2008,** *77*, 021501.

22. Olphen, H. v., An introduction to clay colloid chemistry. *New York: Jonh Wiley & Sons* **1977**.

23. Thompson, D. W.; Butterworth, J. T., *J. Colloid Interface Sci.* **1992,** *151* (1), 236.

24. Knaebel, A.; Bellour, M.; Munch, J. P.; Viasnoff, V.; Lequeux, F.; Harden, J. L., Aging behavior of Laponite clay particle suspensions. *Europhysics Letters* **2000,** *52* (1), 73-79.

25. Angelini, R.; Madsen, A.; Fluerasu, A.; Ruocco, G.; Ruzicka, B., Aging behavior of the localization length in a colloidal glass. *Colloids and Surfaces A: Physicochemical and Engineering Aspects* **2014**.

26. Megen, W. V.; Underwood, S. M., Glass Transition in Colloidal Hard Spheres: Measurement and Mode-Coupling-Theory Analysis of the Coherent Intermediate Scattering Function. *Phys. Rev. E* **1994,** *49*, 4206.

27. Kroy, K.; Cates, M.; Poon, W., Cluster mode-coupling approach to weak gelation in attractive colloids. *Physical review letters* **2004,** *92* (14), 148302.

28. Guo, H.; Bourret, G.; Corbierre, M. K.; Rucareanu, S.; Lennox, R. B.; Laaziri, K.; Piche, L.; Sutton, M.; Harden, J. L.; Leheny, R. L., Nanoparticle motion within glassy polymer melts. *Physical review letters* **2009,** *102* (7), 075702.

29. Yardimci, H.; Leheny, R., Memory in an aging molecular glass. *EPL (Europhysics Letters)* **2003,** *62* (2), 203.

30. Zondervan, R.; Xia, T.; van der Meer, H.; Storm, C.; Kulzer, F.; van Saarloos, W.; Orrit, M., Soft glassy rheology of supercooled molecular liquids. *Proceedings of the National Academy of Sciences* **2008,** *105* (13), 4993-4998.

31. Negi, A.; Osuji, C., Dynamics of a colloidal glass during stress-mediated structural arrest. *EPL (Europhysics Letters)* **2010,** *90* (2), 28003

32. Negi, A. S.; Osuji, C. O., Physical aging and relaxation of residual stresses in a colloidal glass following flow cessation. *Journal of Rheology (1978-present)* **2010,** *54* (5), 943-958

33. Negi, A. S.; Osuji, C. O., Time-resolved viscoelastic properties during structural arrest and aging of a colloidal glass. *Physical Review E* **2010,** *82* (3), 031404.

34. Abou, B.; Bonn, D.; Meunier, J., Aging dynamics in a colloidal glass. *Physical Review E* **2001,** *64* (2), 021510.

35. Jabbari-Farouji, S.; Tanaka, H.; Wegdam, G. H.; Bonn, D., Multiple nonergodic disordered states in Laponite suspensions: A phase diagram. *Physical Review E* **2008,** *78* (6), 061405.

36. Jabbari-Farouji, S.; Zargar, R.; Wegdam, G.; Bonn, D., Dynamical heterogeneity in aging colloidal glasses of Laponite. *Soft Matter* **2012,** *8* (20), 5507-5512.

37. Bonn, D.; Tanase, S.; Abou, B.; Tanaka, H.; Meunier, J., Laponite: Aging and shear rejuvenation of a colloidal glass. *Physical review letters* **2002,** *89* (1), 015701.

38. Bellour, M.; Knaebel, A.; Harden, J.; Lequeux, F.; Munch, J.-P., Aging processes and scale dependence in soft glassy colloidal suspensions. *Physical review E* **2003,** *67* (3), 031405.

39. Cipelletti, L., Manley, S., Ball, R. C., & Weitz, D. A., Universal aging features in the restructuring of fractal colloidal gels. *Physical review letters*, **2000,** *84*(10), 2275.

40. Krall, A.; Weitz, D., Internal dynamics and elasticity of fractal colloidal gels. *Physical review letters* **1998,** *80* (4), 778.

41. Cipelletti, L.; Ramos, L.; Manley, S.; Pitard, E.; Weitz, D.; Pashkovski, E. E.; Johansson, M., Universal non-diffusive slow dynamics in aging soft matter. *Faraday discussions* **2003,** *123*, 237-251.

42. Bandyopadhyay, R.; Liang, D.; Yardimci, H.; Sessoms, D. A.; Borthwick, M. A.; Mochrie, S. G. J.; Harden, J. L.; Leheny, R. L., Evolution of particle-scale dynamics in an aging clay suspension. *Physical Review Letters* **2004,** *93* (22), 228302.

43. Ramos, L., & Cipelletti, L., Ultraslow dynamics and stress relaxation in the aging of a soft glassy system. *Physical review letters*, **2001**, *87*(24), 245503.

44. Pham, K. N.; Egelhaaf, S. U.; Pusey, P. N.; Poon, W. C. K., Glasses in hard spheres with short-range attraction. *Phys Rev E* **2004,** *69* (1), 011503.

45. Atmuri, A. K.; Peklaris, G. A.; Kishore, S.; Bhatia, S. R., A Re-Entrant Glass Transition in Colloidal Disks with Adsorbing Polymer. *Soft Matter* **2012,** *8*, 8965.

46. Atmuri, A. K.; Bhatia, S. R., Polymer-Mediated Clustering of Charged Anisotropic Colloids. *Langmuir* **2013,** *29* (10), 3179-3187.

47. Kishore, S.; Chen, Y.; Ravindra, P.; Bhatia, S. R., The effect of particle-scale dynamics on the macroscopic properties of disk-shaped colloid–polymer systems. *Colloids and Surfaces A: Physicochemical and Engineering Aspects* **2015,** *482*, 585-595.

48. Nelson, A.; Cosgrove, T., A small-angle neutron scattering study of adsorbed poly(ethylene oxide) on laponite. *Langmuir* **2004,** *20* (6), 2298-2304.

49. Nelson, A.; Cosgrove, T., Dynamic light scattering studies of poly (ethylene oxide) adsorbed on laponite: Layer conformation and its effect on particle stability. *Langmuir* **2004,** *20* (24), 10382-10388.

50. Lal, J.; Auvray, L., Interaction of polymer with clays. *J. Appl. Crystallogr.* **2000,** *33* (1), 673

51. Lal, J.; Auvray, L., Interaction of polymer with discotic clay particles. *Mol. Cryst. Liq. Cryst.* **2001,** *356*, 503.

52. Stuart, M. C.; Waajen, F. H.; Cosgrove, T.; Vincent, B.; Crowley, T. L., Hydrodynamic thickness of adsorbed polymer layers. *Macromolecules* **1984,** *17* (9), 1825-1830.

53. Mongondry, P.; Nicolai, T.; Tassin, J. F., Influence of Pyrophosphate or Polyethylene Oxide on the Aggregation and Gelation of Aqueous Laponite Dispersions. *J. Colloid Interface Sci.* **2004,** *275*, 191

54. De Lisi, R.; Gradzielski, M.; Lazzara, G.; Milioto, S.; Muratore, N.; Prevost, S., Aqueous Laponite Clay Dispersions in the Presence of Poly (ethylene oxide) or Poly (propylene oxide) Oligomers and their Triblock Copolymers. *J. Phys. Chem. B* **2008,** *112*, 9328.

55. Loizou, E.; Butler, P.; Porcar, L.; Kesselman, E.; Talmon, Y.; Dundigalla, A.; Schmidt, G., Large scale structures in nanocomposite hydrogels. *Macromolecules* **2005,** *38* (6), 2047-2049

56. Can, V.; Okay, O., Shake gels based on Laponite-PEO mixtures: effect of polymer molecular weight. *Des. Monomers Polym.* **2005,** *8* (5), 453

57. Zebrowski, J.; Prasad, V.; Zhang, W.; Walker, L. M.; Weitz, D. A., Shake-gels: shear-induced gelation of laponite–PEO mixtures. *Colloids Surf., A* **2003,** *213* (2−3), 189.

58. Baghdadi, H. A.; Jensen, E. C.; Easwar, N.; Bhatia, S. R., Evidence for re-entrant behavior in laponite-PEO systems. *Rheologica Acta* **2008,** *47* (2), 121-127

59. Baghdadi, H. A.; Sardinha, H.; Bhatia, S. R., Rheology and gelation kinetics in laponite dispersions containing poly(ethylene oxide). *Journal of Polymer Science Part B-Polymer Physics* **2005,** *43* (2), 233-240.

60. Baghdadi, H. A.; Parrella, J.; Bhatia, S. R., Long-term aging effects on the rheology of neat laponite and laponite-PEO dispersions. *Rheologica Acta* **2008,** *47* (3), 349-357.

61. Zulian, L.; Marques, F. M.; Emilitri, E.; Ruocco, G.; Ruzicka, B., Dual aging behaviour in a clay–polymer dispersion. *Soft Matter* **2014,** *10* (25), 4513-4521.

62. Gennes, P.-G., *Scaling Concepts in Polymer Physics*. 1 ed.; Cornell University Press: Ithica and London, 1979.

63. Ruzicka, B.; Zulian, L.; Ruocco, G., Routes to Gelation in a Clay Suspension. *Phys. Rev. Lett.* **2004,** *93*, 258301

64. Kroon, M.; Wegdam, G. H.; Sprik, R., Dynamic light scattering studies on the sol-gel transition of a suspension of anisotropic colloidal particles. *Phys. Rev. E* **1996,** *54* (6), 6541.

65. Pontoni, D.; Narayanan, T.; Petit, J. M.; Grubel, G.; Beysens, D., Microstructure and dynamics near an attractive colloidal glass transition. *Physical Review Letters* **2003,** *90* (18), 188301

66. Loizou, E.; Porcar, L.; Schexnailder, P.; Schmidt, G.; Butler, P., Shear-Induced Nanometer and Micrometer Structural Responses in Nanocomposite Hydrogels. *Macromolecules* **2010,** *43* (2), 1041-1049

67. Gournis, D.; Floudas, G., "Hairy" plates: Poly(ethylene oxide)-b-polyisoprene copolymers in the presence of laponite clay. *Chem Mater* **2004,** *16* (9), 1686-1692.

68. Krall, A.; Weitz, D., Internal dynamics and elasticity of fractal colloidal gels. *Physical review letters* **1998,** *80* (4), 778.

69. Bouchaud, J.-P.; Pitard, E., Anomalous dynamical light scattering in soft glassy gels. *The European Physical Journal E* **2001,** *6* (3), 231-236

70. Bandyopadhyay, R.; Liang, D.; Yardimci, H.; Sessoms, D.; Borthwick, M.; Mochrie, S.; Harden, J.; Leheny, R., Evolution of particle-scale dynamics in an aging clay suspension. *Physical review letters* **2004,** *93* (22), 228302.

71. Shahin, A.; Joshi, Y. M., Physicochemical Effects in Aging Aqueous Laponite Suspensions. *Langmuir* **2012,** *28* (44), 15674-15686.

72. Kozer, N.; Kuttner, Y. Y.; Haran, G.; Schreiber, G., Protein-protein association in polymer solutions: From dilute to semidilute to concentrated. *Biophys J* **2007,** *92* (6), 2139-2149.

73. Ali, S.; Bandyopadhyay, R., Evaluation of the exfoliation and stability of Na-montmorillonite in aqueous dispersions. *Applied Clay Science* **2015,** *114*, 85-92.

74. Holyst, R.; Bielejewska, A.; Szymanski, J.; Wilk, A.; Patkowski, A.; Gapinski, J.; Zywocinski, A.; Kalwarczyk, T.; Kalwarczyk, E.; Tabaka, M.; Ziebacz, N.; Wieczorek, S. A., Scaling form of viscosity at all length-scales in poly(ethylene glycol) solutions studied by fluorescence correlation spectroscopy and capillary electrophoresis. *Phys Chem Chem Phys* **2009,** *11* (40), 9025-9032.

75. Wyart, F. B.; de Gennes, P. G., Viscosity at small scales in polymer melts. *Eur Phys J E* **2000,** *1* (1), 93-97.

76. Schosseler, F.; Kaloun, S.; Skouri, M.; Munch, J., Diagram of the aging dynamics in laponite suspensions at low ionic strength. *Physical Review E* **2006,** *73* (2), 021401.

# CHAPTER 4

# MICROSTRUCTURE OF COLLOID-POLYMER MIXTURES CONTAINING CHARGED COLLOIDAL DISKS AND WEAKLY-ADSORBING POLYMERS

## 4.1 Introduction

Particles in colloidal dispersions self-assemble under different conditions to form disordered arrested phases/states like colloidal glasses and gels. It is, thus, of importance to understand the formation mechanism and the characteristic nature of these states as it helps in tuning material properties for a specific technological application and in determining the shelf life or long term stability of the material itself. Colloidal glasses and gels can form when the particle volume fraction is increased or when salts, surfactants or polymers are added to the system to modify interactions between particles. Hard-sphere colloidal systems are often used as simple models to understand the physics behind the formation of glasses and gels. For hard-sphere colloids at concentrations close to the fluid-glass transition ($\phi_c \sim 0.58$), the system transitions from a homogeneous liquid phase to an arrested glassy phase primarily due to increasing excluded volume effects[1,2]. On the other hand, fluid-gel transitions can occur along a wider range of concentrations by increasing the range and strength of attractions between particles in the system. One way to achieve this is by adding salts to a charged repulsive colloidal system. The addition of salts increases attractions between particles by screening the electrostatic repulsive interactions. Fractal-like aggregates begin to form, and under certain conditions the fractal structure percolates to form a space-filling gel like network[3]. Colloidal gels can also form by the addition of non-adsorbing polymers to a hard sphere system, which

causes a depletion attraction between particles. Recent studies have shown that the formation of this arrested phase is due to increasing strength of short-range attractions and can be precisely controlled by simply changing the length and the concentration of polymer chains in the system[4,5]. Experiments have also shown that the addition of non-adsorbing polymers to a glassy colloidal system can shift the effective fluid-glass transition to a higher volume fraction, thus making it feasible to work with a fluid phase at higher particle loadings[6]. Understanding the formation of these states in suspensions containing aspherical colloids is however not straightforward, as shape anisotropy and physical aging effects contribute to the existing complexities in the problem.

Laponite® is a model system that is often used to study the structure, phase behavior and dynamics of colloidal disks, as it exhibits a very rich physical behavior. Laponite® is a charged synthetic clay (~25nm wide, ~1nm thick) with an empirical formula of $Na^{+}_{0.7}[(Si_8Mg_{5.5}Li_{0.3})O_{22}(OH)_4]^{-0.7}$. The particles carry a negatively-charged face which is counterbalanced with the $Na^{+}$ ions present in between layers and a pH-governed charge distribution along the edges due to the formation of surface charges during hydration and swelling. Extensive studies have been conducted using techniques such as rheology[7], light, neutron and x-ray scattering experiments[8,9] to probe the structure and phase behavior of aqueous laponite® dispersions at different particle and salt concentrations. Bonn and co-workers used light scattering and conductivity experiments to classify dispersions of laponite® into three different arrested states; (i) Gels ($c_l$ < 1.5wt%), (ii) Repulsive glasses ($c_l$ > 1.5wt%) and (iii) Attractive glasses ($c_l$ < 1.5wt%, high salt conc.), based on the evolution of the relaxation time parameters[10].

Colloidal glasses and gels of laponite® both exhibit solid-like rheological behavior, and there are few experimental methods to distinguish between these two different arrested states. In comparison with spherical colloids, the formation of glassy phases in laponite® occurs at a much lower volume fraction of ~ 0.01. The formation of colloidal glasses in most cases is driven by dominant electrostatic repulsions between particles, and in other cases it is driven by weak inter-particle attractions. Many refer to the latter condition as an "attractive glass," as long lived attractive bonds between particles exist in this structurally arrested phase, and the former state as "Wigner" glasses, although there is still a considerable amount of debate on whether these are gels or glasses[11,12,13]. Similar to the hard sphere system, colloidal gels in laponite® form when clusters begin to span the volume to form a space-filling network. In rheological experiments, glassy systems follow the framework of the SGR model[14] and gels can be identified by using the Winter-Chambon's criterion[15] where a single iso-frequency tan delta point can be correlated with the fractal dimensions in the system. Neutron and x-ray scattering measurements are also used to identify these structures in the colloidal system. Colloidal glasses are homogeneous at larger length scales and correlations are restricted to the interparticle distances, whereas for the colloidal gel, correlations exist at larger distances with the structure factor profiles showing large low-$q$ fluctuations[11,12].

Laponite® gels and glasses have been studied extensively by several groups. However, there is still a considerable amount of debate on whether these systems are really gels or glasses. Several studies in the literature have reported the phase diagram of laponite® as a function of both particle and salt concentration. There seems to be a large consensus on the observation that laponite® particles phase separate at concentrations

below 1% and when the salt concentration is above 20mM[16]. It is also known that for concentrations between 1% and 2%, the suspensions largely evolve to form colloidal gels. However, the final state and microstructure in systems at and above 2% is largely unclear. Small-angle x-ray scattering experiments conducted by Ruzicka and co-workers have found that systems above a concentration of 2% form glassy phases where particles remain frozen and disconnected in the system[17]. Interestingly, results from a recent study by the same group have indicated that while these exists as repulsive glasses during the early aging period, the same system exhibited a repulsive glass – attractive glass transition due to increasing attractions as aging proceeds in the system[18]. On the contrary, studies conducted by Mongondry and Joshi have shown that the particles exist as colloidal gels where attractive bonds do exist between particles[19,20]. Comprehensive set of experiments conducted by Joshi and co-workers have shown that structural arrest in laponite® systems is not driven just by repulsions but also by attractive interactions between particles[20].

The kinetics of structural arrest in laponite® can be modified by the addition of salts to the system. The addition of salts results in the screening of the electrostatic repulsions thereby increasing the van der Waals attraction between particles. The rate of particle aggregation under different salt conditions has been extensively studied by many groups. At very high salt concentrations and at low concentrations of laponite®, the particles begin to aggregate and phase separate under the influence of gravity. Another way of modifying the interactions between the particles is by adding polymers to the system. Several techniques like NMR, reflectometry, x-ray and neutron scattering have been used to study the interaction of polymers with colloidal surfaces[21-24]. Polymers are expected to

contribute to a variety of interactions depending on the nature of the polymer and on the way it interacts with the surfaces of a colloidal particle. While non-adsorbing polymers trigger attractive interactions based on thermodynamic effects, adsorbing polymers can contribute to both steric repulsions and, if chains are sufficiently long, a bridging attraction between particles. Adding short polymer chains to a laponite® system is known to slow down the aggregation process due to steric effects, and adding longer polymer chains leads to the formation of large-scale clusters and space-filling gels in the system[25,26].

Experiments using rheology were previously conducted to study the effect of chain length and concentration of polymers on the macroscopic properties of a laponite®-PEO system. Results from rheological experiments conducted for systems containing 2% laponite® with PEO have shown that two different behaviors exist when the polymer chain length is allowed to vary; (i) retardation in gelation kinetics for molecular weights below 83 kg/mol due to steric effects and (ii) accelerated gelation kinetics for molecular weights above 83 kg/mol because of polymer bridging[27,28]. Studies have also shown that by changing the concentration of small PEO chains, the system transitions through a re-entrant behavior because of increasing depletion attractions in the system. More recently our group has recently studied the effects of varying the concentration of PEO on the macroscopic properties of the system[29,30].

In this chapter, we discuss the use of ultra-small angle x-ray scattering (USAXS) to investigate the microstructure of laponite® systems with poly(ethylene oxide), a weakly adsorbing polymer. In order to systematically examine microstructural changes, we consider two different polymer-colloid size ratios to highlight the effects of long ($R_g/R$ ~

2.4) and short ($R_g/R$ ~ 0.5) polymer chains on the formation of structures in the system. In both cases, the concentration of PEO was allowed to vary between 0.25% and 2.5% (w/w). For the longer PEO chain, this allows us to look at variations in the structure in the concentrated polymer regime. On the contrary, for the shorter PEO chains the range spans regions between dilute and semi-dilute polymer regimes.

## 4.2 Materials and Methods

Laponite® RD was procured from Southern Clay Products (Gonzales, TX, USA) and poly (ethylene) oxide (PEO) with number-average molecular weight, $M_w$, of 20 and 300 kg mol$^{-1}$ were purchased from Sigma Aldrich and used without any further purification.

### 4.2.1 Sample Preparation

Laponite® dispersions were first prepared by adding a calculated amount of clay to de-ionized Millipore water with its pH adjusted to 10 using sodium hydroxide (NaOH) to ensure stability against dissolution. A T25 UltraTurrax homogenizer was used for about 1 minute to disperse particles thoroughly. The solutions were then agitated for 20 minutes and filtered through a 0.45μm filter to remove large aggregates. PEO was then added to obtain the desired concentration. The samples were stirred until the polymer completely dissolved. The samples were then sealed and stored at 25°C to allow them to spontaneously age with time and the aging clock now is set to $t_0$.

### 4.2.2 Ultra-small angle x-ray scattering

Ultra-small angle x-ray scattering measurements were conducted at the Advanced Photon Source (APS), Argonne National Laboratory. Samples for the USAXS experiments were prepared by loading a required amount of dispersion from the samples that were prepared as described in the earlier section, into a 1mm capillary tube. The

capillary tubes were then sealed and the mixtures were allowed to spontaneously age with time. The scattered intensities were recorded over a broad range of scattering wave-vectors, $q$, from ~$10^{-4}$Å to $10^{-1}$Å and the background scattering of pure water was subtracted. The experiment enables us to explore the presence of micron-sized domains at low $q$ and the presence of individual disks at higher $q$.

Table 4.1 lists the experimental system used for this study. $c^* = 3M_w/4\pi R_g^3 N_A$ is the polymer overlap concentration. The amount of polymer needed to saturate a laponite® particle surface exhibits a weak power-law relationship with molecular weight ($\Gamma \sim M_w^{0.05}$). The concentration of PEO bound to the surfaces of a laponite® particle, estimated using NMR relaxation experiments, was found to be ~0.18%. This corresponds to a coverage of 0.4 mg/m$^2$, approximately. Additionally, laponite® has a specific surface area of 900m$^2$/g. Therefore, for every gram of laponite® the amount of PEO at saturation can be calculated as (900 m$^2$/g) x (adsorbed amount at saturation) x (1g/1000 mg). The concentration of PEO needed to saturate or bind to all available particle surfaces ($c_{sat}$) was estimated to be ~0.75% for systems containing 2% laponite® and 1.08% for systems with 3% laponite®. This is strictly based on the assumption that all adsorption surfaces are available to the polymer and that there is a perfectly monodisperse particle size distribution.

Table 4.1 : Experimental system used in this study. Polymer overlap concentration, $c^*$, size ratio $R_g/R$ and the particle surface saturation concentration, $c_{sat}$

| PEO $M_w$ kg/mol | Critical overlap concentration, $c^*$ (%) | Radius of gyration, $R_g$ (nm) | Polymer-colloid size ratio $R_g/R$ | Particle Saturation Concentration, $c_{sat}$ (%) | |
|---|---|---|---|---|---|
| | | | | 2% laponite® ($\phi_c$ ~ 0.0075) | 3% laponite® ($\phi_c$ ~ 0.011) |
| 20 | 2.93 | 6.67 | 0.533 | 0.75 | 1.08 |
| 300 | 0.43 | 30.34 | 2.43 | | |

### 4.3 Results and Discussion

USAXS experiments were carried out on systems containing laponite® RD with and without poly(ethylene oxide). The data reduction and analysis was done using the standard analysis macros that are available using the IGOR software platform[31].

#### 4.3.1 Scattering from laponite® systems without PEO

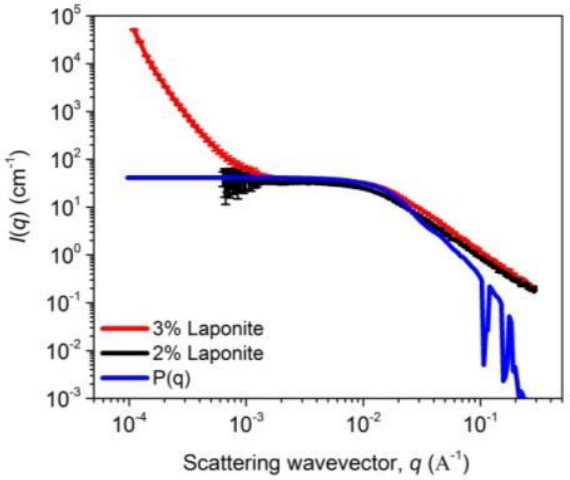


Figure 4.1 : USAXS spectra of neat laponite® systems at a particle concentration of 2% and 3%. Spectra show a low-$q$ upturn with increasing laponite® particle concentration

Figure 4.1 shows the scattering profiles of 2% and 3% laponite® dispersions along with the form factor of a single disk with radius 125Å and thickness of 10Å. The form factor a disk shaped particle is as given below:

$$P(Q) = \int_0^{\pi/2} sin\theta d\theta \left(V_p \Delta\rho\right)^2 \left\{ \frac{sin\left[QH_p cos\theta/2\right]}{QH_p cos\theta/2} * \frac{2J_1\left[QR_p sin\theta\right]}{QR_p sin\theta} \right\}^2$$

where $R_p$ and $H_p$ are the radius and the thickness of the particle respectively, $V_p$ is the volume of one particle and $\Delta\rho$ is the difference in the scattering length densities of laponite® and the solvent, which in this case is water. The x-ray scattering length density of laponite® was calculated according the composition of the grade of laponite® and was estimated to be $2.25*10^{-5}$ Å$^{-2}$. The scattering length density of water $\rho_w = 9.46*10^{-6}$ Å$^{-2}$.

In order to measure the radius of the particle, the scattering from a 1% dilute suspension of laponite® was recorded. The characteristic size of the particle was estimated by using a simple Guinier analysis (Appendix B, Figure B3) and was found to be ca. 12.9±0.125 nm. For a homogeneous phase of single disks, the data along the high $q$ range ($q$ > 0.02 Å$^{-1}$) typically exhibits a $q^{-2}$ dependency. In the case of the 2% and 3% laponite® systems, this value of slope was found to be less than 2 which might be indicative of the presence of some polydispersity in the system. Along the intermediate regions of $q$ (0.002 Å$^{-1}$< $q$ < 0.08 Å$^{-1}$), we observe a plateau in the intensity for both the 2% and the 3% laponite® system. At lower $q$ values ($q$ < 0.002 Å$^{-1}$), we observe an upturn in the intensity for the more concentrated laponite® suspension. The scattering profile exhibits a power law dependence in this $q$ range, with the intensity scaling as $I \sim Aq^{-x}$. A similar upturn in the low-$q$ region has been observed in neat laponite®

suspensions by Bhatia and co-workers[32]. Such low-$q$ upturns are a characteristic feature of fractals or dense aggregates in the system and are commonly seen in colloidal gels.

### 4.3.2 Scattering of laponite® systems with High-$M_w$ PEO

The addition of a high molecular weight PEO increases the rate of gelation primarily due to bridging effects which begin to play an important role as the size of the polymer chains is now equivalent to the interparticle distances. There are a few studies in the literature that discuss the phase behavior of laponite® with 300 kg/mol PEO[33] and the dynamic responses of these systems to the application of different magnitudes of shear[34]. In a recent work by Prasad and co-workers, static and dynamic light scattering experiments were conducted to classify the phase behavior laponite®-PEO systems with different concentrations of laponite® and PEO. They observed different types of behavior in these systems; (i) reversible shake gels formed on the application of a high amount of shear, (ii) some systems shear thickened at high deformation rates and (iii) viscous samples remained fluid-like and showed no shear thickening or shake gel like behavior[35].

Figure 4.2 shows the scattering profiles of suspensions with 2% laponite® and 300 kg/mol PEO. For comparison, the scattering spectra of 2% laponite® has been shown alongside each system's scattering profile. The scattered intensity profiles in the higher $q$ do not change with increasing PEO concentration, which implies that the structural arrangement at the particle-scale level is not altered greatly with increasing PEO content. The slope of the intensity profile along the higher $q$ regions is ~ -1.79 ± 0.04. This is slightly less than the slope that would be expected for monodisperse disks, -2, which could indicate either polydispersity or a contribution from PEO chains, even though the laponite® disks scatter more strongly than the PEO chains. In laponite®-PEO systems at

higher polymer concentrations, where $c_p/c^* > 1.0$, it is reasonable to expect that there will be some contribution from the scattering of the entangled polymer chains in the system. We examined the scattering of polymer solutions at the highest concentration with water at pH 10 as the solvent at 25°C (Figure B4).

For regions of $q < 0.02$ Å$^{-1}$ we observe that the scattered intensities are no longer flat, and they begin to exhibit a power law dependence with $q$. Small upturns in the intermediate $q$ regions indicate the presence of structures at length scales greater than ~300 Å. As we increase the concentration of PEO in the system, we observe a non-monotonic variation in the slopes of the low-$q$ upturn in the regions of $q< 0.001$ Å$^{-1}$. To analyze the scattering in the $q$ range between 0.001Å$^{-1}$ and 0.0001Å$^{-1}$ we fit the curves with a power law $Aq^{-x}$, where $-x$ is the power law slope in this region. The curves showing the fits are presented in Figure B5 (Appendix B) and the values of the power law slopes of these fits are shown in Figure 4.3. In the full aging regime, 2% laponite® system does not exhibit a power law behavior at low-$q$ but is instead homogeneous at large length scales. However, with increasing concentration of PEO the exponents vary between 2.25 and 3.5.

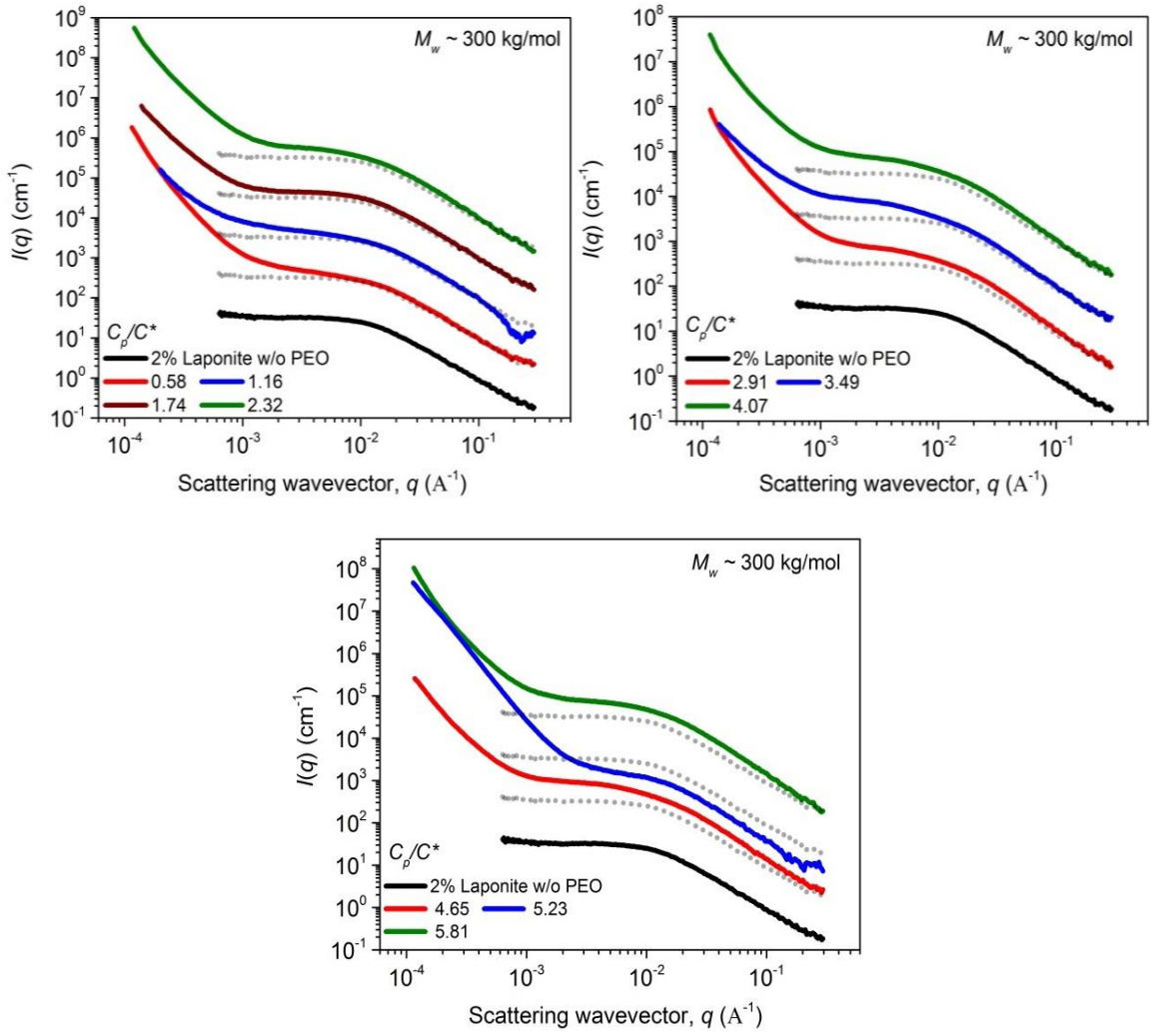


Figure 4.2 : USAXS spectra of suspensions with 2% laponite® and 300 kg/mol PEO. The scattering profiles have been vertically shifted for clarity. The dotted profiles (•••) show the scattering from the 2% laponite® without PEO.

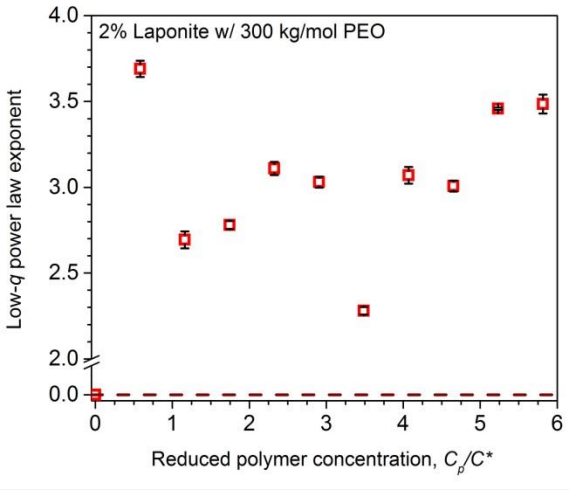


Figure 4.3 : Power law exponent obtained by fitting the low-$q$ region with $q^{-x}$. The fits to the spectra are shown in Figure B5 (Appendix B).

Similarly, we looked at the variations in the scattering profiles of suspensions containing a higher particle fraction of $\phi_c \sim 0.011$. Figure 4.4 shows the USAXS spectra of 3% laponite® – 300 kg/mol PEO systems. Suspensions containing a higher particle concentration transition to an arrested phase at shorter timescales. In the case of the 3% laponite® system, we observe a low-$q$ dependence for all compositions suggesting the existence of a network-like structure. With the addition of PEO to this system, changes in the structure are observed through the variations in this low-$q$ dependence of the scattering intensities. A higher scattering intensity in systems with PEO concentrations ($c_p/c^*$) between 2.5 and 5 is expected as we now have larger number of scattering entities and as the concentration of PEO increases we expect that the number of entanglements in the polymers is more. We analyze the low-$q$ dependence by fitting the USAXS spectra in the region of $q < 0.001$ Å$^{-1}$ with the power law $\sim q^{-x}$. The results of these fits are presented in Figure 4.5 and the scattering profiles showing these fits are presented in Figure B6. As

shown in Figure 4.5, the variations in the power law exponents for systems with different PEO concentrations is non-uniform and falls within a range of 2.2 and 3.8.

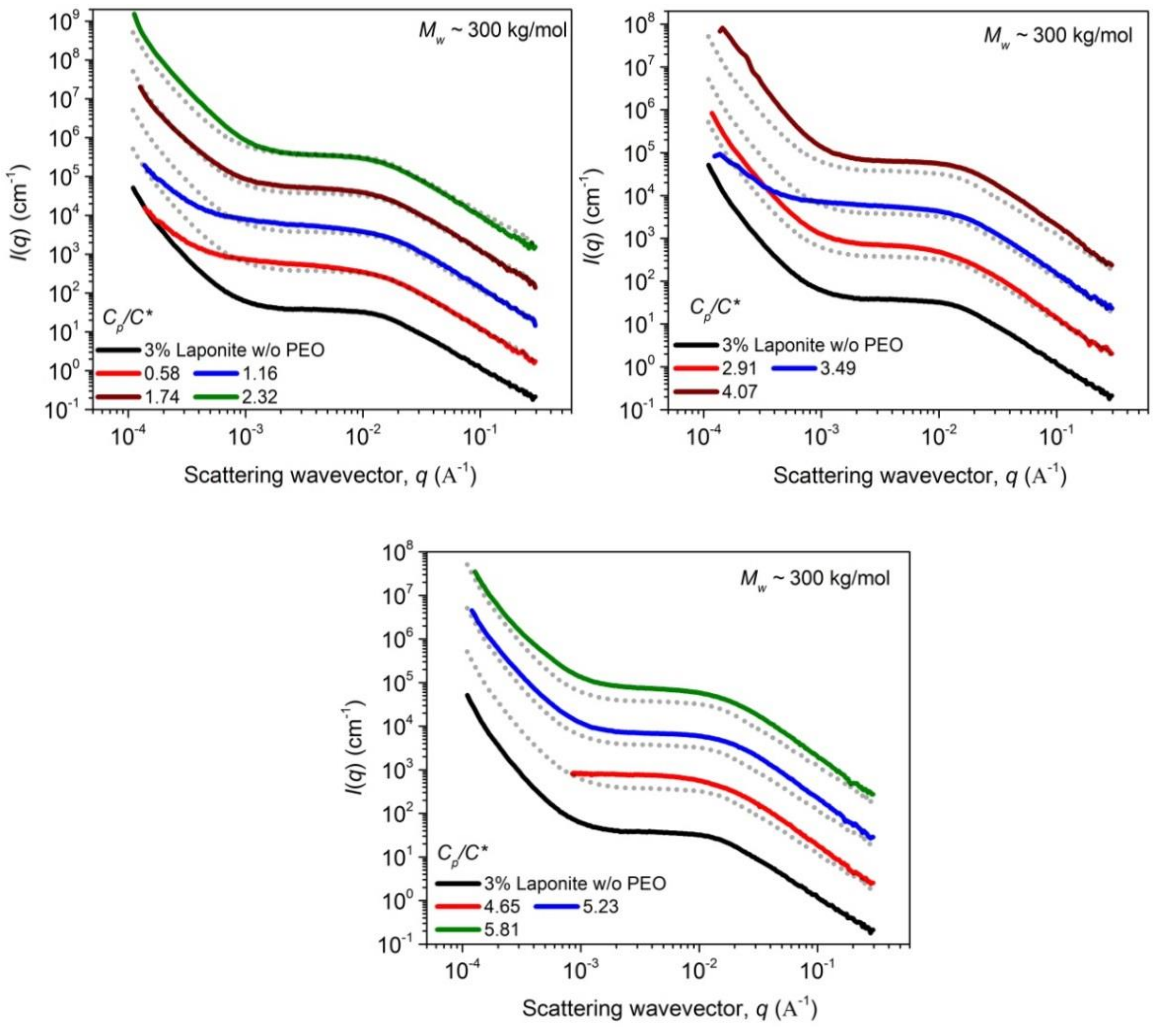


Figure 4.4 : USAXS spectra of systems with 3% laponite® and various concentrations of the 300 kg/mol PEO. The scattering profiles have been vertically shifted for clarity. The dotted profiles (•••) show the scattering from the 3% laponite® without PEO.

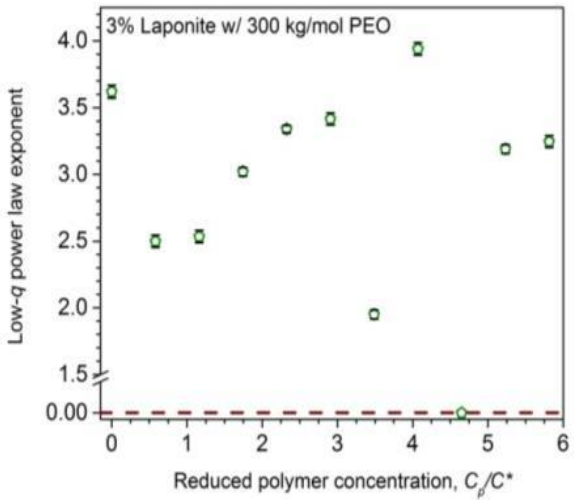


Figure 4.5 : Values of the power law exponents obtained by fitting the low-$q$ upturn to $\sim Aq^{-x}$. The fits to the spectra are shown in Figure B6 (Appendix B).

The most distinct feature in these scattering profiles is the strong $q$ dependence in the low-$q$ region. This type of scattering has been previously observed in laponite® PEO mixtures containing 3% laponite® and 2% PEO with molecular weights 100 kg/mol, 300 kg/mol and 600 kg/mol. In this work, SANS and USANS experiments showed that the low-$q$ scattering scaled as $q^{-1.55}$ and this confirmed the presence of large-scale open structures where the polymer coated particles are tethered together to form a sponge-like network. However, as we can see from the power law fits, the presence of free polymer chains does have some influence on the microstructure in the system.

Figures 4.3 and 4.5 indicate that several laponite®-PEO systems exhibit an excess scattering with power law exponents varying between -3 and -4. These values are indicative of surface scattering where a power law value of -3 corresponds to the scattering from very rough surfaces. On the other hand, a value of -4 is often described by a Porod like scattering from smooth objects. A similar $q$-dependence was observed in hard-sphere colloidal silica systems with a non-adsorbing polymer by Zukoski and co-

workers. This unusually high *q*-dependence was attributed to the formation of dense, polydisperse aggregates with rough surfaces. Using various physical models, they were able to determine that the aggregates were 5-8 particle diamters in size[36].

With respect to the systems that we are studying, we observe large scale fluctuations from 0.002 $Å^{-1}$ to $10^{-4}$ $Å^{-1}$. In real space, this corresponds to length scales between 0.3μm to 6μm. The formation of large-scale structures in laponite®-PEO was previosuly investigated in systems containing 3% laponite® by Schmidt and co-workers. Cryo-TEM and SEM imaging of their laponite®-PEO systems show the existence of clay-rich and clay poor regions in the systems. This heterogenous distribution in the structure can be described by the Debye-Bueche model which is given by the following equation[37]:

$$I(q) \sim \frac{I_0}{(1 + q^2 \xi_v^2)^2}$$

where $I_0$ is the average mass which takes into the differences in the number densities between the dense aggregates and the dilute spaces within the network. $\xi_v$ is a correlation length that describes the distance between the dilute regions surrounding the dense aggregates in the system. In order to obtain values of the parameters $I_0$ and $\xi_v$, we rearrange the above equation to obtain an expression of the form $y = mx + c$ (shown in the Appendix). We plot $I(q)^{-1/2}$ vs $(qD)^2$ and make a linear least square fit over a small range of $q$ where a linearity is observed. Here, the observed slope $m = (\xi_v/D)^2 * I_0^{-1/2}$ and the intercept $c$ is $I_0^{-1/2}$.

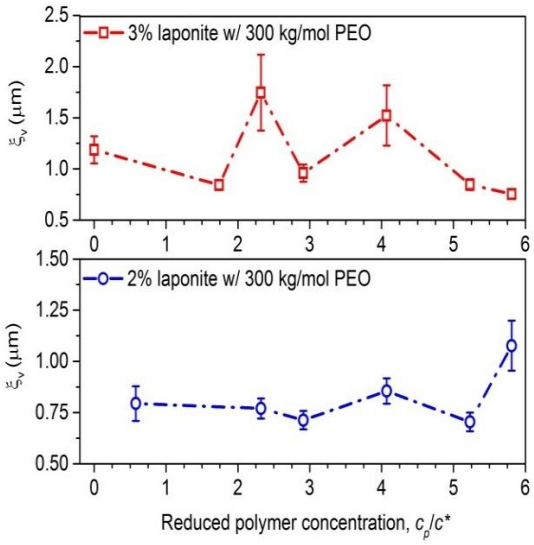


Figure 4.6 : Debye Bueche analysis for systems with laponite® and PEO that exhibit a low-*q* power law scattering with an exponent between 3.1 and 4. Values of the heterogeneity correlation length ($\xi_v$) were obtained by using a linear least square fit over regions of ($qD$) < 0.245. The Debye Bueche plots are shown in the Appendix B (Figure B7).

Figure 4.6 shows the changes in the heterogenity parameter, $\xi_v$, for systems exhibiting a power law exponent greater than 3. For the series of samples containing 2% laponite®, the parameter $\xi_v$ were found to vary non-uniformly with changes in the PEO concentration and the values were typically between 0.75μm and 1μm. On the other hand, for the series of samples containing 3% laponite®, this correlation length is expected to decrease as the interparticle distance is smaller than when compared to the 2% laponite® system, and polymer bridging results in the formation of more compact or tighter aggregates in the system.

### 4.3.3 Scattering of laponite® with Low-$M_w$ PEO

Figures 4.7 – 4.10 show the USAXS spectra of the colloidal system with low molecular weight PEO.

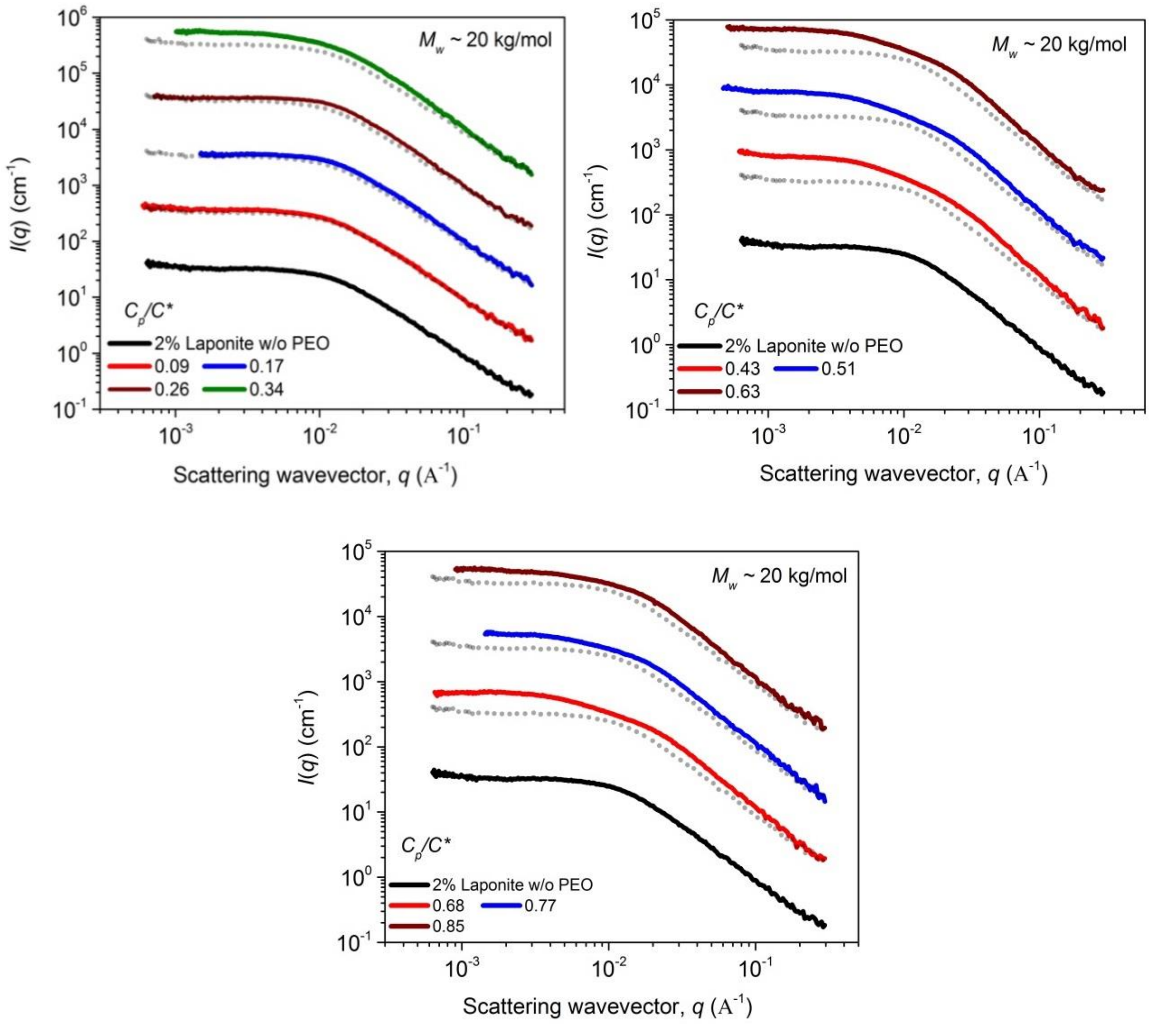


Figure 4.7 : USAXS spectra of suspensions containing 2% laponite® with varying concentrations of 20 kg/mol PEO. The scattered intensity profiles have been vertically shifted for clarity. The dotted profiles (•••) show the scattering from the 2% laponite® without PEO.

The polymer to colloid size ratio in this case is nearly 0.5. In contrast with the systems containing long PEO chains, the USAXS spectra do not show any characteristic excess scattering in the lower *q*-regions which suggests that there are no large domains or structures in these systems. The intensity profile is flat along the intermediate ranges of *q* (0.002 Å$^{-1}$ – 0.02 Å$^{-1}$) and the slopes in the high-*q* region are ca. -1.8 – -1.9, which are

close to the high-$q$ scattering expected for disk-like objects. As above, the slope is a little different than -2, but we expect these differences to occur because of two contributing factors; (i) there may be some polydispersity in the system and (ii) polymer chains also contribute to the scattering. With the addition of a small amount of PEO in the system, we do not observe any remarkable change in the USAXS spectra. However, at a concentration of $c_p/c^* = 0.26$, there is an appearance of a weak correlation peak at a $q$-value of 0.001Å$^{-1}$. Correlation peaks occur as a result of increasing interactions between two neighboring particles. In this case, this is expected to occur as interparticle distances decrease due to increasing local attractions in the system. At intermediate concentrations of PEO, we observe a scattering profile that is qualitatively different than what is observed in systems with smaller amounts of PEO. For concentrations beyond 0.34, the profiles show the existence of two Guinier regions and one Porod region. Such features are seen when the scattering arises either from non-spherical objects in the system or from two different populations of the same kind. The description of scattering from aspherical objects has been elaborately discussed by Hammouda, and a generalized model has been proposed[38].

According to the generalized Guinier Porod model:

$$I(q) = \frac{G_2}{q^{s_2}} \exp\left(\frac{-q^2 R_{g2}^2}{3 - s_2}\right) \qquad q \leq q_2$$

$$I(q) = \frac{G_1}{q^{s_1}} \exp\left(\frac{-q^2 R_{g1}^2}{3 - s_1}\right) \qquad q_2 \leq q \leq q_1$$

$$I(q) = \frac{D}{q^d} \qquad q \geq q_1$$

where $s_1$ and $s_2$ are dimensionality parameters; $G_1$, $G_2$ and $D$ are the scaling factors for the Guinier and the Porod regions respectively; and $R_{g1}$ and $R_{g2}$ describe the dimensions of the object. $q_1$ and $q_2$ are cut off values marking the transition between the three regions in the spectra and are calculated internally using the conditions of continuity. For spherical systems both $s_1$ and $s_2$ are 0 owing to its shape symmetry, and for cylindrical objects, $s_2 = 0$ and $s_1 = 1$. The Porod exponent usually describes the nature of the scattering inhomogeneities in the system; a Porod exponent of 2 represents the scattering from Gaussian polymer chains or can also represent the scattering from platelets or disks. An exponent of 5/3 represents the scattering from swollen polymer chains in a good solvent.

The scattering spectra of systems with 2% laponite® and intermediate concentrations of PEO were successfully fit with the GP model using the non-linear least square fitting and is shown in Figure 4.8. Table 4.2 lists the values of the parameters obtained by fitting the data with the generalized GP model. For all of the systems that were examined using this model, the dimensionality parameter $s_1$ was neither 1 nor 0 indicating that the scattering objects were of some intermediary structure. Assuming the extreme limit of this being a cylinder, as a first guess we estimate the radius $R$ as $R_{g1}*2^{1/2}$ and the length $L$ as $12^{1/2}/(R_{g2}^2 - R_{g1}^2)^{1/2}$.

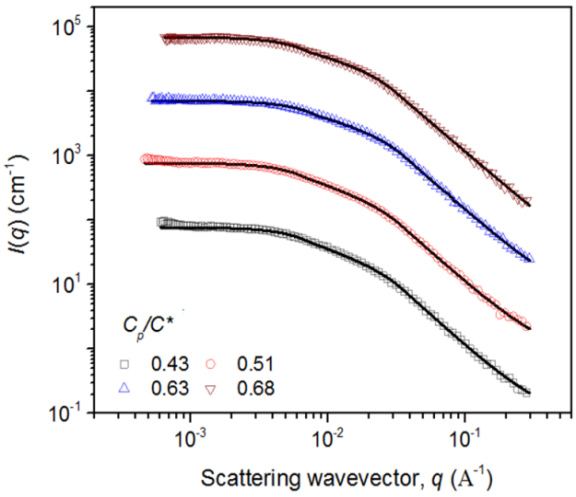


Figure 4.8 : USAXS spectra of 2% laponite® systems with 20kg/mol PEO at different concentrations. Open symbols indicate scattering data, while solid lines indicate the fit of the data with the Guinier Porod Model.

Table 4.2 : Best fit parameters obtained by fitting data to the Guinier-Porod model.

| laponite®-PEO ($c_p/c^*$) | $s_1$ | $R_{g1}$ (nm) | $R$ (nm) | $R_{g2}$ (nm) | $L$ (nm) |
|---|---|---|---|---|---|
| 0.43 | 0.78 ±0.006 | 3.13 ±0.034 | 4.42 ±0.07 | 17.53 ±0.10 | 59.66 |
| 0.51 | 0.75 ±0.006 | 3.22 ±0.035 | 4.55 ±0.07 | 18.96 ±0.12 | 64.73 |
| 0.63 | 0.64 ±0.0065 | 3.67 ±0.038 | 5.19 ±0.08 | 18.10 ±0.03 | 61.40 |
| 0.68 | 0.62 ±0.0069 | 3.79 ±0.039 | 5.36 ±0.08 | 18.36 ±0.18 | 62.24 |
| 0.77 | 0.47 ±0.008 | 4.61 ±0.048 | 6.52 ±0.10 | 16.42 ±0.22 | 53.88 |

The results from fitting the spectra to the GP model indicate very small changes in the microstructure at length scales beyond the particle size. Considering the fact that the scattering objects are not cylindrical but some intermediate structures between a spherical and a cylindrical object we make an attempt at quantifying these structures using the Elliptical cylindrical model[39].

The Elliptical Cylinder (EC) model considers the scattering to be originating from a cylindrical object with an elliptical cross section[40]. In this model, an elliptical cylinder of length *L* has a minor radius and a major radius and the ellipticity parameter (ν) which is the ratio of the major over the minor radius is always greater than 1.

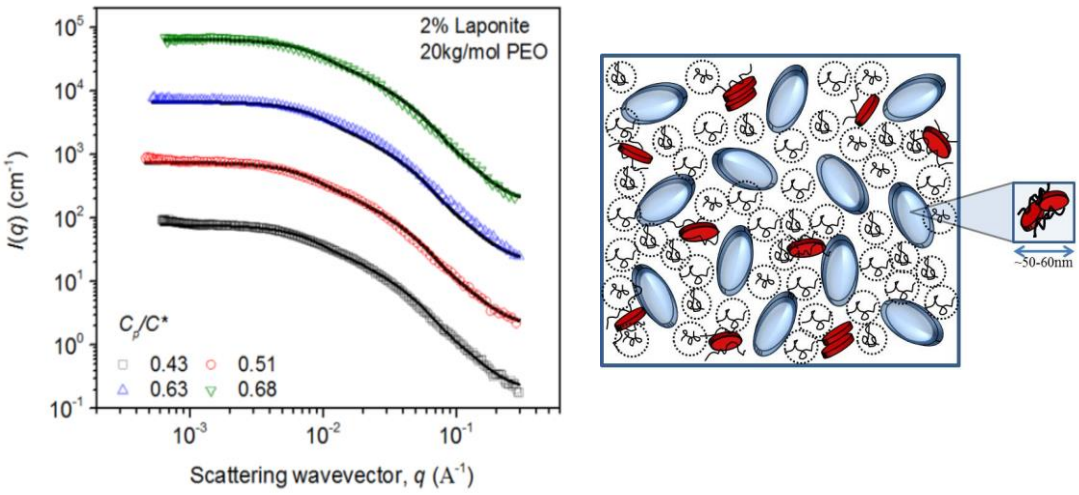


Figure 4.9 : (a) USAXS spectra of 2% laponite® systems with 20kg/mol PEO at different concentrations. Open symbols indicate scattering data, while solid lines indicate the fit of the data with the Elliptical Cylinder model and (b) schematic representation of the intermediate structure as seen in these systems.

Table 4.3 : Best-fit parameters obtained by fitting data to the Elliptical Cylinder Model

| 20 kg/mol PEO ($c_p/c^*$) | Minor Radius (nm) | ν = Major/Minor | Major Radius (nm) | Length (nm) | Bkg ($cm^{-1}$) | Reduced $\chi^2$ |
|---|---|---|---|---|---|---|
| 0.43 | 0.75 ±0.002 | 5.76 ±0.034 | 4.32 | 59.06 ±0.23 | 0.21 ±0.001 | 2.77 |
| 0.51 | 0.709 ±0.002 | 6.09 ±0.036 | 4.32 | 60.69 ±0.25 | 0.21 ±0.001 | 2.68 |
| 0.63 | 0.742 ±0.002 | 5.80 ±0.03 | 4.30 | 52.31 ±0.21 | 0.22 ±0.001 | 3.09 |
| 0.68 | 0.744 ±0.002 | 5.49 ±0.03 | 4.08 | 53.49 ±0.213 | 0.19 ±0.001 | 3.72 |

The scattering spectra of the same set of systems that were analyzed using the generalized GP model were successfully fit with the EC model (Figure 4.9) and the reduced chi-squared ($\chi^2$) parameter was found to be less than 4.0. Results of the fit of this model to the spectra are shown in Table 4.3. The results from fitting the spectra to the EC model suggest that these are fairly consistent with the results derived from fitting the spectra to the GP model. The major and the minor radii do not vary greatly with increasing PEO concentration. The major radius was found to be ca. 4nm for all the systems. However, we observe that the lengths of these objects vary non-uniformly between 52nm and 61nm.

In order to investigate the effects of particle concentration on the microstructure in these systems, a similar set of experiments were conducted for systems with 3% laponite®. At higher particle fractions of $\phi_c \sim 0.011$, we do not observe the formation of large-scale structures in the system. The structure is homogenous along intermediate ranges of $q$ for systems with PEO concentrations above 0.28. For systems containing PEO, the slope at higher $q$ is sometimes 2 or slightly greater than 2, which is reasonable as polymer chains are expected to contribute to some scattering in the higher $q$ regions. With the addition of small amount of PEO, we observe a small peak in the scattering intensity. However, as we keep adding more polymer chains to the system the correlation peak is no longer observed in this region and a flat intensity plateau is observed at higher concentrations of PEO. At intermediate concentrations of PEO, contrary to 2% laponite® series, we do not observe the formation of intermediate structures in the samples. Attempts to fit the USAXS spectra to a polydisperse core-shell cylinder model failed as the parameter fit results yielded unphysical values. This can be expected as the system is

concentrated and increasing interference effects will render it difficult to extract meaningful values of the radial and face side shell thicknesses.

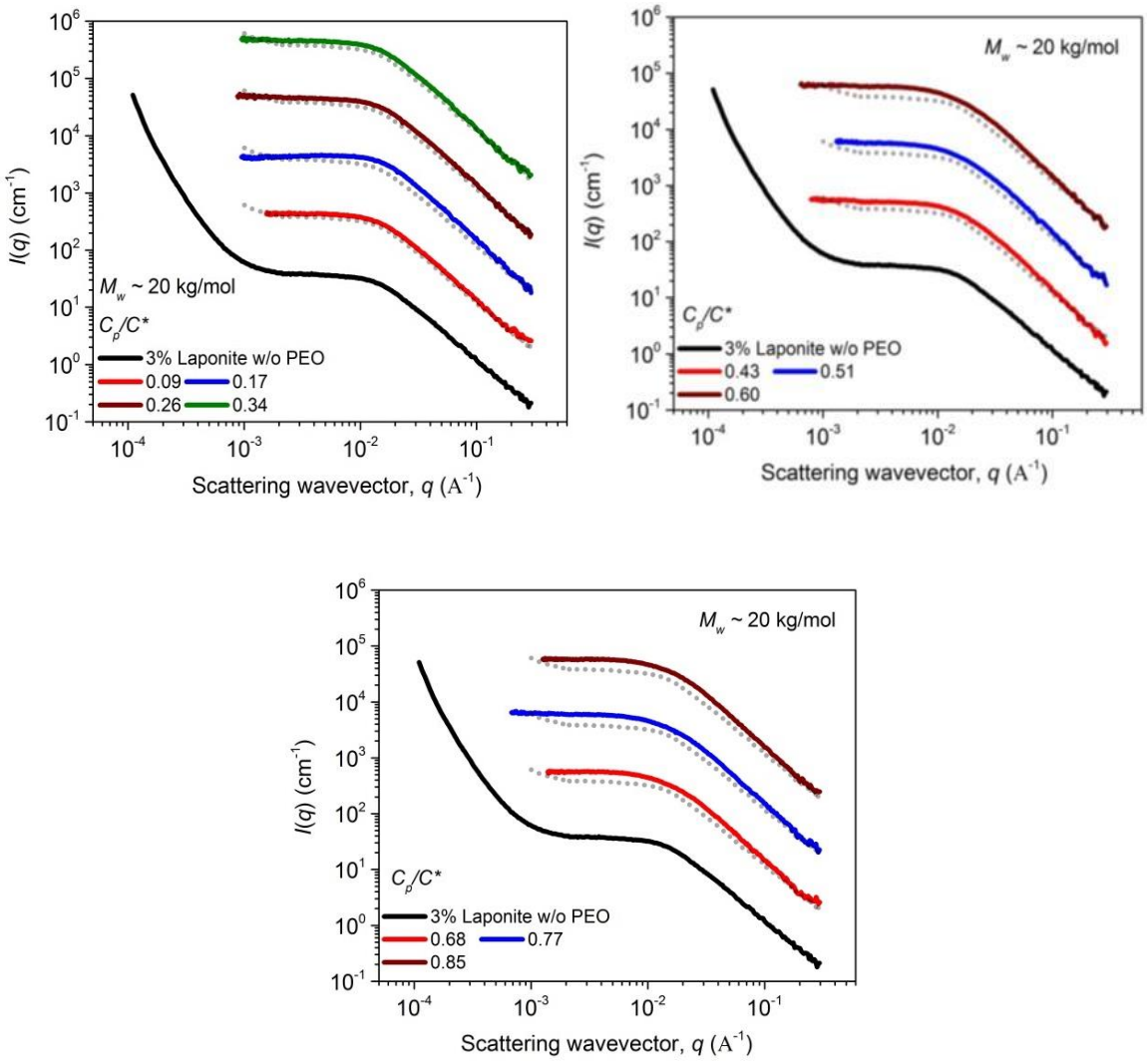


Figure 4.10 : USAXS spectra of suspensions containing 3% laponite® with varying concentrations of 20 kg/mol PEO. The scattered intensity profiles have been vertically shifted for clarity. The dotted profiles (•••) show the scattering from the 3% laponite® without PEO truncated at ~$q$~0.001Å$^{-1}$ for a better comparison.

The scattering spectra for both the higher $M_w$ and lower $M_w$ PEO indicate that the formation of intermediate structures in the system is definitely influenced by the concentration of particles within the volume. The interparticle distances are expected to

decrease as the concentration of laponite® increases. Now with the addition of PEO to the system, the effective volume fraction decreases because formation of complexes. In the case of the series of samples containing 2% laponite® and 300 kg/mol PEO, the adsorbed polymer chains initially contribute to the formation of dense complexes that are approx. 3-4 times the size of the particle. As more polymer is added to the system, particles begin to add up to the edges of the cluster and this is probably why the structure of the objects along intermediate and particle length scales do not vary with the addition of PEO. With the addition of PEO, increasing repulsions between polymers and between polymer coated complexes result in formation of denser clusters. In the case of systems with 3% laponite®, the interparticle distances are now shorter so this results in the formation of denser aggregates. For the series of samples containing the 20 kg/mol PEO, the short and weak attraction strengths result in the formation of very small structures. In the case of the 2% laponite® series, the ellipsoidal structures that form at intermediate PEO concentrations are almost 2 particle diameters long and the thickness is about 4nm which is basically the lateral thickness that takes into account the polymer shell thickness.

**4.4 Conclusions**

A systematic study of the influence of polymers on the microstructure in laponite®-PEO systems has been conducted using ultra small-angle x-ray scattering (USAXS). The focus was to understand how the microstructure contributed to the formation of an arrested phase in an aging colloid-polymer mixture. Two specific cases were considered; (i) polymer-colloid size ratio was 0.5 and (ii) polymer-colloid size ratio was 2.5 and the particle concentration was fixed either at 2% (~0.0075) or 3% (~0.011). As the polymer concentration is allowed to increase, we find:

(i) there is no systematic increase or decrease in the excess scattering at low-*q* for systems with 300 kg/mol PEO at both particle fractions and the effected size of the cluster is about 3-6 times the effective diameter of the particle,

(ii) the shorter polymer chains do not remarkably change the structure at large length scales but influence the formation of ellipsoidal or prolate objects at intermediate concentrations,

(iii) at higher particle fractions, the formation of intermediate structures is avoided because the interparticle distances between particle are initially shorter and thus a more closely packed structure is expected to form at higher polymer concentrations.

## 4.5 References


1. Pusey, P. N.; Van Megen, W., Observation of a Glass-Transition in Suspensions of Spherical Colloidal Particles. *Physical Review Letters* **1987,** *59* (18), 2083-2086.

2. Megen, W. V.; Underwood, S. M., Glass Transition in Colloidal Hard Spheres: Measurement and Mode-Coupling-Theory Analysis of the Coherent Intermediate Scattering Function. *Phys. Rev. E* **1994,** *49*, 4206.

3. Trappe, V., Prasad, V., Cipelletti, L., Segre, P. N., & Weitz, D. A., Jamming phase diagram for attractive particles. *Nature* **2001,** *411*(6839), 772-775.

4. Bergenholtz, J.; Fuchs, M., Nonergodicity transitions in colloidal suspensions with attractive interactions. *Physical Review E* **1999,** *59* (5), 5706-5715.

5. Bergenholtz, J.; Poon, W. C. K.; Fuchs, M., Gelation in Model Colloid-Polymer Mixtures. *Langmuir* **2003,** *19*, 4493.

6. Ilett, S. M.; Orrock, A.; Poon, W.; Pusey, P., Phase behavior of a model colloid-polymer mixture. *Physical Review E* **1995,** *51* (2), 1344.

7. Bonn, D.; Tanase, S.; Abou, B.; Tanaka, H.; Meunier, J., Laponite: Aging and shear rejuvenation of a colloidal glass. *Physical review letters* **2002,** *89* (1), 015701.

8. Pontoni, D.; Narayanan, T., Ultra-small-angle X-ray scattering studies of attractive colloidal glass transition. *Journal Of Applied Crystallography* **2003,** *36*, 787-790.

9. Pham, K. N., Petekidis, G., Vlassopoulos, D., Egelhaaf, S. U., Pusey, P. N., & Poon, W. C. K., Yielding of colloidal glasses. *EPL (Europhysics Letters)*, **2006**, *75*(4), 624.

10. Jabbari-Farouji, S.; Tanaka, H.; Wegdam, G. H.; Bonn, D., Multiple nonergodic disordered states in Laponite suspensions: A phase diagram. *Physical Review E* **2008,** *78* (6), 061405.

11. Bonn, D.; Kellay, H.; Tanaka, H.; Wegdam, G.; Meunier, J., Laponite: What is the difference between a gel and a glass? *Langmuir* **1999,** *15* (22), 7534-7536.

12. Bonn, D.; Tanaka, H.; Wegdam, G.; Kellay, H.; Meunier, J., Aging of a Colloidal "Wigner" Glass. *Eur. Phys. Lett.* **1999,** *45*, 52.

13. Jabbari-Farouji, S.; Wegdam, G.; Bonn, D., Gels and Glasses in a Single System: Evidence for an Intricate Free-Energy Landscape of Glassy Materials. *Phys. Rev. Lett.* **2007,** *99*, 065701.

14. Sollich, P., Lequeux, F., Hébraud, P., & Cates, M. E., Rheology of soft glassy materials. *Physical review letters*, **1997,** *78*(10), 2020.

15. Winter, H. H., & Chambon, F., Analysis of linear viscoelasticity of a crosslinking polymer at the gel point. *Journal of Rheology (1978-present)*, **1986**, *30*(2), 367-382.

16. Angelini, R.; Zulian, L.; Fluerasu, A.; Madsen, A.; Ruocco, G.; Ruzicka, B., Dichotomic aging behaviour in a colloidal glass. *Soft Matter* **2013,** *9* (46), 10955-10959.

17. Angelini, R.; Zaccarelli, E.; de Melo Marques, F. A.; Sztucki, M.; Fluerasu, A.; Ruocco, G.; Ruzicka, B., Glass–glass transition during aging of a colloidal clay. *Nature Communications* **2014,** *5*.

18. Mongondry, P.; Tassin, J. F.; Nicolai, T., Revised state diagram of Laponite dispersions. *Journal of colloid and interface science* **2005,** *283* (2), 397-405.

19. Saha, D.; Bandyopadhyay, R.; Joshi, Y. M., A Dynamic Light Scattering Study and DLVO Analysis of Physicochemical Interactions in Colloidal Suspensions of Charged Disks. *Langmuir* **2015**.

20. Jatav, S., & Joshi, Y. M., Analyzing fractal gel of charged oblate nanoparticles in suspension using time resolved rheometry and DLVO theory.*Faraday Discussions* **2015**

21. Lal, J.; Auvray, L., Interaction of polymer with clays. *J. Appl. Crystallogr.* **2000,** *33* (1), 673.

22. Lal, J.; Auvray, L., Interaction of polymer with discotic clay particles. *Mol. Cryst. Liq. Cryst.* **2001,** *356*, 503.

23. Nelson, A.; Cosgrove, T., A small-angle neutron scattering study of adsorbed poly(ethylene oxide) on laponite. *Langmuir* **2004,** *20* (6), 2298-2304.

24. Nelson, A.; Cosgrove, T., Dynamic light scattering studies of poly(ethylene oxide) adsorbed on laponite: Layer conformation and its effect on particle stability. *Langmuir* **2004,** *20* (24), 10382-10388.

25. Mongondry, P.; Nicolai, T.; Tassin, J. F., Influence of Pyrophosphate or Polyethylene Oxide on the Aggregation and Gelation of Aqueous Laponite Dispersions. *J. Colloid Interface Sci.* **2004,** *275*, 191.

26. Baghdadi, H. A.; Sardinha, H.; Bhatia, S. R., Rheology and gelation kinetics in laponite dispersions containing poly (ethylene oxide). *J. Polym. Sci., Part B: Polym. Phys.* **2005,** *43* (2), 233.

27. Baghdadi, H. A.; Jensen, E. C.; Easwar, N.; Bhatia, S. R., Evidence for re-entrant behavior in laponite-PEO systems. *Rheologica Acta* **2008,** *47* (2), 121-127.

28. Baghdadi, H. A.; Parrella, J.; Bhatia, S. R., Long-term aging effects on the rheology of neat laponite and laponite-PEO dispersions. *Rheologica Acta* **2008,** *47* (3), 349-357.

29. Atmuri, A. K.; Peklaris, G. A.; Kishore, S.; Bhatia, S. R., A Re-Entrant Glass Transition in Colloidal Disks with Adsorbing Polymer. *Soft Matter* **2012,** *8*, 8965.

30. Kishore, S.; Chen, Y.; Ravindra, P.; Bhatia, S. R., The effect of particle-scale dynamics on the macroscopic properties of disk-shaped colloid–polymer systems. *Colloids and Surfaces A: Physicochemical and Engineering Aspects* **2015,** *482*, 585-595.

31. Ilavsky, J.; Jemian, P. R., Irena: tool suite for modeling and analysis of small-angle scattering. *Journal of Applied Crystallography* **2009,** *42*, 347-353.

32. Bhatia, S.; Barker, J.; Mourchid, A., Scattering of Disk Like Particle Suspensions: Evidence for Repulsive Interactions and Large Length Scale Structure from Static Light Scattering and Ultra-Small-Angle-Neutron-Scattering. *Langmuir* **2001,** *19*, 532.

33. Loizou, E.; Butler, P.; Porcar, L.; Kesselman, E.; Talmon, Y.; Dundigalla, A.; Schmidt, G., Large scale structures in nanocomposite hydrogels. *Macromolecules* **2005,** *38* (6), 2047-2049.

34. Schmidt, G.; Nakatani, A. I.; Butler, P. D.; Han, C. C., Small-angle neutron scattering from viscoelastic polymer-clay solutions. *Macromolecules* **2002,** *35* (12), 4725-4732.

35. Zebrowski, J.; Prasad, V.; Zhang, W.; Walker, L. M.; Weitz, D. A., Shake-gels: shear-induced gelation of laponite–PEO mixtures. *Colloids Surf., A* **2003,** *213* (2−3), 189.

36. Shah, S. A.; Chen, Y. L.; Ramakrishnan, S.; Schweizer, K. S.; Zukoski, C. F., Microstructure of dense colloid–polymer suspensions and gels. *J. Phys.: Condens. Matter* **2003,** *15*, 4751.

37. Debye, P., & Bueche, A. M., Scattering by an inhomogeneous solid.*Journal of Applied Physics*, **1949**, *20*(6), 518-525.

38. Hammouda, B., A new Guinier-Porod model. *Journal of Applied Crystallography*, **2010**, *43*(4), 716-719.

39. Feigin, L. A., & Svergun, D. I., *Structure analysis by small-angle X-ray and neutron scattering* **1987,** (pp. 68-73). G. W. Taylor (Ed.). New York: Plenum Press.

40. Guinier, A.; Fournet, G., *Small-angle scattering of X-rays*. New York : Wiley: **1955**.

# CHAPTER 5

# CONCLUSIONS AND FUTURE WORK

## 5.1 Concluding Remarks

This thesis explored the macroscopic behavior, microstructure and dynamics of colloidal disks in mixtures containing poly (ethylene oxide), a weakly adsorbing non-ionic polymer. The objective of this work was to develop an understanding of how adsorbing polymers influence the interactions between particles in the system. The effects of varying simple parameters like polymer chain length, concentration and the particle concentration on the properties of the colloid-polymer system were observed at different length scales using techniques such as rheology, dynamic light scattering, x-ray photon correlation spectroscopy and ultra-small angle x-ray scattering. These observations would serve as a benchmark that would allow for a more effective way to incorporate aspherical colloids in systems (e.g emulsions, polymer blends, drug delivery formulations) that are used in developing products for different applications.

Chapter 2 discussed the macroscopic behavior of mixtures containing laponite®, a charged disk-shaped colloid and poly (ethylene oxide), a non-ionic polymer that weakly interacts with the surfaces of the colloidal particle. The early aging behavior of these systems was observed using rheology and dynamic light scattering (DLS). At a fixed particle concentration of 2%, the effect of different concentrations of 4.6 kg/mol, 20 kg/mol and 35 kg/mol PEO on the viscoelastic properties of the laponite® suspension were measured. Oscillatory stress and frequency sweep tests showed the existence of three distinct types of behavior with increasing polymer concentration. First, the addition

of PEO resulted in a decrease in the elasticity due to increasing steric effects. Then, upon increasing the concentration of PEO, a colloid re-entrant behavior was observed. This behavior is typically seen in a hard-sphere colloidal system with a non-adsorbing polymer. Lastly, when the PEO concentration is close to the polymer overlap regime, a metastable fluid-like phase is observed. The aging of suspensions at this composition was found to depend on the polymer chain length. Dynamic light scattering experiments were conducted to measure the microstructural relaxations in the system and results showed that the variations in this parameter were non-uniform with changes in the concentration of PEO. The experiment was able to capture the re-entrant transitions in the dilute polymer regimes. However, along intermediate polymer concentrations the variations in the slow relaxation parameter were small which suggested that structures were undergoing very small re-arrangements in the system. Close to the polymer overlap region, an abrupt increase in the magnitude of the slow relaxation parameters in systems containing 20 kg/mol and 35 kg/mol PEO revealed that structures were now more hindered by the local crowding of polymer chains. Beyond this region, an increased diffusion of clusters was observed.

Chapter 3 discussed the dynamics of complexes and particles in the laponite®-PEO system using x-ray photon correlation spectroscopy (XPCS). The technique allowed for a thorough investigation of the dynamics in this system as it provided measurements of the diffusion of these structures over a range of length scales in a single experiment. Studies were conducted on a series of laponite®-PEO systems at two different particle concentrations of 2% and 3%, with varying PEO molecular weights (20 kg/mol, 35kg/mol and 55 kg/mol) and concentrations (0.25% (w/w) – 2.5% (w/w)). The

measurement showed the presence of three different dynamic regimes in these system; (i) repulsive regime, where long-range repulsions are dominant, (ii) attractive regime, where depletion effects play a major role and (iii) gel regime, where small clusters begin to diffuse faster because of increasing excluded volume effects. The results indicated that any change in the interparticle interactions led to structural reorganizations at smaller length scales due to competing polymer–particle and polymer–polymer interactions, which in turn had major effects on the bulk properties of the system. The observations qualitatively mapped the results from the dynamic light scattering experiments which were discussed in the previous chapter.

Chapter 4 discussed the analysis of the microstructures in the colloid-polymer mixture using ultra small angle x-ray scattering (USAXS). The aim of this experiment was to look at the microstructural changes in laponite® systems with the addition of PEO. Two different cases were considered for this study; (i) where the size of the polymer was nearly twice the size of the particle and (ii) the size of the PEO chain was half the size of the particle. A series of samples were prepared at 2% and 3% laponite®, with varying concentrations of PEO (0.25 – 2.5 %).

For the first case, distinct upturns in the low-$q$ regions of USAXS spectra were observed and this is a characteristic feature of the presence of micron-sized structures in the system. The variations in the upturn however were non-uniform as the PEO concentrations changed in the system. This highlighted the fact that microstructural re-arrangements occurred over intermediate to large length scales in the system with the inner structure remaining intact.

In the second case, however, the USAXS spectra did not show any characteristic upturns in the low-*q* regions in both the 2% and 3% laponite®-PEO series. Along the dilute polymer regime, the addition of a small amount of PEO resulted in some aggregation which was characterized by the presence of a broad peak. However, as the PEO concentration is increased, the USAXS spectra showed the existence of two Guinier regions; one in the intermediate *q* region of 0.02 $Å^{-1}$ - 0.03 $Å^{-1}$ and the other in the lower *q* region of 0.003$Å^{-1}$. These observations pointed to the existence of polydisperse ellipsoidal structures. Model fitting was done using the generalized Guinier-Porod model. The fitting parameters obtained using this model suggested that in this intermediate concentration regime of PEO, the sizes of these structures did not vary greatly until the systems approach *c**.

## 5.2 Future work

### 5.2.1 Non-linear rheology of laponite®-PEO mixtures

It is now well established that the re-entrant behavior in laponite®-PEO systems is driven not only by the influence of the free polymers in the bulk but also by the arrangement of clusters in systems close to the fluid-attractive phase transition. In the case of suspensions containing low Mw PEO, the observations point to the idea that maybe the final states after the re-entrant behavior is a glass rather than an attractive gel. Structurally, if this is an attractive gel or a glass one must then also be able to see upturns at lower values of *q*, as seen by Pontoni and co-workers in their study of spherical particles[1].

Since there is much difficulty in identifying what the final state is, one can then always turn to rheology to find out such information. A thorough study of the yielding

behavior in hard sphere systems with non-adsorbing polymers was conducted earlier by Petekidis and co-workers[2]. Results from this study show that hard sphere glasses exhibit a single yield peak, whereas strong attractive glasses exhibit two yielding peaks. One yield peak characterizes the breakage of attractive bonds, and the other characterizes the rearrangement of nearest neighbors. Such rheological experiments can be very useful in cases where the systems cannot be distinguished by either scattering or visual examination.

### 5.2.2 Experiment design for non-linear rheology:

Proposed samples for this experiment: Mixtures of laponite with 0, 0.25%, 1.5% and 2.5% PEO with a molecular weight of 20 kg/mol or 35 kg/mol.

(TRIOS Software)

Step 1: Conditioning : For 20 minutes at 25°C. The conditioning step allows the sample to relax quiescently so all the loading induced peturbations and history is erased. This is different from pre-shearing where the sample is sheared with a magnitude beyond the yielding point and then allowed to age during the experiment itself. The latter method might be useful in terms of reducing the variability between replicates but we have not seen a large amount of variability when the former method is used. This would be an interesting small project in itself.

Step 2: Oscillation Amplitude Test : Frequency 1Hz; Strain Amplitude: 0.1% to 1000% (Logarithmic Sweep) at 10 points per decade

Step 3: Conduct the same test on the different sample under different frequencies: 0.1Hz and 10Hz. Yielding sometimes is sensitive to the frequency of oscillations.

### 5.2.3 Comparing re-entrant behavior between two concentrated laponite® suspensions

Re-entrant behavior in mixtures containing 2% laponite® and PEO with molecular weights of 20 – 35 kg/mol has been observed, and this dissertation has brought out some useful observations[3,4]. In these systems, rheological experiments were able to beautifully describe the transitions when the systems were in the early aging period. In other words, the transitions between glass-fluid and fluid-glass phases were more apparent in this regime of aging. However, when one compares this type of re-entrancy that is observed with a mixture containing a higher concentration of laponite®, the aging kinetics is more dominant, and the structural equivalency between two systems at a time-point is lost. Hence a time evolution experiment for the more concentrated systems would be more appropriate to compare the effects of chain length and concentration on the dynamics of a system that contains a higher laponite® concentration.

### 5.2.4 Experiment design of time-evolution rheology:

Proposed samples for this experiment: Samples with 2.8% laponite® and higher reach a glassy phase within a week. So an experimental system with 3% laponite® will be ideal for such experiments.

(TRIOS Software)

Step 1: Conditioning for 20mins at 25°C. This is the same as mentioned in the earlier section.

Step 2: Oscillation time sweep: At 1Hz for a duration of 10,000 seconds (~2.8 hours); Sampling interval: 100 seconds per point or one point for every 1000 seconds (whichever appropriate)

### 5.2.5 Imaging of laponite®-PEO systems

Results from the USAXS study have shown the existence of finite-sized clusters in the case of mixtures containing low-Mw PEO and micron-sized dense aggregates in the case of long PEO chains. Attempts have been made previously to obtain an image of the microstructure in these systems using cryo-transmission electron microscopy (Cryo – TEM). Although some information could be derived from it, obtaining an image with a higher resolution often seems to be a great challenge because of the high concentration of PEO employed in most of the systems. Cryo-TEM imaging technique was most recently used to analyze systems containing just neat laponite® alone and some results were recently presented at the Society of Rheology conference by Joshi. Improvements may have been made in the instrumentation so as to be able to properly image these particles. While this technique would allow for a better characterization of the laponite®-PEO systems, sample preparation still seems to be a grand challenge as the procedure requires careful drying of samples on a grid which might result in some changes in the structure itself.

### 5.2.6 Re-entrant behavior in spherical and rod-like particles with adsorbing polymers

The contribution of shape-anisotropy to the aging of colloid-polymer solutions is still not clearly known, and there are very few studies that contribute to the understanding of aging mechanisms in these systems. From Chapter 4, we know that the presence of additional free polymer chains result in the formation of layered structures. Through our rheological experiments, we also know that the elasticity and the aging kinetics increases in this regime of polymer concentration but very little is known about how these

columnar layered structures speed up the aging process and increase the bulk elasticity if these systems are in fact attractive in nature.

There are a few ways to understand this behavior: (i) synthesize an equivalent spherical charged particle that also hydrates and swells when dispersed in water. In this way, a direct comparison can be made to the laponite® system itself. This is probably a better way than using another spherical particle like Ludox where surface characteristics are completely different, or (ii) Examining the behavior of particles with a larger aspect ratio (larger than 1/25 ~ 0.08) will provide some more insight on the kinetics of structural arrest and aging of columnar structures that are seen in laponite®-PEO systems[5].

## 5.3 References


1. Pontoni, D.; Narayanan, T., Ultra-small-angle X-ray scattering studies of attractive colloidal glass transition. *Journal Of Applied Crystallography* **2003,** *36*, 787-790.

2. Pham, K. N., Petekidis, G., Vlassopoulos, D., Egelhaaf, S. U., Pusey, P. N., & Poon, W. C. K., Yielding of colloidal glasses. *EPL (Europhysics Letters)*, **2006**, *75*(4), 624.

3. Kishore, S.; Chen, Y.; Ravindra, P.; Bhatia, S. R., The effect of particle-scale dynamics on the macroscopic properties of disk-shaped colloid–polymer systems. *Colloids and Surfaces A: Physicochemical and Engineering Aspects* **2015,** *482*, 585-595.

4. Atmuri, A. K.; Peklaris, G. A.; Kishore, S.; Bhatia, S. R., A Re-Entrant Glass Transition in Colloidal Disks with Adsorbing Polymer. *Soft Matter* **2012,** *8*, 8965.

5. Solomon, M. J., Spicer, P. T., Microstructural regimes of colloidal rod suspensions, gels, and glasses. *Soft Matter*, **2010**, *6*(7), 1391-1400.

# APPENDIX A

## MACROSCOPIC BEHAVIOR AND DYNAMICS OF LAPONITE® WITH LOW AND INTERMEDIATE $M_w$ PEO

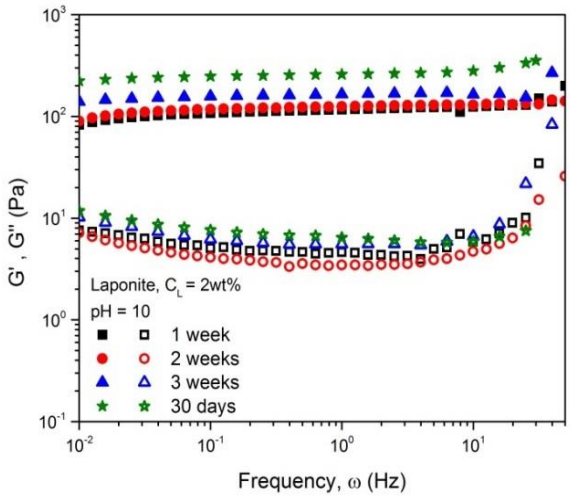


Figure A 1 : The aging behavior of laponite® at a particle concentration of 2wt%. Frequency dependence of the storage (*G'*) and loss modulus (*G''*) at different aging times; (a) 1 week (black squares), (b) 2 weeks (red circles), (c) 3 weeks (blue triangles), (d) 30 days (green stars).

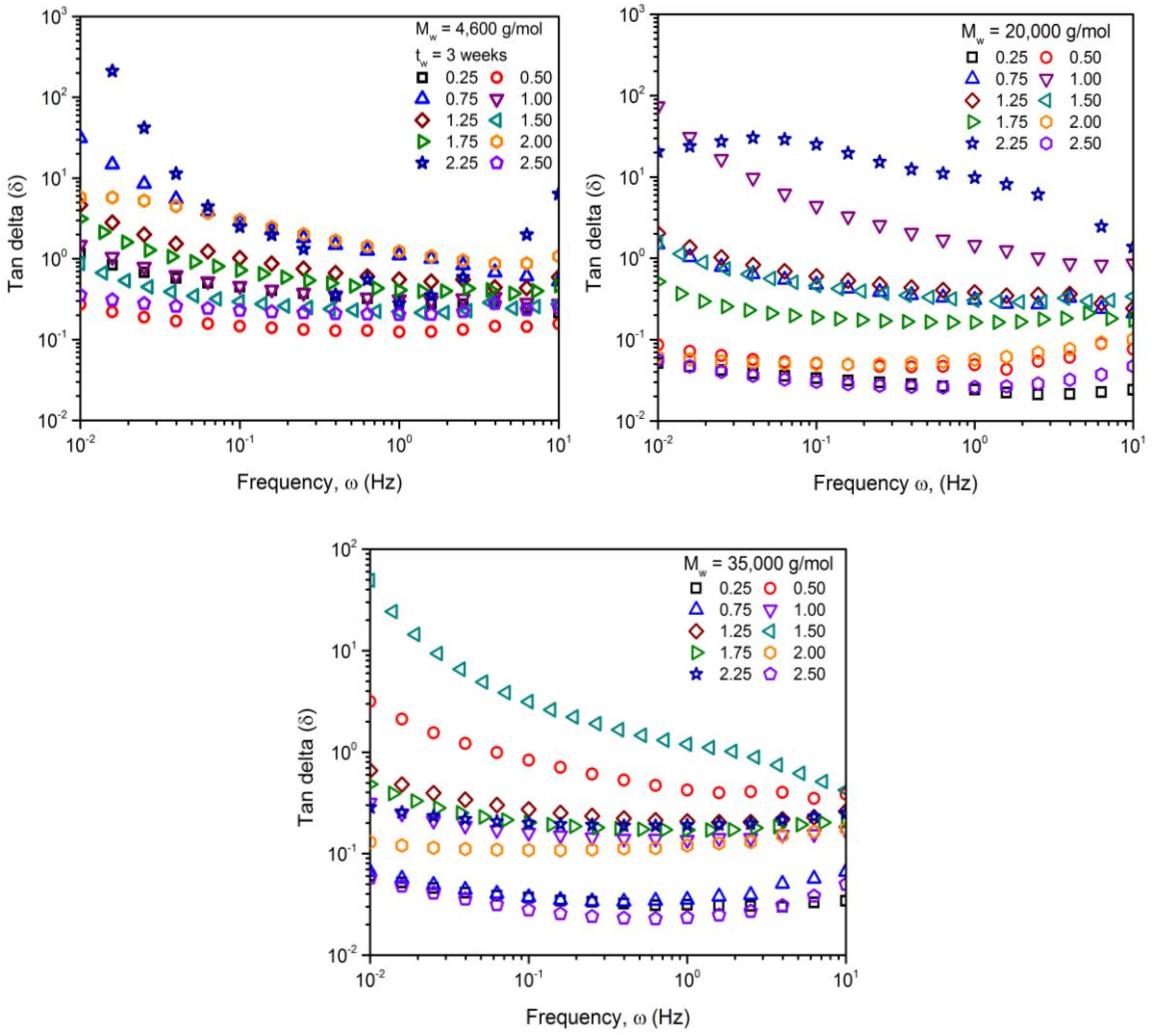


Figure A 2 : Frequency dependence of tan delta ($\delta$) at various polymer concentrations of (a) 4K PEO (top left); (b) 20K PEO (top right); (c) 35K PEO (bottom). The legends represent the polymer concentration $c_p$ in % (w/w). All samples were tested after an aging time of 21 days.

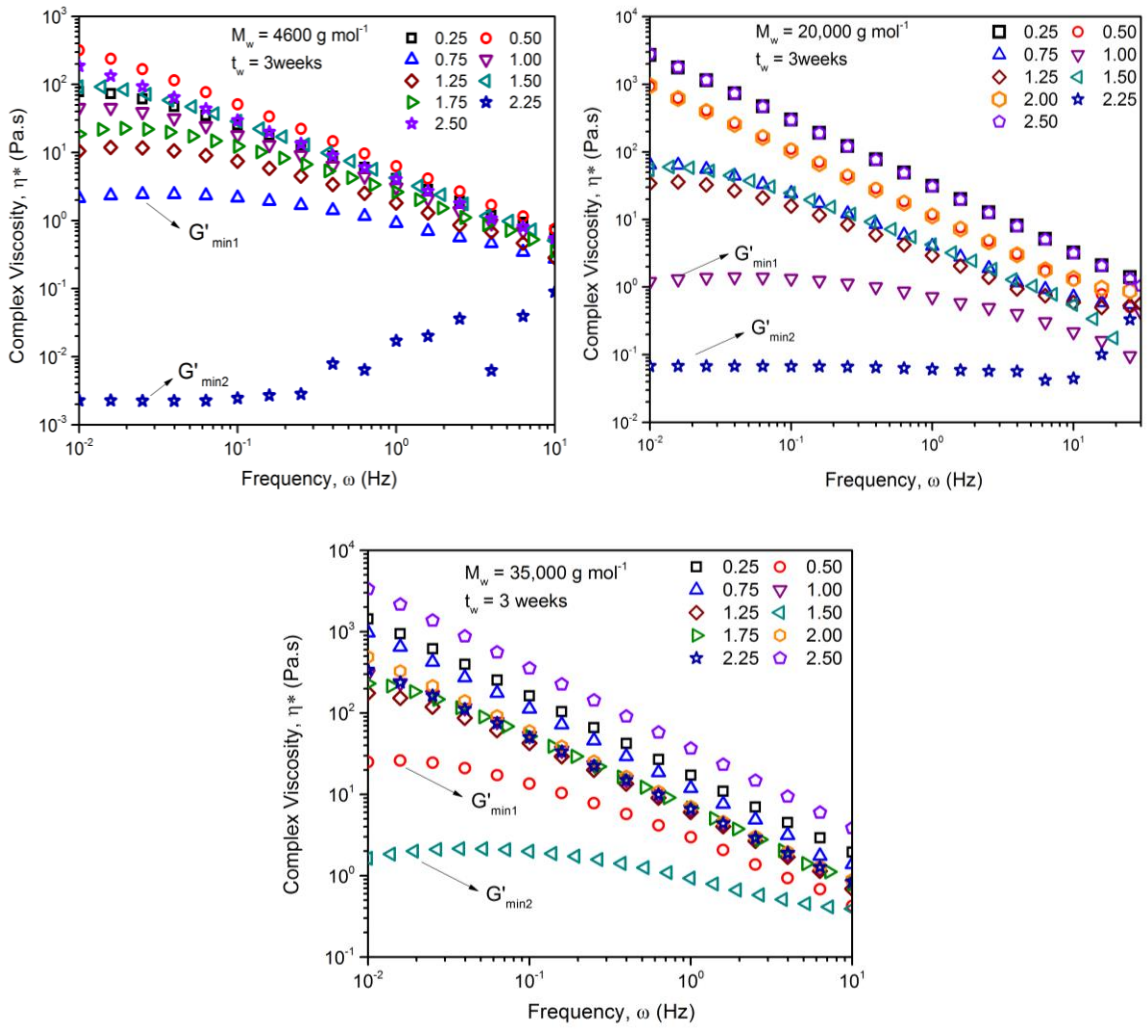


Figure A 3 : Frequency dependence of complex viscosity ($\eta^*$) at various polymer concentrations of (a) 4K PEO (top left); (b) 20K PEO (top right); (c) 35K PEO (bottom). The legends represent the polymer concentration $c_p$ in % (w/w). All samples were tested after an aging time of 21 days.

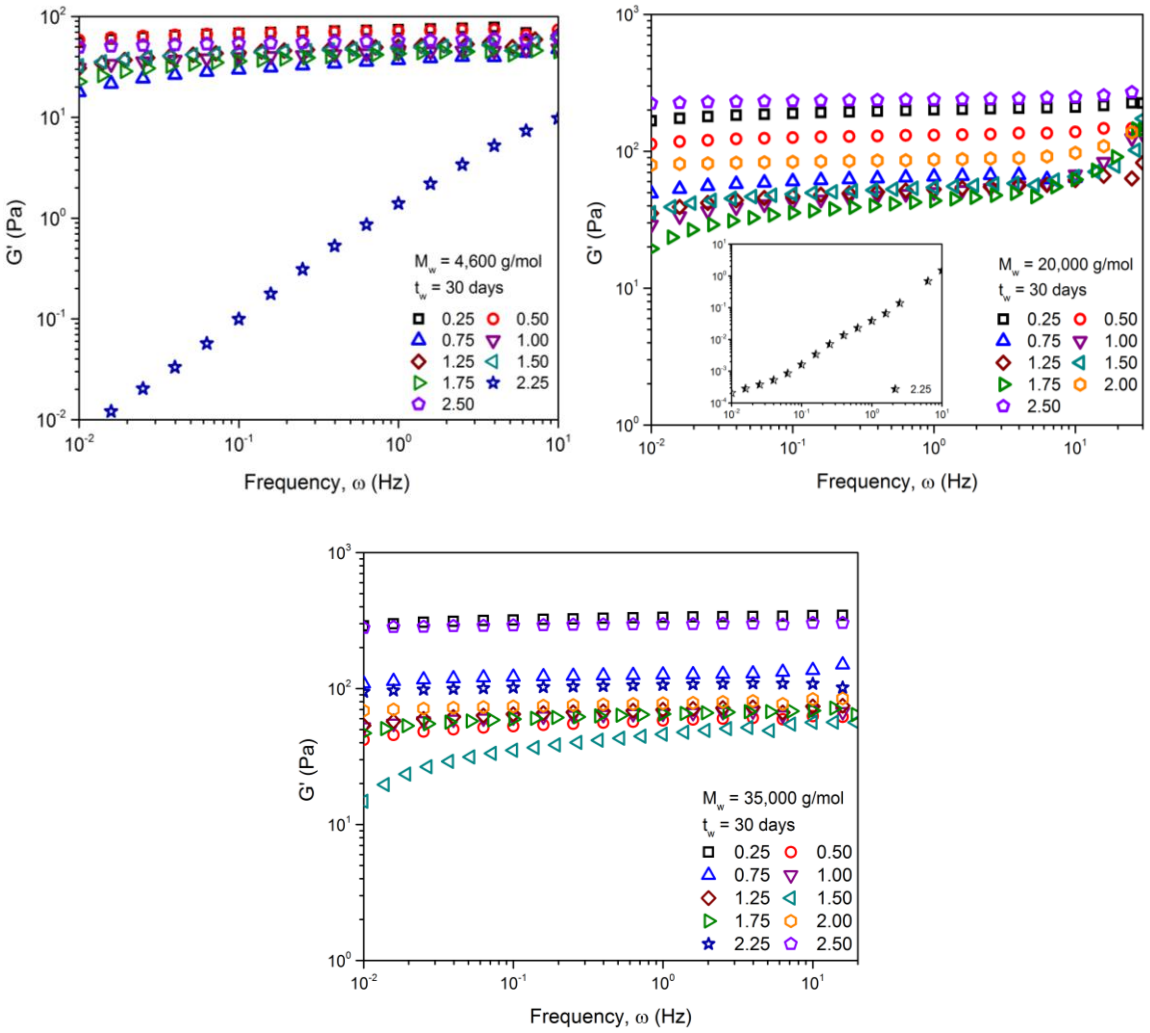


Figure A 4 : Frequency dependence of the storage modulus (*G'*) at different polymer concentrations of (a) 4K PEO (top left); (b) 20K PEO (top right), inset shows the behavior of laponite with 2.25% PEO; (c) 35K PEO (bottom). The legends represent the polymer concentration $c_p$ in % (w/w). All samples were tested at an aging time of 30 days.

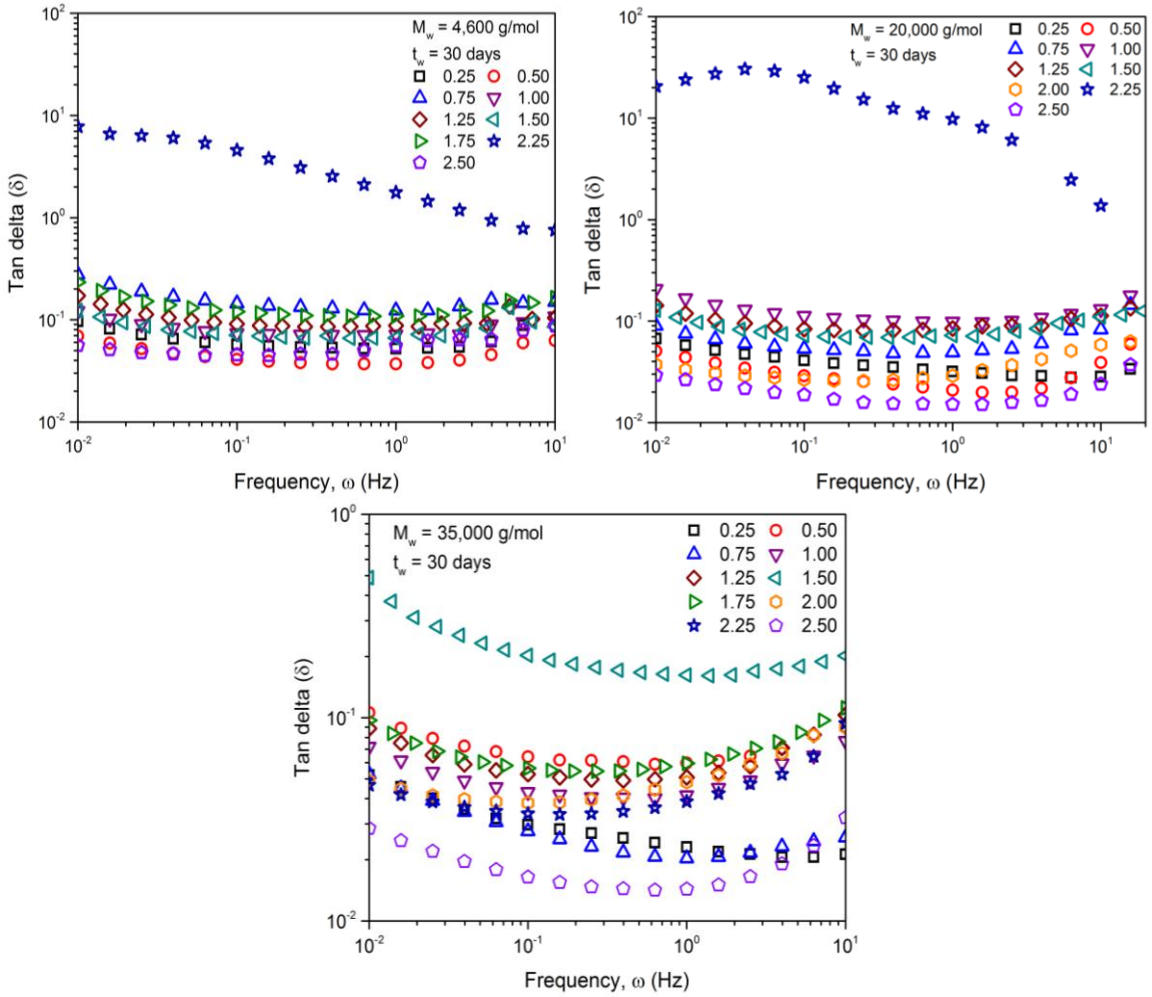


Figure A 5 : Frequency dependence of tan delta ($\delta$) at various polymer concentrations of (a) 4K PEO (top left); (b) 20K PEO (top right); (c) 35K PEO (bottom). The legends represent the polymer concentration $c_p$ in % (w/w). All samples were tested after an aging time of 30 days.

Table A 1 : Average relaxation time ($\tau_R$) obtained from the crossover frequency ($\omega_c$) observed in a rheological experiment conducted after an aging time of 21 days.

| PEO | Crossover Frequency (CF) (21 days) | | |
|---|---|---|---|
| | $c_p$ (wt%) | CF ($\omega_c$) (Hz) | Relaxation Time ($\tau_R \sim 1/\omega_c$) (sec) |
| 20,000 g/mol | 0.75 | 0.0158 | 10.073 |
| | 1.00 | 2.5119 | 0.0633 |
| | 1.5 | 0.0211 | 7.5429 |
| | 2.25 | >5 | <0.0318 |
| 35,000 g/mol | $c_p$ (wt%) | CF ($\omega_c$) (Hz) | Relaxation Time ($\tau_R \sim 1/\omega_c$) (sec) |
| | 0.5 | 0.0631 | 2.5223 |
| | 1.5 | 1.9308 | 0.0824 |
| | 1.75 | 0.001 | 159.155 |
| | 2.25 | <0.001 | >159.155 |

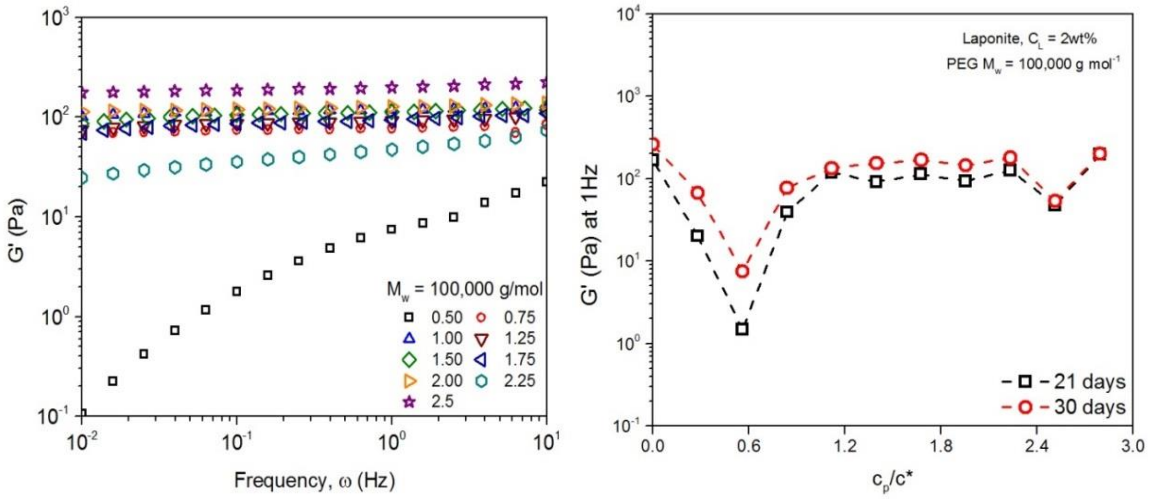


Figure A 6 : Macroscopic behavior of laponite® with 100,000 g/mol PEO. (a) Variation of the storage modulus for different concentrations of 100K PEO (left). The legends represent the polymer concentration $c_p$ in % (w/w). Samples were tested after an aging time of 21 days. (b) storage modulus $G'$ at 1 Hz versus the scaled polymer concentration $(c_p/c^*)$ at an aging time of 21 days (black squares) and 30 days (red circles).

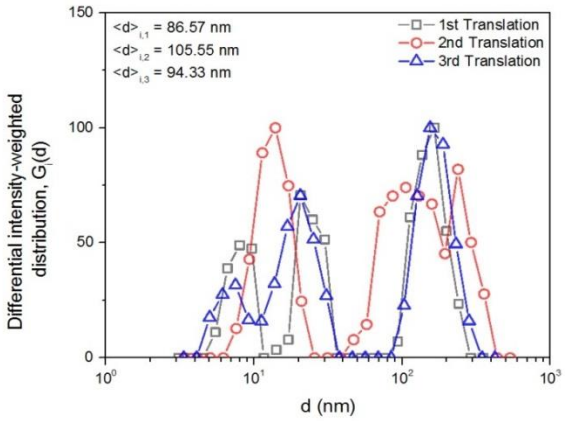


Figure A 7 : The intensity weighted distribution of laponite® particles in water, estimated after an aging time of 2 days. Each distribution is a representation of a different sample volume in the dispersion as the vial is axially rotated to another position. A distribution of single particles and small clusters can be observed.

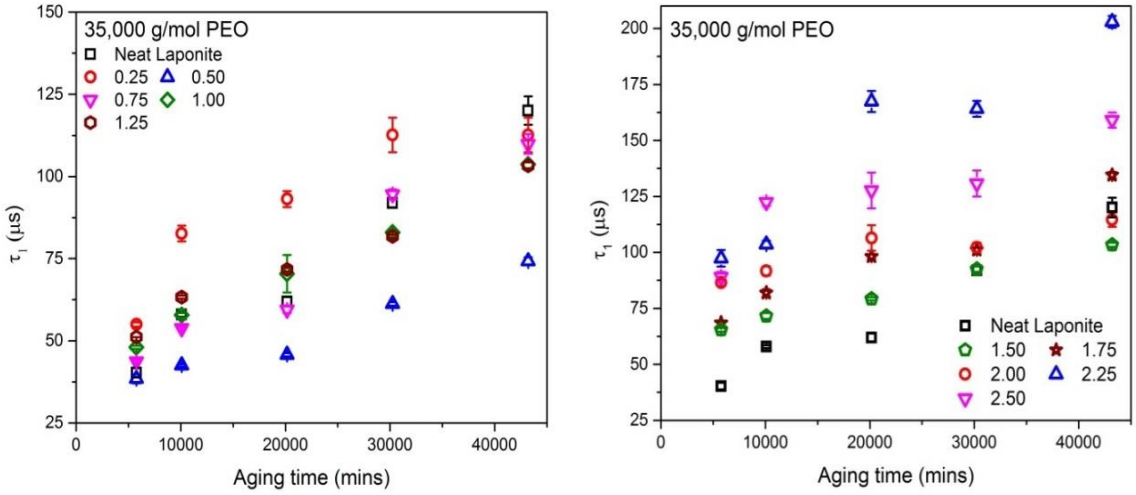

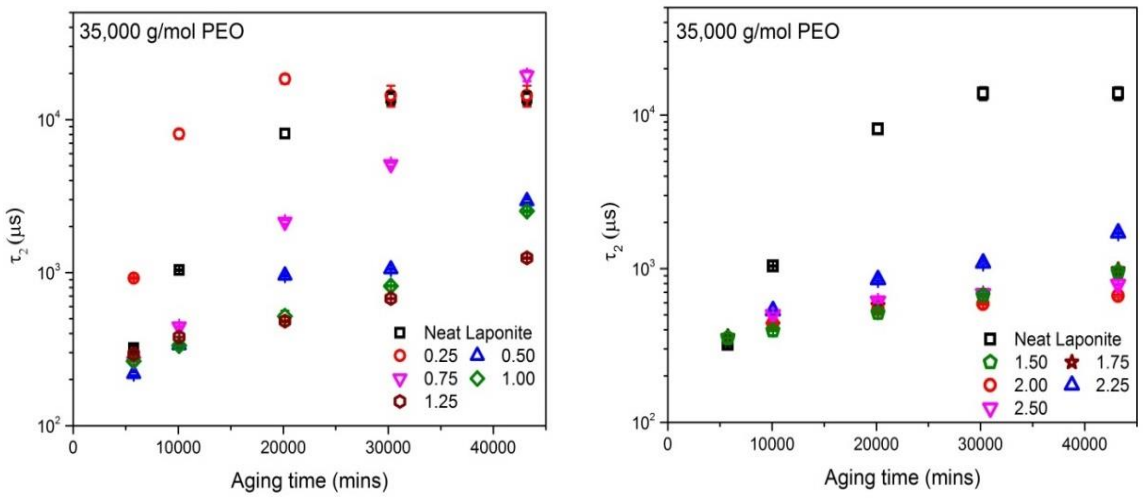


Figure A 8 : The time dependence of the fast (top - left and right) and slow relaxation (bottom - left and right) processes for systems containing 2% laponite® with 35K PEO. The error bars represent the standard deviation of values obtained from fitting the autocorrelation function to the two-step function. The legends represent the concentration of PEO in % (w/w).

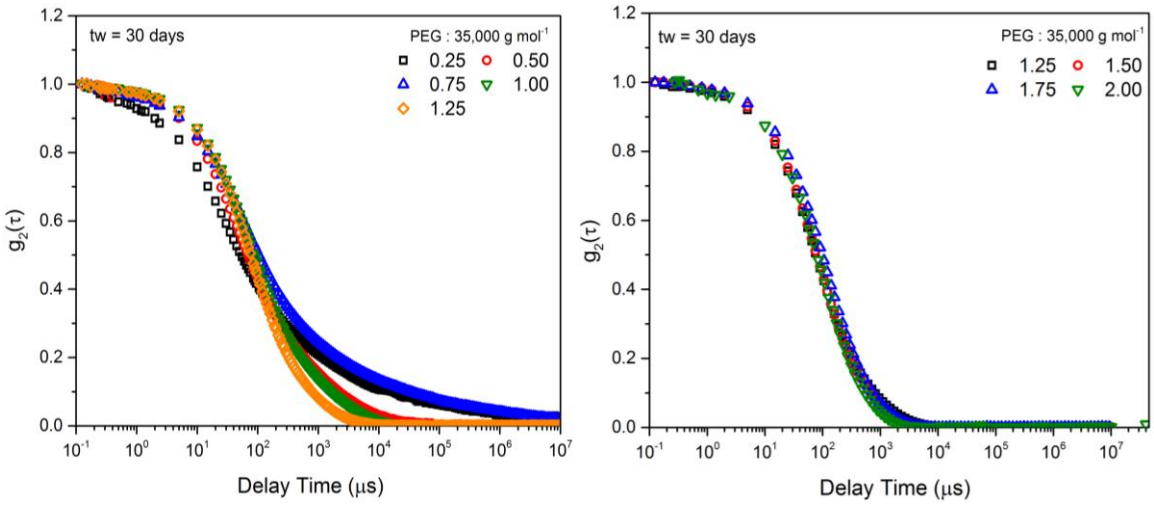

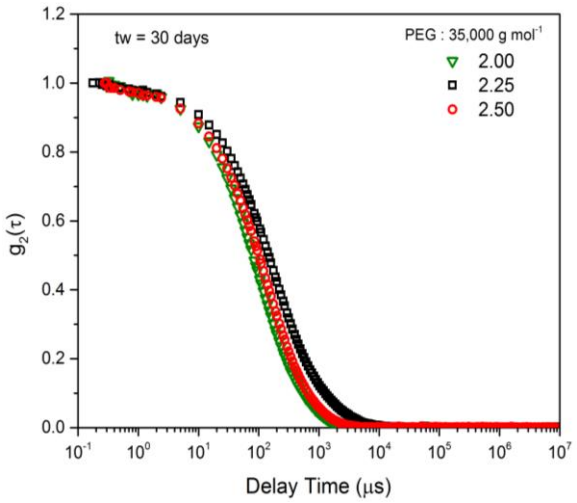


Figure A 9: Autocorrelation function $g_2(\tau)$ for a delay time range between $10^{-1}$ to $10^{7}$ μs for a 2wt% laponite® dispersion with different concentrations of the 35K PEO. The legends represent the polymer concentration $c_p$ in % (w/w). All samples were tested after an aging time of 30 days.

# APPENDIX B

## NON-LINEAR RHEOLOGY AND MICROSTRUCTURE OF LAPONITE®-PEO MIXTURES

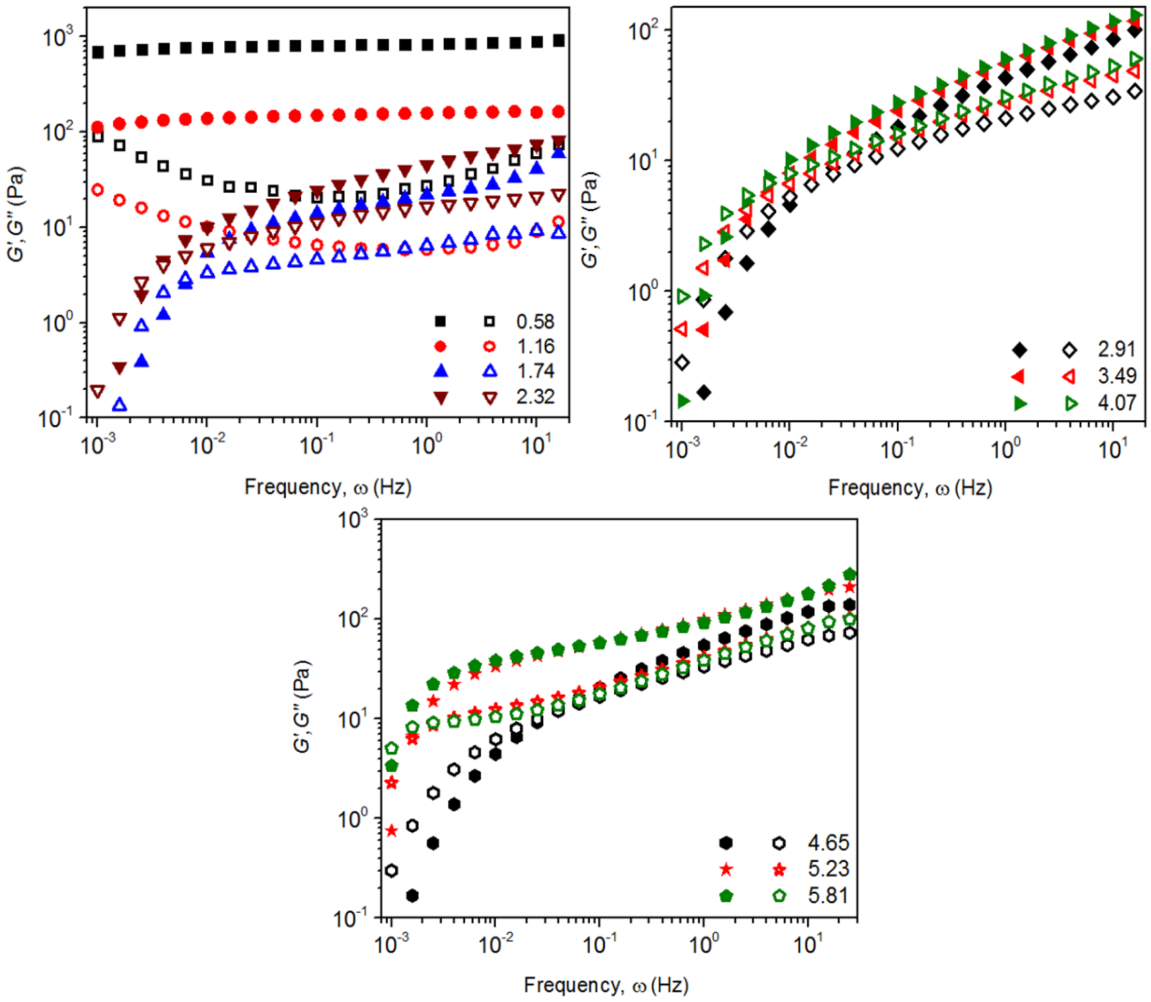


Figure B 1 : Dependence of *G'* and *G''* on the frequency $\omega$, for systems with 2% laponite® and various concentrations of 300 kg/mol PEO.

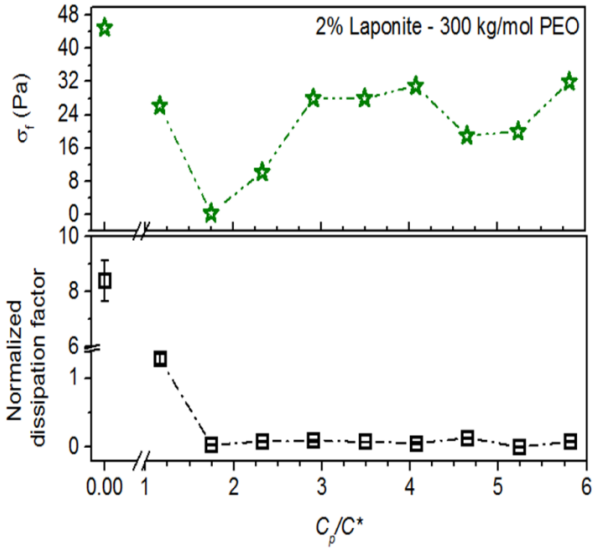


Figure B 2 : Apparent yield stress and normalized dissipation factor for 2% laponite® systems with 300 kg/mol PEO.

We present some results from rheological experiments in Figure B1. Macroscopically, the bulk elasticity of the system decreases with the addition of PEO and systems with PEO concentrations from $C_p/C^*$ ~ 1.7 to 6 exhibit a viscous gel-like behavior. From the oscillatory frequency sweep experiments, we observe that these gel-like systems exhibit a crossover frequency ($\omega_c$) below which $G'' > G'$ and above which $G' > G''$. For PEO concentrations between 1.7 and 5.8, we observe only marginal shifts in the magnitude of this crossover frequency. Below this crossover frequency both the storage and viscous modulus exhibit a $G' \sim \omega^x$ *and* $G'' \sim \omega^x$ dependence respectively. At higher frequencies the dependence is $G' \sim \omega^x$ *and* $G'' \sim \omega^x$ . Although these cross over frequencies are indicative of the strength of these gels, little information about the gel structure can be discerned from rheology alone.

Oscillatory stress sweeps were conducted to examine the viscoelastic response to magnitudes of stresses varying between 0.01 Pa to 100 Pa. With increasing magnitudes of stress, the material begins to yield. Close to yielding, $G'$ decreases and $G''$ exhibits a

single peak before it starts decreasing. The apparent yield stress is the value of stress at which $G'$ and $G''$ cross over, and beyond this crossover stress ($\sigma_y$) the material begins to flow ($G' < G''$). The presence of a peak in $G''$ has also been observed in repulsive and attractive glassy systems. Since yielding occurs around this point, we attribute the presence of this peak to the local rearrangements that take place before the material begins to flow entirely and the height of this is often correlated with the energy dissipation that takes place during the yielding process. The peaks in $G''$ have often been used as a parameter to distinguish between different kinds of glassy systems. In the case of our systems, as we keep increasing the concentration of PEO we observe a broad and shallow peak. Nevertheless, we use these parameters as cues to qualitatively distinguish the structures in the system. We present the values of the yield stresses and the normalized peak height or dissipation factor ($G''_{peak}/< G''_{linear}> - 1$) in Figure B2

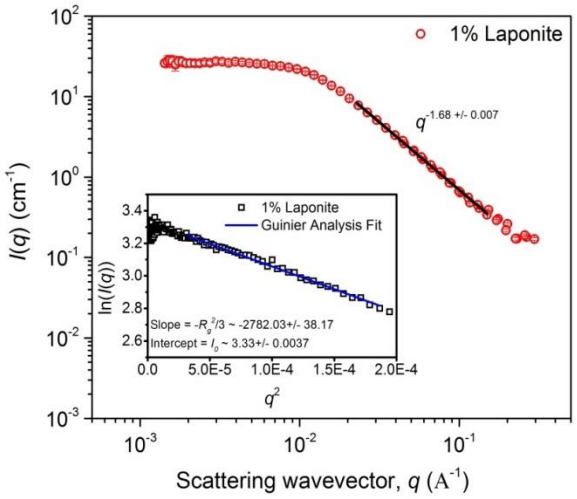


Figure B 3 : Scattered intensity profile for a dilute 1% laponite® suspension (○). The profile corresponds to a solution containing a slightly polydisperse particle distribution with a high-$q$ slope of -1.68. The inset shows the corresponding Guinier Analysis (ln($I(q)$) vs $q^2$ plot) of the same system.

Figure S1 shows the scattering profile of a dilute laponite® suspension. The value of the power law slope obtained from fitting a power law along the high-$q$ region is ~ -1.68 which is lower than what is typically expected from a system containing perfectly non-interacting disks. The absence of any low-$q$ feature indicates that there is no build-up of any structure with aging in this system. The inset in this figure shows a Guinier plot which is often used to estimate the radius of gyration of a particle. A plot of ln($I(q)$) vs $q^2$ for very small values of $q$

The Guinier function (Guinier & Fournet,1955) is given as:

$$\ln\big(I(q)\big) = \ln\big(I(q=0)\big) - \left(\frac{R_g^2 q^2}{3}\right)$$

Where the slope $m$ = - ($Rg$^2)/3 and the intercept $c$ = ln($I(q)$ = 0). For a disc shaped particle the radius is $\sqrt{2}\ R_g$ and from this analysis, the radius was found to be 12.9±0.125 nm.

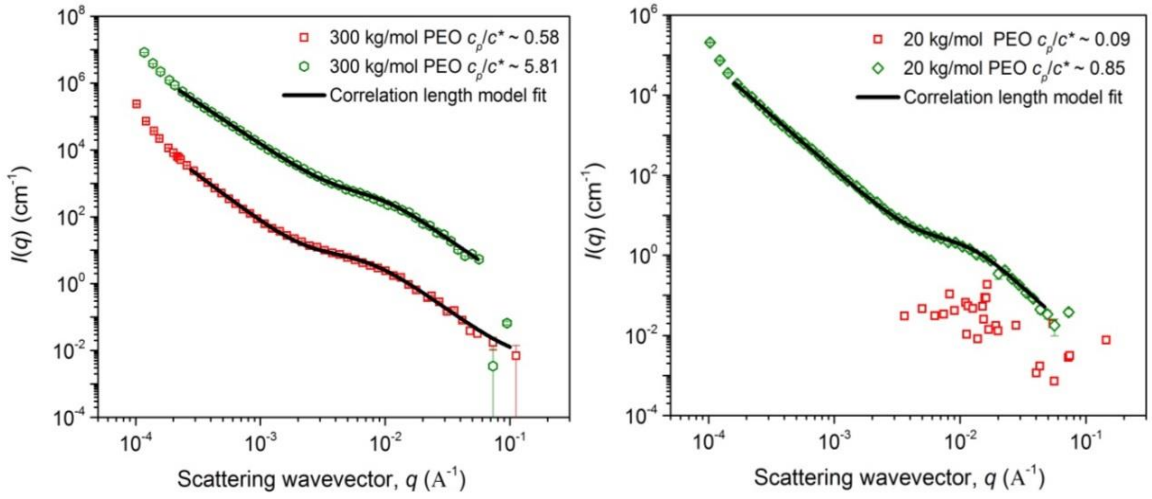


Figure B 4 : Scattering spectra for 20 and 300 kg/mol polymer solutions at the lowest and the highest concentrations. Scattering data is indicated by the open symbols while the fit of the correlation model to the data is indicated by the solid line. The scattering profile for $c_p/c^*$~5.81 has been vertically shifted for better clarity.

The scattering intensities from the polymer solutions at the lowest and highest concentrations of the 20 and 300 kg/mol of PEO are shown in Figure S2. The scattering from the lowest concentration of PEO is very noisy at higher values of $q$. We believe this is expected as the solution is pretty dilute and it is rather difficult to obtain a good scattering data. On the other hand, at the highest concentration of $c_p/c^*$~0.85, we observe a low-$q$ upturn in addition to the high-$q$ scattering. The same can be observed in the case of the scattering from $c_p/c^*$~0.58 and $c_p/c^*$~5.81 300 kg/mol PEO. In order to extract meaningful information, we fit this data with the correlation length model (Hammouda B, Ho DL, and Kline S., 2004) through a nonlinear, least square fit (as shown in Figure B4).

The correlation length model is described by the following function:

$$I(q) = \frac{A}{q^n} + \frac{C}{1 + (q\xi_L)^m} + Bkg$$

where, the first term describes the scattering from clusters and the second term describes the scattering from the polymer chains in the solution. This term characterizes the polymer/solvent interactions and hence the thermodynamics of the system. *n*,*m* and $\xi_L$ are the Porod exponent, Lorentzian exponent and the Lorentzian correlation length respectively. Results of the fit of this model to the USAXS spectra are shown in Table B1. The reduced $\chi^2$ values for all the fits were equal to or less than 2.2, indicating a low error following the fitting process.

Table B 1: Results from Correlation Length Model fit to the 300 kg/mol and 20 kg/mol polymer solution scattering profiles

| **Parameters** | **300 kg/mol PEO** | | **20 kg/mol PEO** |
|---|---|---|---|
| $c_p/c^*$ | **0.58** | **5.81** | **0.85** |
| *n* | 2.887±0.013 | 2.43±0.007 | 2.72±0.0048 |
| $\xi_L$ **(nm)** | **14.68±0.29** | **9.1±0.192** | **7.83±0.143** |
| *m* | 2.569±0.022 | 2.908±0.04 | 3.086± 0.057 |
| *Bkg* ($cm^{-1}$) | 0.008 | 0.01 | 0.005 |

According to the Flory mean-field theory, the radius of gyration of a polymer chain is given as $R_g \sim N^v$ where *v* is the excluded volume parameter. Typically, *v* is ~3/5 under swollen conditions, ~1/2 in theta conditions and ~1/3 in the case of a collapsed chain. In the case of the scattering from polymer solutions, the exponents *n* and *m* are inversely related to the excluded volume parameter. The Lorentzian exponent, *m* for both the 20 kg/mol and 300 kg/mol polymer solutions are between 2 and 3, indicating that the chains are behaving as though in a poor solvent and are present as clusters that contain two or more chains in them. The Lorentzian screening length, $\xi_L$ for the 300 kg/mol PEO series is found to decrease with increasing polymer concentration. In order to check the validity of these results we compare this to the theoretical estimation of the end-to-end

distance, $r_o$, which can be roughly calculated as $bN^v$ where $b$ is the Kuhn length of a PEO chain (~0.76nm), $N$ is the number of Kuhn segments (Mark J and Flory P.,1965) and $v$ is the excluded volume parameter (~0.5 for a good solvent) (Rubinstein M and Colby R. Polymer Physics). The estimated end-to-end chain distance for the 300 kg/mol and 20 kg/mol polymer chain in this case was found to be ~42nm and ~11nm respectively. Clearly, these chain distances are much larger than what is observed from the Correlation length model and thus validates our observation from the results obtained using this model.

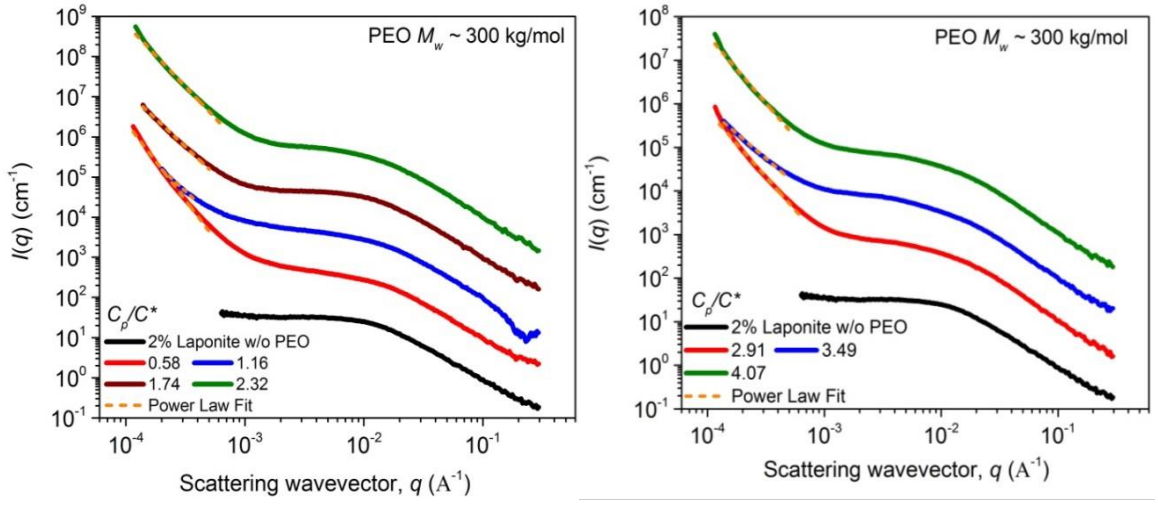

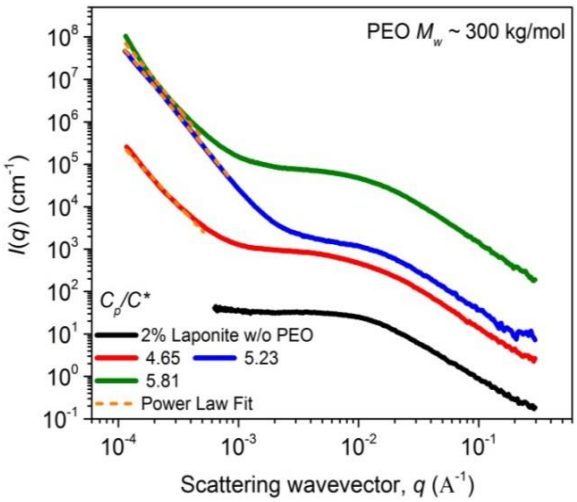


Figure B 5 : USAXS spectra of systems with 2% laponite® with various concentrations ($c_p/c^*$) of 300 kg/mol PEO. Short dashed lines along the low-$q$ regions are power law fits with the best fit slopes depicted in Figure 4.3 of Chapter 4.

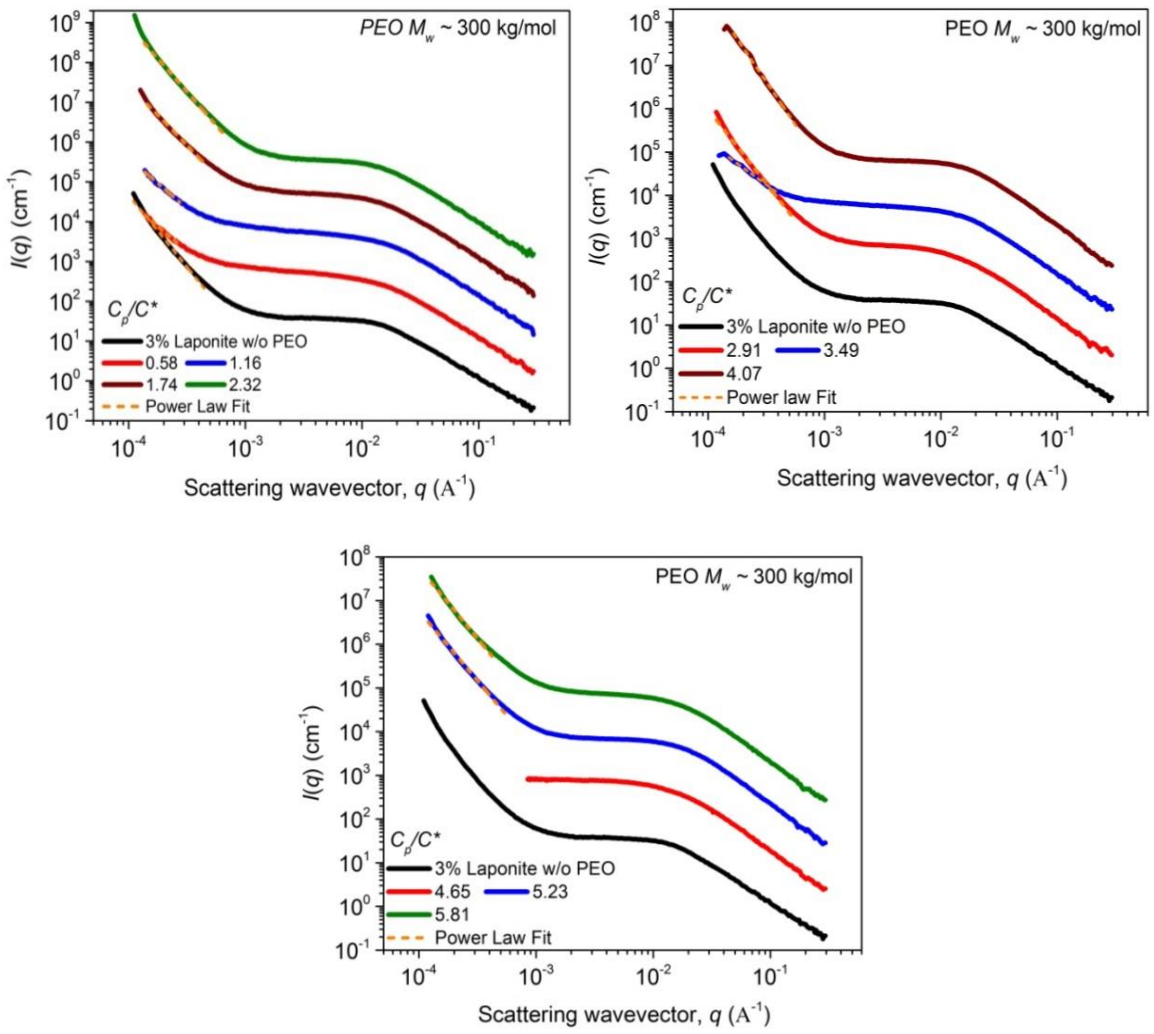


Figure B 6 : USAXS spectra of systems with 3% laponite® with various concentrations ($c_p/c^*$) of 300 kg/mol PEO. Short dashed lines along the low-$q$ regions are power law fits with the best fit slopes depicted in Figure 4.5 of Chapter 4.

Debye Bueche Analysis

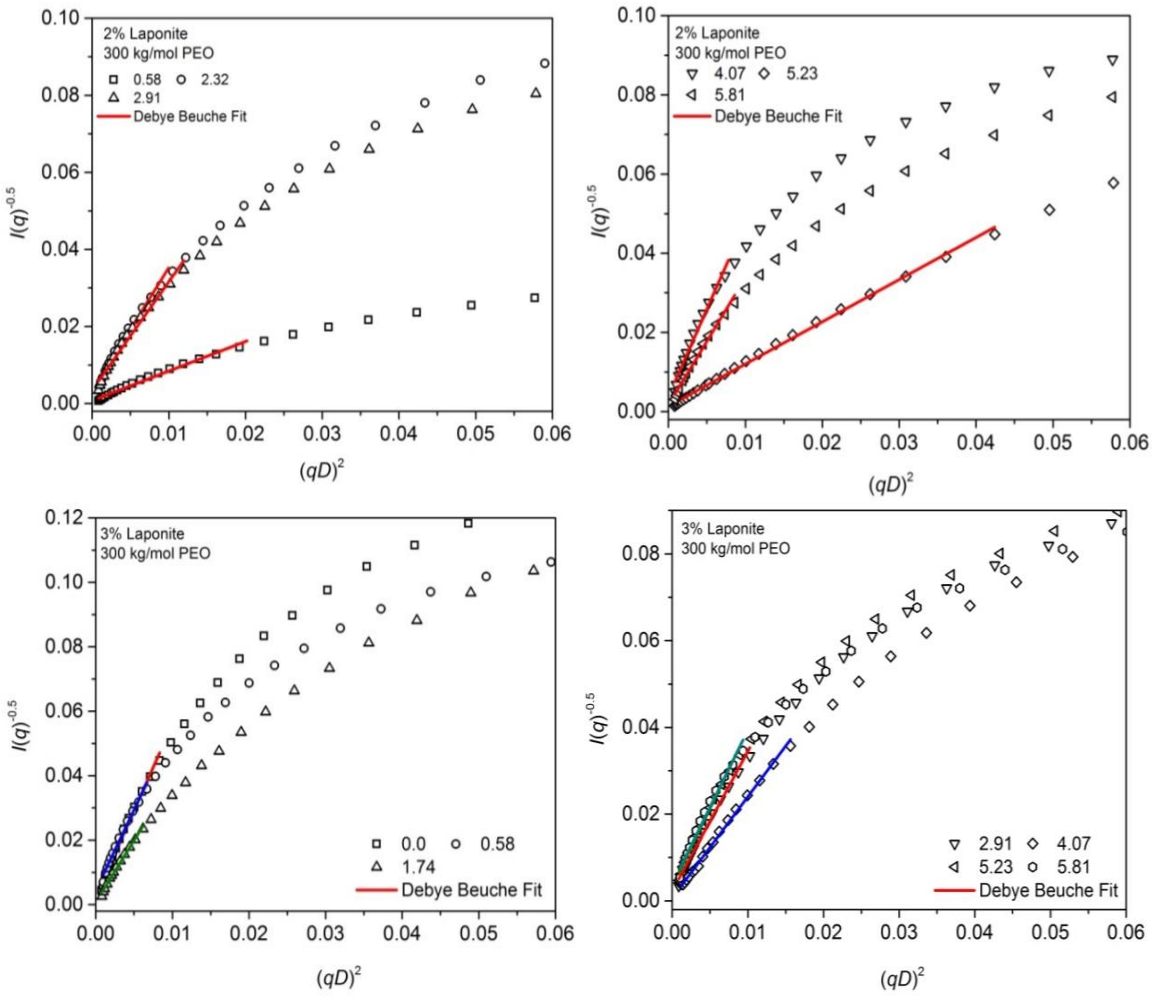


Figure B 7 : Debye Bueche analysis for laponite-PEO systems with a low-q excess scattering and a power law exponent between 3 and 4. The open symbols represent the scattering spectra and the solid lines are the linear least square fits for $(qD)^2 < 0.06$.

The Debye Bueche function is as given below:

$$I(q) \sim \frac{I_0}{(1 + q^2 \xi_v^2)^2}$$

The above equation can be re-written by introducing $D$ as

$$I(q) \sim \frac{I_0}{\left(1 + (qD)^2 \left(\frac{\xi_v}{D}\right)^2\right)^2}$$

$$\frac{1}{I(q)} \sim \frac{\left(1 + (qD)^2 \left(\frac{\xi_v}{D}\right)^2\right)^2}{I_0}$$

Taking a square root on both sides,

$$I(q)^{-1/2} \sim \left(1 + (qD)^2 \left(\frac{\xi_v}{D}\right)^2\right) * I_0^{-1/2}$$

So upon plotting $I(q)^{-1/2}$ vs $(qD)^2$ , we have

Slope $m$ = $\left(\frac{\xi_v}{D}\right)^2 * I_0^{-1/2}$

Intercept, $c$ = $I_0^{-1/2}$

# APPENDIX C

## RHEOLOGICAL BEHAVIOR AS OBSERVED IN LAPONITE® SUSPENSIONS WITH AN ANIONIC POLYELECTROLYTE

The interactions between charged colloidal particles are governed by the presence of long-range repulsions in the system. In cases where short-ranged attractions are also present, there is a competition between the attractions that lead to aggregation and the repulsions leading to stabilization. Experiments and simulation work have shown that short-ranged repulsions lead to the formation of clusters and form a percolating network at larger particle concentrations. However, when the repulsions are long-ranged, the clusters remain disconnected due to dominant repulsions and the systems transition to a glassy phase.

Figure C1 shows the rheological response of materials containing 2% laponite and various concentrations of sodium polyacrylate. As shown in this figure, the systems transition from a glass to a liquid phase with the addition of very small amounts of the charged polymer to the system.

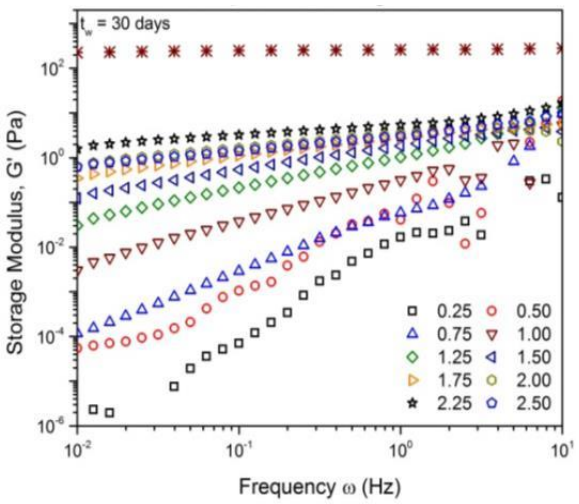


Figure C 1 : Frequency dependence of the storage modulus *G'* for systems with 2% laponite® and various concentrations of 15,000 g/mol of PAA. All samples were tested at an aging time of 30days.

## BIBLIOGRAPHY


Abou, B.; Bonn, D.; Meunier, J., Aging dynamics in a colloidal glass. *Physical Review E* **2001,** *64* (2), 021510.

Adam, M.; Delsanti, M., Dynamical behavior of semidilute polymer solutions in a theta solvent: quasi-elastic light scattering experiments. *Macromolecules* **1985,** *18* (9), 1760-1770.

Agrawal, S. K.; Sanabria-DeLong, N.; Jemian, P. R.; Tew, G. N.; Bhatia, S. R., Micro- to nanoscale structure of biocompatible PLA-PEO-PLA hydrogels. *Langmuir* **2007,** *23* (9), 5039-5044.

Alessi, M. L., Coil-to-Helix Transition of Poly (ethylene oxide) in Solution. **2004**.

Angelini, R.; Zaccarelli, E.; de Melo Marques, F. A.; Sztucki, M.; Fluerasu, A.; Ruocco, G.; Ruzicka, B., Glass–glass transition during aging of a colloidal clay. *Nature Communications* **2014,** *5*.

Angelini, R.; Zulian, L.; Fluerasu, A.; Madsen, A.; Ruocco, G.; Ruzicka, B., Dichotomic aging behaviour in a colloidal glass. *Soft Matter* **2013,** *9* (46), 10955-10959.

Angelini, R.; Madsen, A.; Fluerasu, A.; Ruocco, G.; Ruzicka, B., Aging behavior of the localization length in a colloidal glass. *Colloids and Surfaces A: Physicochemical and Engineering Aspects* **2014**.

Arfin, N.; Bohidar, H., Ergodic-to-nonergodic phase inversion and reentrant ergodicity transition in DNA–nanoclay dispersions. *Soft matter* **2014,** *10* (1), 149-156.

Atmuri, A. K.; Bhatia, S. R., Polymer-Mediated Clustering of Charged Anisotropic Colloids. *Langmuir* **2013,** *29* (10), 3179-3187.

Atmuri, A. K.; Peklaris, G. A.; Kishore, S.; Bhatia, S. R., A Re-Entrant Glass Transition in Colloidal Disks with Adsorbing Polymer. *Soft Matter* **2012,** *8*, 8965.

Avery, R. G.; Ramsay, J. D. F., Colloidal Properties of Synthetic Hectorite Clay Dispersions. *J. Colloid Interface Sci.* **1986,** *109*, 448.

Awasthi, V.; Joshi, Y. M., Effect of temperature on aging and time–temperature superposition in nonergodic laponite suspensions. *Soft Matter* **2009,** *5*, 4991.

Baghdadi, H. A.; Jensen, E. C.; Easwar, N.; Bhatia, S. R., Evidence for re-entrant behavior in laponite-PEO systems. *Rheologica Acta* **2008,** *47* (2), 121-127.

Baghdadi, H. A.; Parrella, J.; Bhatia, S. R., Long-term aging effects on the rheology of neat laponite and laponite-PEO dispersions. *Rheologica Acta* **2008,** *47* (3), 349-357.

Baghdadi, H. A.; Sardinha, H.; Bhatia, S. R., Rheology and gelation kinetics in laponite dispersions containing poly (ethylene oxide). *J. Polym. Sci., Part B: Polym. Phys.* **2005,** *43* (2), 233.

Baghdadi, H. A. Polymer-clay dispersions as soft glassy materials: Rheology, dynamics and structure. ProQuest, 2008.

Balnois, E., Durand-Vidal, S., & Levitz, P., Probing the morphology of Laponite clay colloids by atomic force microscopy. *Langmuir*, **2003,** *19*(17), 6633-6637.

Bandyopadhyay, R.; Liang, D.; Yardimci, H.; Sessoms, D. A.; Borthwick, M. A.; Mochrie, S. G. J.; Harden, J. L.; Leheny, R. L., Evolution of particle-scale dynamics in an aging clay suspension. *Physical Review Letters* **2004,** *93* (22), 228302.

Bandyopadhyay, R.; Liang, D.; Harden, J. L.; Leheny, R. L., Slow dynamics, aging, and glassy rheology in soft and living matter. *Solid state communications* **2006,** *139* (11), 589-598.

Barker, J. G.; Glinka, C. J.; Moyer, J. J.; Kim, M. H.; Drews, A. R.; Agamalian, M., Design and performance of a thermal-neutron double-crystal diffractometer for USANS at NIST. *J. Appl. Crystallogr.* **2005,** *38*, 1004.

Bastide, J.; Leibler, L., Large-scale heterogeneities in randomly cross-linked networks. *Macromolecules* **1988,** *21* (8), 2647.

Bellour, M.; Knaebel, A.; Harden, J.; Lequeux, F.; Munch, J.-P., Aging processes and scale dependence in soft glassy colloidal suspensions. *Physical review E* **2003,** *67* (3), 031405.

Belzung, B.; Lequeux, F.; Vermant, J.; Mewis, J., Flow-induced anisotropy in mixtures of associative polymers and latex particles. *J. Colloid Interface Sci.* **2000,** *224* (1), 179.

Bergenholtz, J.; Fuchs, M., Nonergodicity transitions in colloidal suspensions with attractive interactions. *Physical Review E* **1999,** *59* (5), 5706-5715.

Bergenholtz, J.; Poon, W. C. K.; Fuchs, M., Gelation in Model Colloid-Polymer Mixtures. *Langmuir* **2003,** *19*, 4493.

Bhatia, S. R., Ultra-small-angle scattering studies of complex fluids. *Current Opinion In Colloid & Interface Science* **2005,** *9* (6), 404-411.

Bhatia, S.; Barker, J.; Mourchid, A., Scattering of Disk Like Particle Suspensions: Evidence for Repulsive Interactions and Large Length Scale Structure from Static Light Scattering and Ultra-Small-Angle-Neutron-Scattering. *Langmuir* **2001,** *19*, 532.

Bonn, D.; Kellay, H.; Tanaka, H.; Wegdam, G.; Meunier, J., Laponite: What is the difference between a gel and a glass? *Langmuir* **1999,** *15* (22), 7534-7536.

Bonn, D.; Tanaka, H.; Wegdam, G.; Kellay, H.; Meunier, J., Aging of a Colloidal "Wigner" Glass. *Eur. Phys. Lett.* **1999,** *45*, 52.

Bonn, D.; Tanase, S.; Abou, B.; Tanaka, H.; Meunier, J., Laponite: Aging and shear rejuvenation of a colloidal glass. *Physical review letters* **2002,** *89* (1), 015701.

Bouchaud, J. P.; Pitard, E., Anomalous dynamical light scattering in soft glassy gels. *European Physical Journal E* **2001,** *6* (3), 231-236.

Burns, J. L.; Jameson, G. J.; Biggs, S., The structure and strength of depletion force induced particle aggregates. *Chemical engineering journal* **2000,** *80* (1), 23-30.

Caem, R.; Darley, H. C. H.; Gray, G. R., *Composition and Properties of Drilling and Completion Fluids*. **2011**; p 179.

Campbell, A. I.; Anderson, V. J.; Van Duijneveldt, J. S.; Bartlett, P., Dynamical Arrest in Attractive Colloids: The Effect of Long-Range Repulsion. *Phys. Rev. Lett.* **2005,** *94*, 208301.

Can, V.; Okay, O., Shake gels based on Laponite-PEO mixtures: effect of polymer molecular weight. *Des. Monomers Polym.* **2005,** *8* (5), 453.

Carreau, P. J.; Macdonald, I. F.; Bird, R. B., A nonlinear viscoelastic model for polymer solutions and melts—II. *Chem. Eng. Sci.* **1968,** *23*, 901.

Chang, S. H.; Ryan, M. E.; Gupta, R. K., The effect of pH, ionic strength, and temperature on the rheology and stability of aqueous clay suspensions. *Rheol. Acta* **1993,** *32*, 263.

Chen, W.-R.; Mallamace, F.; Glinka, C. J.; Fratini, E.; Chen, S.-H., Neutron-and light-scattering studies of the liquid-to-glass and glass-to-glass transitions in dense copolymer micellar solutions. *Physical Review E* **2003,** *68* (4), 041402.

Cipelletti, L.; Ramos, L.; Manley, S.; Pitard, E.; Weitz, D. A.; Pashkovski, E. E.; Johansson, M., Universal non-diffusive slow dynamics in aging soft matter, *Faraday Discussions* **2003,** *123*, 423-423.

Cipelletti, L.; Ramos, L., Slow dynamics in glassy soft matter. *Journal of Physics: Condensed Matter* **2005,** *17* (6), R253.

Cox, W. P.; Merz, E. H., Rheology of polymer melts. A correlation of dynamic and steady-flow measurement. *J. Polym. Sci.* **1958,** *28*, 619.

Crichton, M. A.; Bhatia, S. R., Large-scale structure in gels of attractive block copolymer micelles. *Langmuir* **2005,** *21* (22), 10028-10031.

Cummins, H. Z., Liquid, glass, gel: The phases of colloidal Laponite. *J. Non-Crystal. Solids* **2007,** *353*, 3891.

Daga, V. K.; Wagner, N. J., Linear viscoelastic master curves of neat and laponite-filled poly (ethylene oxide)–water solutions. *Rheol. Acta* **2006,** *45* (6), 813.

Dawson, K. A., The glass paradigm for colloidal glasses, gels, and other arrested states driven by attractive interactions. *Current opinion in colloid & interface science* **2002,** *7* (3), 218-227.

de Bruyn, J. R.; Pignon, F.; Tsabet, E.; Magnin, A., Micron-scale origin of the shear-induced structure in Laponite–poly (ethylene oxide) dispersions. *Rheol. Acta* **2008,** *47* (1), 63.

Debye, P., & Bueche, A. M., Scattering by an inhomogeneous solid.*Journal of Applied Physics*, **1949**, *20*(6), 518-525.

De Gennes, P.-G., *Scaling concepts in polymer physics*. Cornell university press: **1979**.

De Lisi, R.; Gradzielski, M.; Lazzara, G.; Milioto, S.; Muratore, N.; Prevost, S., Aqueous Laponite Clay Dispersions in the Presence of Poly (ethylene oxide) or Poly (propylene oxide) Oligomers and their Triblock Copolymers. *J. Phys. Chem. B* **2008,** *112*, 9328.

Degroot, J. V.; Macosko, C. W.; Kume, T.; Hashimoto, T., *J. Colloid Interface Sci.* **1994,** *166* (2), 404.

Delhorme, M.; Jonsson, B.; Labbez, C., Monte Carlo simulations of a clay inspired model suspension: the role of rim charge. *Soft Matter* **2012,** *8* (37), 9691-9704.

Devanand, K.; Selser, J. C., Asymptotic behavior and long-range interactions in aqueous solutions of poly (ethylene oxide). *Macromolecules* **1991,** *24*, 5943.

Dimon, P.; Sinha, S. K.; Weitz, D. A.; Safinya, C. R.; Smith, G. S.; Varady, W. A.; Lindsay, H. M., Structure Of Aggregated Gold Colloids. *Physical Review Letters* **1986,** *57* (5), 595-598.

Eberle, A. P. R.; Wagner, N. J.; Castañeda-Priego, R., Dynamical Arrest Transition in Nanoparticle Dispersions with Short-Range Interactions. *Phys. Rev. Lett.* **2011,** *106*, 105704.

Eckert, T.; Bartsch, E., Re-Entrant Glass Transition in a Colloid-Polymer Mixture with Depletion Attraction. *Phys. Rev. Lett.* **2002,** *89*, 125701.

Fall, A.; Bonn, D., Shear thickening of Laponite suspensions with poly(ethylene oxide). *Soft Matter* **2012,** *8* (17), 4645-4651.

Feigin, R. I.; Napper, D. H., Depletion stabilization and depletion flocculation. *Journal of Colloid and Interface Science* **1980,** *75* (2), 525-541.

Feigin, L. A., & Svergun, D. I. (). *Structure analysis by small-angle X-ray and neutron scattering* **1987,** (pp. 68-73). G. W. Taylor (Ed.). New York: Plenum Press.

Fluerasu, A.; Moussaïd, A.; Madsen, A.; Schofield, A., Slow dynamics and aging in colloidal gels studied by x-ray photon correlation spectroscopy. *Physical Review E* **2007,** *76* (1), 010401.

Foffi, G.; Zaccarelli, E.; Buldyrev, S.; Sciortino, F.; Tartaglia, P., Aging in Short-Ranged Attractive Colloids: A Numerical Study. *J. Chem. Phys.* **2004,** *120*, 8824.

Fossum, J. O., Physical phenomena in clays. *Phys. A* **1999,** *270*, 270.

Gabriel, J. C. P.; Sanchez, C.; Davidson, P., Observation of nematic liquid-crystal textures in aqueous gels of smectite clays. *J. Phys. Chem.* **1996,** *100*, 11139.

Gennes, P.-G., *Scaling Concepts in Polymer Physics*. 1 ed.; Cornell University Press: Ithica and London, **1979**.

Gili, T.; Capuani, S.; Maraviglia, B., Nonergodic arrested state in diluted clay suspensions monitored by triple-quantum 23Na nuclear magnetic resonance. *J. Phys. Chem. B* **2007,** *111*, 7092.

Gleissle, W.; Hochstein, B., Validity of the Cox–Merz rule for concentrated suspensions. *J. Rheol.* **2003,** *47*, 897.

Glinka, C. J.; Barker, J. G.; Hammouda, B.; Krueger, S.; Moyer, J. J.; Orts, W. J., *J. Appl. Crystallogr.* **1998,** *31*, 430.

Goetze, W. in Liquids, Freezing and Glass Transition (eds Hansen, J. P., Levesque, D. & Zinn-Justin, J.) 287 (North Holland, Amsterdam, **1991**).

Gournis, D.; Floudas, G., "Hairy" plates: Poly(ethylene oxide)-b-polyisoprene copolymers in the presence of laponite clay. *Chemistry of Materials* **2004,** *16* (9), 1686-1692.

Grandjean, J.; Mourchid, A., Re-entrant glass transition and logarithmic decay in a jammed micellar system. Rheology and dynamics investigation. *EPL (Europhysics Letters)* **2004,** *65* (5), 712.

Guinier, A.; Fournet, G., *Small-angle scattering of X-rays*. New York : Wiley: **1955**.

Guo, H. Y.; Ramakrishnan, S.; Harden, J. L.; Leheny, R. L., Connecting nanoscale motion and rheology of gel-forming colloidal suspensions. *Physical Review E* **2010,** *81* (5), 050401.

Guo, H. Y.; Ramakrishnan, S.; Harden, J. L.; Leheny, R. L., Gel formation and aging in weakly attractive nanocolloid suspensions at intermediate concentrations. *Journal of Chemical Physics* **2011,** *135* (15), 154903.

Hammouda, B.; Ho, D. L.; Kline, S., Insight into Clustering in Poly(ethylene oxide) Solutions. *Macromolecules* **2004,** *37*, 6932-6937.

Hammouda, B., A new Guinier-Porod model. *Journal of Applied Crystallography*, **2010**, *43*(4), 716-719.

Hansen, J. P., & McDonald, I. R., *Theory of Simple Liquids: With Applications to Soft Matter*. Academic Press.

Hayes, C.; Bokobza, L.; Boue, F.; Mendes, E.; Monnerie, L., Relaxation dynamics in bimodal polystyrene melts: a fourier-transform infrared dichroism and small-angle neutron scattering study. *Macromolecules* **1996,** *29* (14), 5036.

Holyst, R.; Bielejewska, A.; Szymanski, J.; Wilk, A.; Patkowski, A.; Gapinski, J.; Zywocinski, A.; Kalwarczyk, T.; Kalwarczyk, E.; Tabaka, M.; Ziebacz, N.; Wieczorek, S. A., Scaling form of viscosity at all length-scales in poly(ethylene glycol) solutions studied by fluorescence correlation spectroscopy and capillary electrophoresis. *Physical Chemistry Chemical Physics* **2009,** *11* (40), 9025-9032.

Ilavsky, J.; Jemian, P. R., Irena: tool suite for modeling and analysis of small-angle scattering. *Journal of Applied Crystallography* **2009,** *42*, 347-353.

Ilett, S. M.; Orrock, A.; Poon, W.; Pusey, P., Phase behavior of a model colloid-polymer mixture. *Physical Review E* **1995,** *51* (2), 1344.

Israelachvili, J. N., *Intermolecular and surface forces: revised third edition*. Academic press: **2011**.

Jabbari-Farouji, S.; Tanaka, H.; Wegdam, G. H.; Bonn, D., Multiple nonergodic disordered states in Laponite suspensions: A phase diagram. *Physical Review E* **2008,** *78* (6), 061405.

Jabbari-Farouji, S.; Wegdam, G.; Bonn, D., Gels and Glasses in a Single System: Evidence for an Intricate Free-Energy Landscape of Glassy Materials. *Phys. Rev. Lett.* **2007,** *99*, 065701.

Jabbari-Farouji, S.; Zargar, R.; Wegdam, G.; Bonn, D., Dynamical heterogeneity in aging colloidal glasses of Laponite. *Soft Matter* **2012,** *8* (20), 5507-5512.

Jatav, S., & Joshi, Y. M., Analyzing fractal gel of charged oblate nanoparticles in suspension using time resolved rheometry and DLVO theory.*Faraday Discussions* **2015**

Joshi, Y. M., Model for cage formation in colloidal suspension of laponite. *J. Chem. Phys.* **2007,** *127*, 081102.

Joshi, Y. M.; Reddy, G. R. K., Aging in a colloidal glass in creep flow: Time-stress superposition. *Phys. Rev. E* **2008,** *77*, 021501.

Joshi, Y. M.; Reddy, G. R. K.; Kulkarni, A. L.; Kumar, N.; Chhabra, R. P., Rheological behaviour of aqueous suspensions of laponite: new insights into the ageing phenomena. *Proceedings of the Royal Society A: Mathematical, Physical and Engineering Science* **2008,** *464* (2090), 469-489.

Kadoma, I. A.; vanEgmond, J. W., "Tuliplike" scattering patterns in wormlike micelles under shear flow. *Phys. Rev. Lett.* **1996,** *76* (23), 4432.

Kawaguchi, S.; Imai, G.; Suzuki, J.; Miyahara, A.; Kitano, T.; Ito, K., Aqueous solution properties of oligo-and poly (ethylene oxide) by static light scattering and intrinsic viscosity. *Polymer* **1997,** *38* (12), 2885-2891.

Kim, Y. H.; Gihm, S. H.; Park, C. R.; Lee, K. Y.; Kim, T. W.; Kwon, I. C.; Chung, H.; Jeong, S. Y., Structural Characteristics of Size-Controlled Self-Aggregates of Deoxycholic Acid-Modified Chitosan and Their Application as a DNA Delivery Carrier. *Bioconjugate Chem.* **2001,** *12*, 932.

Kishore, S.; Chen, Y.; Ravindra, P.; Bhatia, S. R., The effect of particle-scale dynamics on the macroscopic properties of disk-shaped colloid–polymer systems. *Colloids and Surfaces A: Physicochemical and Engineering Aspects* **2015,** *482*, 585-595.

Klajner, P.; Kaloun, S.; Munch, J. P.; Hebraud, P., Restricted diffusion of small probe particles in a laponite dispersion. *Physical Review E* **2013,** *88* (3).

Kline, S. R., Reduction and analysis of SANS and USANS data using IGOR Pro. *Journal Of Applied Crystallography* **2006,** *39*, 895-900.

Knaebel, A.; Bellour, M.; Munch, J. P.; Viasnoff, V.; Lequeux, F.; Harden, J. L., Aging behavior of Laponite clay particle suspensions. *Europhysics Letters* **2000,** *52* (1), 73-79.

Kohli, I.; Mukhopadhyay, A., Diffusion of Nanoparticles in Semidilute Polymer Solutions: Effect of Different Length Scales. *Macromolecules* **2012,** *45* (15), 6143-6149.

Kozer, N.; Kuttner, Y. Y.; Haran, G.; Schreiber, G., Protein-protein association in polymer solutions: From dilute to semidilute to concentrated. *Biophysical Journal* **2007,** *92* (6), 2139-2149.

Krall, A.; Weitz, D., Internal dynamics and elasticity of fractal colloidal gels. *Physical review letters* **1998,** *80* (4), 778.

Kramb, R. C.; Zhang, R.; Schweizer, K. S.; Zukoski, C. F., Re-Entrant Kinetic Arrest and Elasticity of Concentrated Suspensions of Spherical and Nonspherical Repulsive and Attractive Colloids. *J. Chem. Phys.* **2011,** *134*, 014503.

Kramb, R. C.; Zukoski, C. F., Yielding in Dense Suspensions: Cage, Bond, and Rotational Confinements. *J. Phys.: Condens. Matter* **2011,** *23*, 035102.

Kroon, M.; Vos, W. L.; Wegdam, G. H., Structure and formation of a gel of colloidal disks. *Phys. Rev. E* **1998,** *57* (2), 1962.

Kroon, M.; Wegdam, G. H.; Sprik, R., Dynamic light scattering studies on the sol-gel transition of a suspension of anisotropic colloidal particles. *Phys. Rev. E* **1996,** *54* (6), 6541.

Kroy, K.; Cates, M.; Poon, W., Cluster mode-coupling approach to weak gelation in attractive colloids. *Physical review letters* **2004,** *92* (14), 148302.

Kulkarni, A. M.; Dixit, N. M.; Zukoski, C. F., Ergodic and Non-Ergodic Phase Transitions in Globular Protein Suspensions. *Faraday Discuss.* **2003,** *123*, 37.

Labanda, J.; Llorens, Influence of Sodium Polyacrylate on the Rheology of Aqueous Laponite Dispersions. *J. Colloid Interface Sci.* **2005,** *289*, 86.

Labanda, J.; Llorens, J., Rheology of Laponite Colloidal Dispersions Modified by Sodium Polyacrylates. *Colloids Surf., A: Physicochem. Eng. Aspects* **2004,** *249*, 127.

Labanda, J.; Llorens, J., Effect of aging time on the rheology of Laponite dispersions. *Colloids Surf. A* **2008,** *329*, 1.

Labanda, J.; Sabatè, J.; Llorens, J., Rheology Changes of Laponite Aqueous Dispersions Due to the Addition of Sodium Polyacrylates of Different Molecular Weights. *Colloids Surf., A: Physicochem. Eng. Aspects* **2007,** *301*, 8.

Lal, J.; Auvray, L., Interaction of polymer with clays. *J. Appl. Crystallogr.* **2000,** *33* (1), 673.

Lal, J.; Auvray, L., Interaction of polymer with discotic clay particles. *Mol. Cryst. Liq. Cryst.* **2001,** *356*, 503.

Larson, R. G., *The Structure and Rheology of Complex Fluids*. **1999**.

Larson-Smith, K.; Pozzo, D. C., Scalable Synthesis of Self-Assembling Nanoparticle Clusters Based on Controlled Steric Interactions. *Soft Matter* **2011,** *7*, 5339.

Laurati, M.; Petekidis, G.; Koumakis, N.; Cardinaux, F.; Schofield, A. B.; Brader, J. M.; Fuchs, M.; Egelhaaf, S. U., Rheology, Structure and Dynamics of Colloid-Polymer Mixtures: from Liquids to Gels. *J. Chem. Phys.* **2009,** *130*, 134907.

Levitz, P.; Lecolier, E.; Mourchid, A.; Delville, A.; Lyonnard, S., Liquid-solid transition of Laponite suspensions at very low ionic strength: Long-range electrostatic stabilisation of anisotropic colloids. *Europhys. Lett.* **2000,** *49* (5), 672.

Li, J.; Jiang, J.; Li, C.; Lin, M. Y.; Schwarz, S. A.; Rafailovich, M. H.; Sokolov, J., Effect of Temperature on Shear-Induced Anisotropic Structure in Polymer Clay Hydrogels. *Macromol. Rapid Commun.* **2006,** *27*, 1787.

Lin-Gibson, S.; Kim, H.; Schmidt, G.; Han, C. C.; Hobbie, E. K., Shear-induced structure in polymer–clay nanocomposite solutions. *J. Colloid Interface Sci.* **2004,** *274* (2), 515.

Lin-Gibson, S.; Schmidt, G.; Kim, H.; Han, C. C.; Hobbie, E. K., Shear-induced mesostructure in nanoplatelet-polymer networks. *J. Chem. Phys.* **2003,** *119* (15), 8080.

Loizou, E.; Butler, P.; Porcar, L.; Kesselman, E.; Talmon, Y.; Dundigalla, A.; Schmidt, G., Large scale structures in nanocomposite hydrogels. *Macromolecules* **2005,** *38* (6), 2047-2049.

Loizou, E.; Butler, P.; Porcar, L.; Schmidt, G., Dynamic responses in nanocomposite hydrogels. *Macromolecules* **2006,** *39* (4), 1614-1619.

Loizou, E.; Porcar, L.; Schexnailder, P.; Schmidt, G.; Butler, P., Shear-Induced Nanometer and Micrometer Structural Responses in Nanocomposite Hydrogels. *Macromolecules* **2009,** *43* (2), 1041-1049.

Lu, P. J.; Conrad, J. C.; Wyss, H. M.; Schofield, A. B.; Weitz, D. A., Fluids of Clusters in Attractive Colloids. *Phys. Rev. Lett.* **2006,** *96*, 028306.

Lu, P. J.; Zaccarelli, E.; Ciulla, F.; Schofield, A. B.; Sciortino, F.; Weitz, D. A., Gelation of Particles with Short-Range Attraction. *Nat. Lett.* **2008**, 453.

Ma, L. L.; Johnston, K. P., Small Multifunctional Nanoclusters (Nanoroses) for Targeted Cellular Imaging and Therapy. *ACS Nano* **2009,** *3*, 2686.

Madsen, A.; Leheny, R. L.; Guo, H.; Sprung, M.; Czakkel, O., Beyond simple exponential correlation functions and equilibrium dynamics in x-ray photon correlation spectroscopy. *New Journal of Physics* **2010,** *12* (5), 055001.

Magda, J.; Fredrickson, G.; Larson, R.; Helfand, E., Dimensions of a polymer chain in a mixed solvent. *Macromolecules* **1988,** *21* (3), 726-732.

Malwitz, M. M.; Butler, P. D.; Porcar, L.; Angelette, D. P.; Schmidt, G., *J. Polym. Sci., Part B: Polym. Phys.* **2004,** *42* (17), 3102.

Meakin, P., Formation of fractal clusters and networks by irreversible diffusion-limited aggregation. *Physical Review Letters* **1983,** *51* (13), 1119.

Megen, W. V.; Underwood, S. M., Glass Transition in Colloidal Hard Spheres: Measurement and Mode-Coupling-Theory Analysis of the Coherent Intermediate Scattering Function. *Phys. Rev. E* **1994,** *49*, 4206.

Mendes, E.; Oeser, R.; Hayes, C.; Boue, F.; Bastide, J., Small-angle neutron scattering study of swollen elongated gels: butterfly patterns. *Macromolecules* **1996,** *29* (17), 5574.

Merkel, T. C.; Freeman, B. D.; Spontak, R. J.; He, Z.; Pinnau, I.; Meakin, P.; Hill, A. J., *Science* **2002,** *296* (5567), 519.

Mongondry, P.; Nicolai, T.; Tassin, J. F., Influence of Pyrophosphate or Polyethylene Oxide on the Aggregation and Gelation of Aqueous Laponite Dispersions. *J. Colloid Interface Sci.* **2004,** *275*, 191.

Mongondry, P.; Tassin, J. F.; Nicolai, T., Revised state diagram of Laponite dispersions. *Journal of colloid and interface science* **2005,** *283* (2), 397-405.

Morariu, S.; Bercea, Gels based poly (ethylene oxide)-laponite mixtures. M., *Rev. Roum. Chim.* **2006,** *51*, 433.

Morariu, S.; Bercea, M., Influence of Poly (ethylene oxide) on the Aggregation and Gelation of Laponite Dispersions in Water. *Rev. Roum. Chim.* **2007,** *52*, 147.

Morariu, S.; Bercea, M., Effect of addition of polymer on the rheology and electrokinetic features of Laponite RD aqueous dispersions. *J. Chem. Eng. Data* **2009,** *54*, 54.

Morariu, S.; Bercea, M., Effect of Temperature and Aging Time on the Rheological Behavior of Aqueous Poly(ethylene glycol)/Laponite RD Dispersions. *The Journal of Physical Chemistry B* **2011,** *116* (1), 48-54.

Mori, Y.; Togashi, K.; Nakamura, K., Colloidal Properties of Synthetic Hectorite Clay Dispersion Measured by Dynamic Light Scattering and Small Angle X-Ray Scattering. *Adv. Powder Technol.* **2001,** *12*, 45.

Mourchid, A.; Lecolier, E.; Van Damme, H.; Levitz, P., On Viscoelastic, Birefringent, and Swelling Properties of Laponite Clay Suspensions: Revisited Phase Diagram. *Langmuir* **1998,** *14*, 4718.

Mourchid, A.; Delville, A.; Levitz, P., Sol-gel transition of colloidal suspensions of anisotropic particles of laponite. *Faraday Discussions* **1995,** *101* (0), 275-285.

Nelson, A.; Cosgrove, T., A small-angle neutron scattering study of adsorbed poly(ethylene oxide) on laponite. *Langmuir* **2004,** *20* (6), 2298-2304.

Nelson, A.; Cosgrove, T., Dynamic light scattering studies of poly(ethylene oxide) adsorbed on laponite: Layer conformation and its effect on particle stability. *Langmuir* **2004,** *20* (24), 10382-10388.

Nicolai, T.; Cocard, S., Structure of gels and aggregates of disk-like colloids. *The European Physical Journal E* **2001,** *5* (2), 221-227.

Nosrati, A.; Addai-Mensah, J.; Skinner, W., Rheology of aging aqueous muscovite clay dispersions. *Chem. Eng. Sci.* **2011,** *66*, 119.

Ogden, A.; Lewis, J., Effect of nonadsorbed polymer on the stability of weakly flocculated suspensions. *Langmuir* **1996,** *12* (14), 3413-3424.

Ohno, K.; Koh, K.; Tsujii, Y.; Fukuda, T., *Macromolecules* **2002,** *35*, 8989.

Oppong, F. K.; Coussot, P.; de Bruyn, J. R., Gelation on the microscopic scale. *Physical Review E* **2008,** *78* (2), 021405.

Osterman, N.; Babic, D.; Poberaj, I.; Dobnikar, J.; Ziherl, P., Observation of Condensed Phases of Quasiplanar Core- Softened Colloids. *Phys. Rev. Lett.* **2007,** *99*, 248301.

Pellens, L.; Corrales, R. G.; Mewis, J., General nonlinear rheological behavior of associative polymers. *J. Rheol.* **2004,** *48*, 380.

Petit, L.; Barentin, C.; Colombani, J.; Ybert, C.; Bocquet, L., Size dependence of tracer diffusion in a Laponite colloidal gel. *Langmuir* **2009,** *25* (20), 12048-12055.

Pham, K. N.; Egelhaaf, S. U.; Pusey, P. N.; Poon, W. C. K., Glasses in Hard Spheres with Short-Range Attraction. *Phys. Rev. E* **2004,** *69*, 011503.

Pham, K. N.; Puertas, A. M.; Bergenholtz, J.; Egelhaaf, S. U.; Moussaid, A.; Pusey, P. N.; Schofield, A. B.; Cates, M. E.; Fuchs, M.; Poon, W. C. K., Multiple Glassy States in a Simple Model System. *Science* **2002,** *296*, 104.

Pham, K.; Egelhaaf, S.; Moussaıd, A.; Pusey, P., Ensemble-averaging in dynamic light scattering by an echo technique. *Review of scientific instruments* **2004,** *75* (7), 2419-2431.

Pignon, F.; Magnin, A.; Piau, J. M.; Cabane, B.; Lindner, P.; Diat, O., Yield stress thixotropic clay suspension: Investigations of structure by light, neutron, and x-ray scattering. *Phys. Rev. E* **1997,** *56* (3), 3281.

Pignon, F.; Piau, J. M.; Magnin, A., Structure and pertinent length scale of a discotic clay gel. *Phys. Rev. Lett.* **1996,** *76* (25), 4857.

Pignon, F.; Magnin, A.; Piau, J.-M., Butterfly light scattering pattern and rheology of a sheared thixotropic clay gel. *Physical Review Letters* **1997,** *79* (23), 4689.

Pontoni, D.; Narayanan, T., Ultra-small-angle X-ray scattering studies of attractive colloidal glass transition. *Journal Of Applied Crystallography* **2003,** *36*, 787-790.

Pontoni, D.; Narayanan, T.; Petit, J. M.; Grubel, G.; Beysens, D., Microstructure and dynamics near an attractive colloidal glass transition. *Physical Review Letters* **2003,** *90* (18), 188301.

Poon, W. C. K.; Renth, F.; Evans, R. M. L.; Fairhurst, D. J.; Cates, M. E.; Pusey, P. N., Colloid-polymer mixtures at triple coexistence: Kinetic maps from free-energy landscapes. *Physical Review Letters* **1999,** *83* (6), 1239-1242.

Poon, W. C. K.; Pirie, A. D.; Pusey, P. N., Gelation in colloid-polymer mixtures. *Faraday Discussions* **1995,** *101* (0), 65-76.

Pozzo, D. C.; Walker, L. M., Reversible shear gelation of polymer-clay dispersions. *Colloids And Surfaces A-Physicochemical And Engineering Aspects* **2004,** *240* (1-3), 187-198.

Puertas, A. M.; Fuchs, M.; Cates, M. E., Aging in Attraction-Driven Colloidal Glasses. *Phys. Rev. E* **2007,** *75*, 031401.

Pujala, R. K.; Bohidar, H. B., Slow dynamics, hydration and heterogeneity in Laponite dispersions. *Soft Matter* **2013,** *9* (6), 2003-2010.

Pusey, P. N.; Van Megen, W., Observation of a Glass-Transition in Suspensions of Spherical Colloidal Particles. *Physical Review Letters* **1987,** *59* (18), 2083-2086.

Pusey, P.; Van Megen, W., Dynamic light scattering by non-ergodic media. *Physica A: Statistical Mechanics and its Applications* **1989,** *157* (2), 705-741.

Pusey, P. N., van Megen, W., Underwood, S. M., Bartlett, P., & Ottewill, R. H., Colloidal fluids, crystals and glasses. *Journal of Physics: Condensed Matter*, **1990**, *2*(S), SA373.

Ramakrishnan, S.; Gopalakrishnan, V.; Zukoski, C. F., Clustering and Mechanics in Dense Depletion and Thermal Gels. *Langmuir* **2005,** *21*, 9917.

Ramakrishnan, S.; Shah, S. A.; Ruggeri, L.; Chen, Y. L.; Schweizer, K. S.; Zukoski, C. F., Collective Diffusion in Colloid-Polymer Suspensions: Relative Role of Thermodynamics and Hydrodynamics. *Langmuir* **2009,** *25*, 10507.

Ramsay, J. D. F.; Lindner, P., Small-Angle Neutron-Scattering Investigations Of The Structure Of Thixotropic Dispersions Of Smectite Clay Colloids. *Journal Of The Chemical Society-Faraday Transactions* **1993,** *89* (23), 4207-4214.

Ramsay, J. D. F.; Swanton, S. W.; Bunce, J., Swelling And Dispersion Of Smectite Clay Colloids - Determination Of Structure By Neutron-Diffraction And Small-Angle Neutron-Scattering. *Journal Of The Chemical Society-Faraday Transactions* **1990,** *86* (23), 3919-3926.

Ramzi, A.; Zielinski, F.; Bastide, J.; Boue, F., Butterfly patterns: small-angle neutron scattering from deuterated mobile chains in a randomly cross-linked polystyrene network. *Macromolecules* **1995,** *28* (10), 3570.

Roe, R. J., *Methods of X-Ray and Neutron Scattering in Polymer Science*. **2000**.

Ruzicka, B.; Zulian, L.; Ruocco, G., Routes to Gelation in a Clay Suspension. *Phys. Rev. Lett.* **2004,** *93*, 258301.

Ruzicka, B.; Zulian, L.; Ruocco, G., More on the phase diagram of laponite. *Langmuir* **2006,** *22* (3), 1106-1111.

Ruzicka, B.; Zaccarelli, E., A fresh look at the Laponite phase diagram. *Soft Matter* **2011,** *7* (4), 1268-1286.

Ruzicka, B.; Zulian, L.; Ruocco, G., Ageing dynamics in Laponite dispersions at various salt concentrations. *Philosophical Magazine* **2007,** *87* (3-5), 449-458.

Ruzicka, B., Zaccarelli, E., Zulian, L., Angelini, R., Sztucki, M., Moussaïd, A., Sciortino, F. , Observation of empty liquids and equilibrium gels in a colloidal clay. *Nature materials,* **2011**. *10*(1), 56-60.

Saha, D.; Bandyopadhyay, R.; Joshi, Y. M., A Dynamic Light Scattering Study and DLVO Analysis of Physicochemical Interactions in Colloidal Suspensions of Charged Disks. *Langmuir* **2015**.

Saunders, J. M.; Goodwin, J. W.; Richardson, R. M.; Vincent, B., A small-angle X-ray scattering study of the structure of aqueous laponite dispersions. *Journal Of Physical Chemistry B* **1999,** *103* (43), 9211-9218.

Schaefer, D. W.; Martin, J. E.; Wiltzius, P.; Cannell, D. S., Fractal Geometry Of Colloidal Aggregates. *Physical Review Letters* **1984,** *52* (26), 2371-2374.

Schexnailder, P.; Loizou, E.; Porcar, L.; Butler, P.; Schmidt, G., Heterogeneity in nanocomposite hydrogels from poly(ethylene oxide) cross-linked with silicate nanoparticles. *Phys Chem Chem Phys* **2009,** *11* (15), 2760-6.

Schmidt, G.; Nakatani, A. I.; Butler, P. D.; Karim, A.; Han, C. C., Shear orientation of viscoelastic polymer-clay solutions probed by flow birefringence and SANS. *Macromolecules* **2000,** *33* (20), 7219.

Schmidt, G.; Nakatani, A. I.; Han, C. C., Rheology and flow-birefringence from viscoelastic polymer-clay solutions. *Rheologica Acta* **2002,** *41* (1-2), 45-54.

Schmidt, G.; Nakatani, A. I.; Butler, P. D.; Han, C. C., Small-angle neutron scattering from viscoelastic polymer-clay solutions. *Macromolecules* **2002,** *35* (12), 4725-4732.

Sciortino, F.; Tartaglia, P.; Zaccarelli, E., One Dimensional Cluster Growth and Branching Gels in Colloidal Systems with Short-Range Depletion Attractive and Screened Electrostatic Repulsion. *J. Phys. Chem. B* **2005,** *109*, 21942.

Sciortino, F., Disordered materials: One liquid, two glasses. *Nature materials* **2002,** *1* (3), 145-146.

Sciortino, F.; Mossa, S.; Zaccarelli, E.; Tartaglia, P., Equilibrium cluster phases and low-density arrested disordered states: the role of short-range attraction and long-range repulsion. *Physical review letters* **2004,** *93* (5), 055701.

Segre, P. N., Prasad, V., Schofield, A. B., & Weitz, D. A., Glasslike kinetic arrest at the colloidal-gelation transition. *Physical Review Letters*, **2001**, *86*(26), 6042.

Shah, S. A.; Chen, Y. L.; Ramakrishnan, S.; Schweizer, K. S.; Zukoski, C. F., Microstructure of dense colloid–polymer suspensions and gels. *J. Phys.: Condens. Matter* **2003,** *15*, 4751.

Shah, S. A.; Ramakrishnan, S.; Chen, Y. L.; Schweizer, K. S.; Zukoski, C. F., Scattering Studies of the Structure of Colloid-Polymer Suspensions and Gels. *Langmuir* **2003,** *19*, 5128.

Shahin, A.; Joshi, Y. M., Hyper-aging dynamics of nanoclay suspension. *Langmuir* **2012,** *28*, 5826-5833.

Shahin, A.; Joshi, Y. M., Physicochemical Effects in Aging Aqueous Laponite Suspensions. *Langmuir* **2012,** *28* (44), 15674-15686.

Shahin, A.; Joshi, Y. M., Irreversible aging dynamics and generic phase behavior of aqueous suspensions of laponite. *Langmuir* **2010,** *26* (6), 4219-4225.

Shaukat, A.; Sharma, A.; Joshi, Y. M., Time–aging time–stress superposition in soft glass under tensile deformation field. *Rheol. Acta* **2010,** *49*, 1093-1101.

Shibayama, M.; Karino, T.; Miyazaki, S.; Okabe, S.; Takehisa, T.; Haraguchi, K., Small-angle neutron scattering study on uniaxially stretched poly (N-isopropylacrylamide)-clay nanocomposite gels. *Macromolecules* **2005,** *38* (26), 10772-10781.

Shibayama, M.; Suda, J.; Karino, T.; Okabe, S.; Takehisa, T.; Haraguchi, K., Structure and dynamics of poly (N-isopropylacrylamide)-clay nanocomposite gels. *Macromolecules* **2004,** *37* (25), 9606.

Shin, H.; Grason, G. M.; Santangelo, C. D., Mesophases of Soft-Sphere Aggregates. *Soft Matter* **2009,** *5*, 3629.

Shukla, A.; Joshi, Y. M., Ageing under oscillatory stress: Role of energy barrier distribution in thixotropic materials. *Chem. Eng. Sci.* **2009,** *64*, 4668.

Sollich, P., Lequeux, F., Hébraud, P., & Cates, M. E., Rheology of soft glassy materials. *Physical review letters*, **1997,** *78*(10), 2020.

Somani, R. H.; Yang, L.; Hsiao, B. S.; Sun, T.; Pogodina, N. V.; Lustiger, A., Shear-induced molecular orientation and crystallization in isotactic polypropylene: Effects of the deformation rate and strain. *Macromolecules* **2005,** *38* (4), 1244.

Sudeepto, S.; Yuping, X.; Sanat, K. K.; Hoichang, Y.; Amitabh, B.; Derek, L. H.; Lisa, H.; Justin, B. H.; Kenneth, S. S., Chain Conformations and Bound-Layer Correlations in Polymer Nanocomposites. *Physical Review Letters* **2007,** *98* (12), 128302.

Sun, W.; Wang, T.; Wang, C.; Liu, X.; Tong, Z., Scaling of the dynamic response of hectorite clay suspensions containing poly (ethylene glycol) along the universal route of aging. *Soft Matter* **2013,** *9* (27), 6263-6269.

Surve, M.; Pryamitsyn, V.; Ganesan, V., Nanoparticles in solutions of adsorbing polymers: Pair interactions, percolation, and phase behavior. *Langmuir* **2006,** *22* (3), 969-981.

Swenson, J.; Smalley, M. V.; Hatharasinghe, H. L. M., Mechanism and strength of polymer bridging flocculation. *Physical Review Letters* **1998,** *81* (26), 5840-5843.

Takeda, M.; Matsunaga, T.; Nishida, T.; Endo, H.; Takahashi, T.; Shibayama, M., Rheo-SANS Studies on Shear Thickening in Clay− Poly (ethylene oxide) Mixed Solutions. *Macromolecules* **2010,** *43* (18), 7793-7799.

Tanaka, H.; Jabbari-Farouji, S.; Meunier, J.; Bonn, D., Kinetics of Ergodic-to-Nonergodic Transitions in Charged Colloidal Suspensions: Aging and Gelation. *Phys. Rev. E* **2005,** *71*, 021402.

Tanaka, H.; Meunier, J.; Bonn, D., Nonergodic States of Charged Colloidal Suspensions: Repulsive and Attractive Glasses and Gels. *Phys. Rev. E* **2004,** *69*, 031404.

Tang, S.; Wang, X.; Lei, J.; Hu, Z.; Deng, S.; Ju, H., Pt-Dispersed Flower-Like Carbon Nano Sheet Aggregation for Low-Over Potential Electrochemical Biosensing. *Biosens. Bioelectron.* **2010,** *26*, 432.

Tawari, S. L.; Koch, D. L.; Cohen, C., Electrical double-layer effects on the brownian diffusivity and aggregation rate of laponite clay particles. *Journal of Colloid and Interface Science* **2001,** *240* (1), 54-66.

Thompson, D. W.; Butterworth, J. T., The nature of laponite and its aqueous dispersions. *J. Colloid Interface Sci.* **1992,** *151* (1), 236.

Toledano, J. C. F.; Sciortino, F.; Zaccarelli, E., Colloidal Systems with Competing Interactions: From an Arrested Repulsive Cluster Phase to a Gel. *Soft Matter* **2009,** *5*, 2390.

Trappe, V.; Sandkuhler, P., Colloidal gels - low-density disordered solid-like states. *Current Opinion in Colloid & Interface Science* **2004,** *8* (6), 494-500.

Trappe, V., Prasad, V., Cipelletti, L., Segre, P. N., & Weitz, D. A. , Jamming phase diagram for attractive particles. *Nature* **2001,** *411*(6839), 772-775.

Tuinier, R.; Fan, T.-H., Scaling of nanoparticle retardation in semi-dilute polymer solutions. *Soft Matter* **2008,** *4* (2), 254-257.

Turner, A. J.; Nair, S.; Lai, Z.; Cheng, C.; Bhatia, S. R., Controlled Aggregation of Colloidal Particles for Toner Applications. *J. Appl. Polym. Sci.* **2011,** *122*, 1358.

Van Oss, C.; Arnold, K.; Coakley, W., Depletion flocculation and depletion stabilization of erythrocytes. *Cell biophysics* **1990,** *17* (1), 1-10.

Vermant, J., Large-scale structures in sheared colloidal dispersions. *Curr. Opin. Colloid Interface Sci.* **2001,** *6* (5−6), 489.

Wheeler, E. K.; Izu, P.; Fuller, G. G., Structure and rheology of wormlike micelles. *Rheol. Acta* **1996,** *35* (2), 139.

Winter, H. H., & Chambon, F., Analysis of linear viscoelasticity of a crosslinking polymer at the gel point. *Journal of Rheology (1978-present)*, **1986**, *30*(2), 367-382.

Wyart, F. B.; de Gennes, P. G., Viscosity at small scales in polymer melts. *European Physical Journal E* **2000,** *1* (1), 93-97.

Zaccarelli, E., Colloidal gels: equilibrium and non-equilibrium routes. *Journal of Physics-Condensed Matter* **2007,** *19* (32), 323101.

Zaccarelli, E.; Lu, P. J.; Ciulla, F.; Weitz, D. A.; Sciortino, F., Gelation as Arrested Phase Separation in Short-Ranged Attractive Colloid-Polymer Mixtures. *J. Phys.: Condens. Matter* **2008,** *20*, 494242.

Zaccarelli, E.; Poon, W. C., Colloidal glasses and gels: The interplay of bonding and caging. *Proceedings of the National Academy of Sciences* **2009,** *106* (36), 15203-15208.

Zebrowski, J.; Prasad, V.; Zhang, W.; Walker, L. M.; Weitz, D. A., Shake-gels: shear-induced gelation of laponite–PEO mixtures. *Colloids Surf., A* **2003,** *213* (2−3), 189.

Zhang, S.; Lee, J.; Sun, S., Controlled Synthesis of Monodisperse Magnetic Nanoparticles in Solution Phase. *Open Surf. Sci. J.* **2012,** *4*, 26.

Zhang, X.; Servos, M. R.; Liu, J., Ultrahigh nanoparticle stability against salt, pH, and solvent with retained surface accessibility via depletion stabilization. *Journal of the American Chemical Society* **2012,** *134* (24), 9910-9913.

Zulian, L.; Marques, F. M.; Emilitri, E.; Ruocco, G.; Ruzicka, B., Dual aging behaviour in a clay–polymer dispersion. *Soft Matter* **2014,** *10* (25), 4513-4521.

Zulian, L.; Ruzicka, B.; Ruocco, G., Influence of an adsorbing polymer on the aging dynamics of Laponite clay suspensions. *Philosophical Magazine* **2008,** *88* (33-35), 4213-4221.